Synthesis, characterization and *in vitro* antiplasmodial evaluation of 4-& 8-aminoquinoline based-hybrid compounds

by

Xhamla Nqoro

University of Fort Hare
Together in Excellence

2018

Synthesis, characterization and *in vitro* antiplasmodial evaluation of 4-& 8-aminoquinoline based-hybrid compounds

Nqoro, Xhamla (201300305)

Dissertation submitted in partial fulfillment for MSc degree in chemistry

Faculty of science and agriculture Chemistry department

University of Fort Hare

Supervisor: Prof Blessing A. Aderibigbe

Declaration

"I declare that this dissertation submitted for the degree of MSc in Chemistry department, University of Fort Hare, Alice campus is my own original work. It has not been previously submitted for any degree or examination in any other institution of higher learning. I further declare that all sources cited or quoted are indicated and acknowledged in a comprehensive list of references."

____2018-12-03_____   _____

Date   Signature

Dedication

I dedicate this work to my family, my Mother, siblings, and cousins. Nolungisa Joyce Nqoro,

Nceba Ronald Nqoro, Babalwa Nqoro, Ayabulela Nqoro, Siphenkosi Nqoro, Ukhonaye Nqoro,

Lunje-uthando Gwala, Chwayita Nqoro, and Andisiwe Jekwa "changes".

Abstract

Malaria is a deadly disease and its drug resistance has been reported to be a challenge globally. The death toll caused by malaria has increased rapidly in different regions of the world. Quinoline scaffold molecules are combined with other classes of antimalarials to tackle drug resistance. The combination of quinoline scaffolds with other antimalarial compounds and metals-based drugs have been reported to be a potential approach to overcome drug resistance common in the currently used antimalarials. 4-Aminoquinoline was hybridized with selected organic molecules and metal-based compounds to form a class of hybrid compounds containing either an amide bond or ester bond as a linker between the parent molecules. 4-Aminoquinoline derivatives are known compounds and they were prepared via known synthetic routes and characterized. The hybrid compounds were characterized and the FTIR results confirmed the successful linkage of 4-aminoquinoline derivatives to selected organic scaffolds to form hybrid compounds. NMR results confirmed the successful formation of hybrid compounds. MS showed signals of the hybrid molecules confirming the successful isolation of the hybrid compounds. *In vitro* antiplasmodial assay was performed against asexual parasite and chloroquine was used as a reference drug. The percentage inhibition effects of the hybrid compounds were in a range of 96-102% at 5 µM and 36-96% at 1 µM suggesting that the percentage inhibition effect of the hybrid compounds was influenced by the drug concentration. Hybridization of either 4-aminosalicylic scaffold or ferrocene butanoic acid with 4-aminoquinoline derivatives is a potential synthetic route that can result in potent antimalarials. However, more research is needed to fully understand the structure-activity relationship of these hybrid compounds.

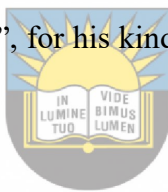**Key words**: Malaria, *P. falciparum*, aminoquinoline, hybrid compounds

Acknowledgements

Conference and Publication
Conference

1. X. Nqoro and B.A. Aderibigbe: Synthesis and characterization of 4-aminoquinoline-based hybrid compounds as potential antimalarials. Bio Africa convention 27th-29th August 2018, Durban ICC South Africa.

2. X. Nqoro and B.A. Aderibigbe: synthesis, characterization and in vitro assay of metal-based hybrid compounds containing aminoquinoline and antifolates as potential antimalarials. Postgraduate day 2018 7th November 2018, University of Fort Hare South Africa

Publication

1. X. Nqoro, T. Naki, B.A. Aderibigbe "Quinoline-Based Hybrid Compounds with Antimalarial Activity" Molecules **2017**

List of Abbreviations

AEE: 2(2-Aminoethoxy)ethanol

EDDA: 2-(2-(2-aminoethoxy)ethoxy)ethanamine

$C_7H_7NO_2$: 4-aminosalicylic acid

$CHCl_3$: Chloroform

°C: Degrees Celsius

PDA: 1.3-diaminopropane

DCM: Dichloromethane

DCC: N.N'-Dicyclohexylcarbodiimide

Dhfr: Dihydrofolate reductase

DMAP: 4-Dimethylaminopyridine

DMF: Dimethylformide

DMSO: Dimethylsulfoxide

EtOH: Ethanol

EA: Ethanolamine

EtOAc: Ethyl acetate

EDA: Ethyldiamine

$FeC_{14}H_{14}O_3$: Ferrocene butanoic acid

FTIR: Fourier-transform infrared spectroscopy

HZN: Hydrazine hydrate

HSU: N-Hydroxysuccinimide

LC-MS: Liquid chromatography mass spectroscopy

MeOH: Methanol

mmol: millimole

NMR: Nuclear magnetic resonance

ppm: parts per million

P. falciparum: *Plasmodium falciparum*

Pfcrt: *Plasmodium falciparum* chloroquine resistant transporter

*Pf*EXP1: *Plasmodium falciparum* Export Protein1

Pfmdr1: *Plasmodium falciparum* multidrug resistance

cm^{-1}: per centimeter

ROS: Relative oxygen species

TLC: Thin layer chromatography

Table of Contents

x

List of schemes

List of Tables

List of Figures

Chapter 1
1. Introduction

Malaria is a parasitic disease hosted by humans through the bite of a female *Anopheles* mosquito[1–3]. The malaria life cycle starts in the vector mosquito and continues in its host (humans), by injecting the parasites to the host's blood stream. The parasite undergoes multiple stages inside the host invading the blood and the liver cells, where they mature and multiply asexually into gametocytes[4]. The cycle continues when an uninfected mosquito feeds on the infected human thereby ingesting blood containing parasitic gametes to its mid-gut, where sexual reproduction takes place producing sporozoites. In each stage of the malaria infection, different symptoms present itself that can alert the medical teams to administer treatment. Each stage of malaria infection requires different treatment with different classes of antimalarials. Malaria is caused by five plasmodium parasitic species but the most dominant and deadly one is *P. falciparum* which is highly resistant to most antimalarial drugs in the sub-tropical regions[4,5].
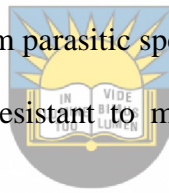
Cases of severe malaria are mostly reported in tropical and sub-tropical regions of the world and in places where there is a high rate of poverty[5]. The common victims or the easy targets of malaria infection are immune deficient people, pregnant women, and children[6–10]. The statistics released in 2017 by the World Health Organisation (WHO) stated that 216 million infections were reported, with an increased record of about 5 million cases when compared to 2015[8,9,11,12]. Furthermore, 445 000 deaths were associated with malaria infection[8,9]. Most malaria cases are reported in the African region followed by South-East Asia and the Eastern Mediterranean region, respectively[13–15].

Different approaches have been designed to treat malaria intracellular and extracellular. Extracellular treatment includes vector control such as [awareness, vaccines, indoor residual sprays (IRS) and long-lasting insecticidal nets (LNs)]. These controls have also assisted in

minimizing the spread of malaria[16]. Even though practices such as vector control have managed to decrease the death rate between 2000 to 2015 by approximately 37-45%, the resistance of *P. falciparum* is still alarming[17,18]. Vector control has been proven to be insufficient for the complete eradication of malaria, and currently, there is no vaccine that can totally prevent the infection[9,19,20]. With vector control lacking effectiveness, intracellular treatment remains the best approach for malarial treatment[19].

Intracellular treatment has remained the key approach for the treatment of malaria and is still the most effective approach. The class of 4-aminoquinolines (chloroquine) were the first and most effective antimalarials for the treatment of malaria back in 1940`s[21]. Chloroquine was the first effective antimalarial and remained the drug of choice until *P. falciparum* developed varying degrees of resistance[22]. Chloroquine is being used as the first aid drug in areas where malaria mostly endangers people's lives[23,24]. The malaria parasite has developed resistance to chloroquine and its derivatives. Scientists have designed a combination of different antimalarials to enhance their efficacy. At present, the approaches used for the design of antimalarials with enhanced therapeutic efficacy are the hybridization of antimalarial drugs with antibiotics or antigens and the re-design of currently existing antimalarial drugs for targeted drug delivery for the treatment of malaria[1,25]. Treatment of malaria via combination therapy resulted in a high cure rate when compared to the use of a single antimalarial with the cure rate of 20-40%[23]. Combination therapy is the future and hope against drug resistance.

1.1. Problem statement

The resistance of the malaria parasites to most of the currently used antimalarials has become the major problem that hinders the total eradication of the disease. Chloroquine was the first drug of choice to treat malaria but the ever-growing resistance of *P. falciparum* has made it ineffective. The resistance of the malaria parasite to most of the currently available antimalarials has instilled fear in people, mostly in the African region where about 80% of the

cases are reported annually[19]. The drug resistance associated with the presently used antimalarial drugs is the cause of the increase in death rates globally. The malaria transmission is triggered by *P47* the parasite's protein that mediates *P. falciparum* (Pfs47) invasion to the mosquito's immune and *Pfs47* which allows the parasite to adapt into new and different vector species globally[26]. The malaria parasite resistance is linked to gene mutations. The *P. falciparum* multidrug resistance (*Pfmdr1*) and *P. falciparum* chloroquine-resistant transporter (*Pfcrt*) gene mutations cause a high level of malaria parasite resistance[27–31]. This increases the rate of chloroquine efflux by the parasite. Gene mutations also cause other diseases like sickle cell anaemia[32] such that even when a malaria victim is cured it can still suffer from the potentially fatal condition of sickle cell anemia the blood cell disease[33,34]. Patients carrying resistant *pfcrt* 76T gene allele were reported to likely fail chloroquine treatment compared to the ones that carry sensitive K76 gene allele of the parasite, though this could not predict treatment failure for a patient who's been initially infected with resistant parasite[35]. The most affected areas by malaria in South Africa are three provinces namely KwaZulu-Natal, Limpopo, and Mpumalanga[36,37] meaning that about 6 million people in South Africa are at the risk of the disease[36]. In KwaZulu-Natal, most cases are reported in UMkhanyakude, uThungulu, and Zululand which is about 80% of the cases reported in the region[36]. An estimation of South Africa's population at risk of malaria was accounted to be 10% living in malaria-endemic regions caused by *P. falciparum*[38].

1.2.   Motivation & Rationale

The ongoing resistance of the malarial parasite has been the main problem ever since it became resistant to chloroquine. Chloroquine alone is less effective hence the new approach of combination therapy has been recommended to be the future and a promising tool in malarial treatment[19]. Combination therapy via hybridization of two or more molecules through their active sites, to form one molecule with the combined effect of its precursors is an effective

approach to overcome drug resistance[18,36,37]. Hybrid molecules have the ability to treat the malarial parasites at different stages of its life cycle[38]. Hybrid molecules overcome the malarial resistance by increasing efficacy of the individual molecule in the hybrid. 4-aminoquinoline molecules and their derivatives are recommended for hybridization with other antimalarials[39]. The class of 4-aminoquinoline scaffolds is reviewed as promising precursors for combination therapy with metal-based molecules as well as other classes of antimalarials via selected functionalities[30].

1.3. Aim

To synthesize 4- and 8-aminoquinoline-based hybrid compounds for evaluation against drug resistance.

1.4. Objectives

1. To synthesize and characterize 4-and 8-aminoquinoline hybrid compounds.

2. To conduct *in vitro* antiplasmodial evaluation of 4- and 8-aminoquinoline hybrid compounds.
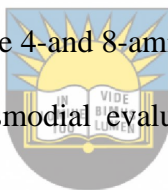
References

1. MacMillan DS, Murray J, Sneddon HF, Jamieson C, Watson AJB. Evaluation of alternative solvents in common amide coupling reactions: Replacement of dichloromethane and N,N-dimethylformamide. *Green Chem*. 2013;15(3):596-600. doi:10.1039/c2gc36900a

2. Nqoro X, Tobeka N, Aderibigbe BA. Quinoline-based hybrid compounds with antimalarial activity. *Molecules*. 2017;22(12). doi:10.3390/molecules22122268

3. Cowman AF, Crabb BS. Invasion of red blood cells by malaria parasites. *Cell*. 2006;124(4):755-766. doi:10.1016/j.cell.2006.02.006

4. Capela R, Magalhães J, Miranda D, Machado MSV, Margarida A, Inês SS, Moni G, Jiri R, Philip JF, Raquel P, Maria JM, Rui P, Miguel L, Francisca. Endoperoxide-8-aminoquinoline hybrids as dual-stage antimalarial agents with enhanced metabolic stability. *Eur J Med Chem*. 2018;149:69-78. doi:10.1016/j.ejmech.2018.02.048

5. Lynch D. 4-aminoquinolines as Antimalarial Drugs. *Trinity Student Sci Rev*. 2016;2(September 2015):196-210. https://trinityssr.files.wordpress.com/2016/06/4th-chem.pdf.

6. Vandekerckhove S, D'Hooghe M. Quinoline-based antimalarial hybrid compounds. *Bioorganic Med Chem*. 2015;23(16):5098-5119. doi:10.1016/j.bmc.2014.12.018

7. Sinha M, Dola VR, Agarwal P, Srivastava K, Haq W, Puri, SK. Katti, SB. Antiplasmodial activity of new 4-aminoquinoline derivatives against chloroquine resistant strain. *Bioorganic Med Chem*. 2014;22(14):3573-3586. doi:10.1016/j.bmc.2014.05.024

8. Chopra R, Chibale K, Singh K. Pyrimidine-chloroquinoline hybrids: Synthesis and antiplasmodial activity. *Eur J Med Chem*. 2018;148:39-53.

doi:10.1016/j.ejmech.2018.02.021

9.   Kumar S, Bhardwaj TR, Prasad DN, Singh RK. Drug targets for resistant malaria: Historic to future perspectives. *Biomed Pharmacother*. 2018;104(March):8-27. doi:https://doi.org/10.1016/j.biopha.2018.05.009

10.   Luzzatto L. G6PD deficiency: A polymorphism balanced by heterozygote advantage against malaria. *Lancet Haematol*. 2015;2(10):e400-e401. doi:10.1016/S2352-3026(15)00191-X

11.   Ashley EA, Pyae Phyo A, Woodrow CJ. Malaria. *Lancet*. 2018;391. doi:10.1016/S0140-6736(18)30324-6

12.   Health Organization W. *World Malaria Report 2017*.; 2017. doi:10.1071/EC12504

13.   World Health Organization. World Malaria Report 2015. *World Health*. 2015:243. doi:ISBN 978 92 4 1564403

14.   Kondaparla S, Soni A, Manhas A, Srivastava K, Puri SK, Katti SB. Antimalarial activity of novel 4-aminoquinolines active against drug resistant strains. *Bioorg Chem*. 2017;70:74-85. doi:10.1016/j.bioorg.2016.11.010

15.   Jones RA, Panda SS, Hall CD. European Journal of Medicinal Chemistry Quinine conjugates and quinine analogues as potential antimalarial agents. *Eur J Med Chem*. 2015;97:335-355. doi:10.1016/j.ejmech.2015.02.002

16.   Ngufor C, Fagbohoun J, Critchley J, N'Guessan R, Todjinou D, Malone D, Akogbeto M, Rowland M. Which intervention is better for malaria vector control: Insecticide mixture long-lasting insecticidal nets or standard pyrethroid nets combined with indoor residual spraying? *Malar J*. 2017;16(1):1-9. doi:10.1186/s12936-017-1987-5

17.   Singh S, Agarwal D, Sharma K, Sharma M, Nielsen MA, Alifrangis M, Singh AK, Gupta RD, Awasthi SK. 4-Aminoquinoline derivatives : Synthesis, in vitro and in vivo antiplasmodial activity against chloroquine-resistant parasites. *Eur J Med Chem*. 2016;122:394-407. doi:10.1016/j.ejmech.2016.06.033

18.   Reddy PL, Khan SI, Ponnan P, Tripathi M, Rawat DS. Design, synthesis, and evaluation of 4-aminoquinoline-purine hybrids as potential antiplasmodial agents. *Eur J Med Chem*. 2017;126:675-686. doi:10.1016/j.ejmech.2016.11.057

19.   Maurya SS, Khan SI, Bahuguna A, Kumar D, Rawat DS. Synthesis, antimalarial activity, heme binding and docking studies of N-substituted 4-aminoquinoline-pyrimidine molecular hybrids. *Eur J Med Chem*. 2017;129:175-185. doi:10.1016/j.ejmech.2017.02.024

20.   Kanishchev OS, Lavoignat A, Picot S, Médebielle M, Bouillon JP. New route to the 5-((arylthio- and heteroarylthio)methylene)-3-(2,2,2- trifluoroethyl)-furan-2(5H)-ones - Key intermediates in the synthesis of 4-aminoquinoline γ-lactams as potent antimalarial compounds. *Bioorganic Med Chem Lett*. 2013;23(22):6167-6171. doi:10.1016/j.bmcl.2013.08.108

21.   Wongsrichanalai C, Pickard AL, Wernsdorfer WH, Meshnick SR. Epidemiology of drug-resistant malaria. *Lancet Infect Dis*. 2002;2(4):209-218. doi:10.1016/S1473-3099(02)00239-6

22.   Foley M, Tilley L. Quinoline antimalarials: Mechanisms of action and resistance. *Int J Parasitol*. 1997;27(2):231-240. doi:10.1016/S0020-7519(96)00152-X

23.   Canfield CJ, Hall AP, MacDonald BS, Neuman DA, Shaw JA. Treatment of falciparum malaria from Vietnam with a phenanthrene methanol (WR 33063) and a quinoline methanol (WR 30090). *Antimicrob Agents Chemother*. 1973;3(2):224-227.

doi:10.1128/AAC.3.2.224

24. Almeida A De, Arez AP, Cravo PVL, Virgílio E. Analysis of genetic mutations associated with anti-malarial drug resistance in Plasmodium falciparum from the Democratic Republic of East Timor. 2009;7:1-7. doi:10.1186/1475-2875-8-59

25. Edaye S, Tazoo D, Bohle DS, Georges E. 3-Iodo-4-aminoquinoline derivative sensitises resistant strains of Plasmodium falciparum to chloroquine. *Int J Antimicrob Agents*. 2016;47(6):482-485. doi:10.1016/j.ijantimicag.2016.03.016

26. Molina-Cruz A, Canepa GE, Barillas-Mury C. Plasmodium P47: a key gene for malaria transmission by mosquito vectors. *Curr Opin Microbiol*. 2017;40:168-174. doi:10.1016/j.mib.2017.11.029

27. Talisuna AO, Langi P, Mutabingwa TK, Van Marck E, Speybroeck N, Egwang TG, Watkins WW, Hastings IM, D'Alessandro U, Intensity of transmission and spread of gene mutations linked to chloroquine and sulphadoxine-pyrimethamine resistance in falciparum malaria. *Int J Parasitol*. 2003;33(10):1051-1058. doi:10.1016/S0020-7519(03)00156-5

28. Bamaga OAA, Mahdy MAK, Lim YAL. Survey of chloroquine-resistant mutations in the Plasmodium falciparum pfcrt and pfmdr-1 genes in Hadhramout, Yemen. *Acta Trop*. 2015;149(November 2005):59-63. doi:10.1016/j.actatropica.2015.05.013

29. Chaijaroenkul W, Ward SA, Mungthin M, Johnson D, Owen A, Bray PG, Na-Bangchang K. Sequence and gene expression of chloroquine resistance transporter (pfcrt) in the association of in vitro drugs resistance of Plasmodium falciparum. *Malar J*. 2011;10:1-9. doi:10.1186/1475-2875-10-42

30. Kar NP, Chauhan K, Nanda N, Kumar A, Carlton JM, Das A. Comparative assessment on the prevalence of mutations in the Plasmodium falciparum drug-resistant genes in

two different ecotypes of Odisha state, India. *Infect Genet Evol*. 2016;41:47-55. doi:10.1016/j.meegid.2016.03.014

31. Chauhan K, Pande V, Das A. DNA sequence polymorphisms of the pfmdr1 gene and association of mutations with the pfcrt gene in Indian Plasmodium falciparum isolates. *Infect Genet Evol*. 2014;26:213-222. doi:10.1016/j.meegid.2014.05.033

32. Luzzatto L. Genes expressed in red cells could shape a malaria attack. *Lancet Haematol*. 2018;5(8):e322-e323. doi:10.1016/S2352-3026(18)30110-8

33. Malaria resistance genes in Everlasting flowers ? Rules for 3D protein – DNA. *Trends Genet*. 2001;17(9):9525-9525.

34. Akanbi OM, Odaibo AB, Olatoregun R, Ademowo AB. Role of malaria induced oxidative stress on anaemia in pregnancy. *Asian Pac J Trop Med*. 2010;3(3):211-214. doi:10.1016/S1995-7645(10)60011-9

35. Sibley CH. Understanding drug resistance in malaria parasites: Basic science for public health. *Mol Biochem Parasitol*. 2014;195(2):107-114. doi:10.1016/j.molbiopara.2014.06.001

36. Mutegeki E, John M, Mukaratirwa S. Acta Tropica Assessment of individual and household malaria risk factors among women in a South African village. *Acta Trop*. 2018;175(2017):71-77. doi:10.1016/j.actatropica.2016.12.007

37. Behera SK, Morioka Y, Ikeda T, Doi T, Ratnam JV, Nonaka M, Tsuzuki A, Imai C, Kim Y, Hashizume M, Iwami S, Kruger P, Maharaj R, Sweijd N, Minakawa N. Malaria incidences in South Africa linked to a climate mode in southwestern Indian Ocean. *Environ Dev*. 2018;27(June):47-57. doi:10.1016/j.envdev.2018.07.002

38. Maharaj R, Morris N, Seocharan I, Kruger P, Moonasar D, Mabuza A, Raswiswi E, Raman, Jaishree. The feasibility of malaria elimination in South Africa. 2012:1-10.

39. Pinheiro LCS, Boechat N, Ferreira MDLG, Júnior CCS, Jesus AML, Leite MMM, Souza NB, Krettli AU. Anti-Plasmodium falciparum activity of quinoline-sulfonamide hybrids. *Bioorganic Med Chem*. 2015;23(17):5979-5984. doi:10.1016/j.bmc.2015.06.056

40. Lombard MC, N'Da DD, Breytenbach JC, Smith PJ, Lategan CA. Synthesis, in vitro antimalarial and cytotoxicity of artemisinin- aminoquinoline hybrids. *Bioorganic Med Chem Lett*. 2011;21(6):1683-1686. doi:10.1016/j.bmcl.2011.01.103

41. Hansen FK, Sumanadasa SDM, Stenzel K, Duffy S, Meister S, Marek L, Schmetter R, Kuna K, Hamacher A, Mordmüller B, Kassack MU, Winzeler EA, Avery VM, Andrews KT, Kurz T. Discovery of HDAC inhibitors with potent activity against multiple malaria parasite life cycle stages. *Eur J Med Chem*. 2014;82:204-213. doi:10.1016/j.ejmech.2014.05.050

42. Kondaparla S, Manhas A, Dola VR, Srivastava K, Puri SK, Katti SB. Design, synthesis and antiplasmodial activity of novel imidazole derivatives based on 7-chloro-4-aminoquinoline. *Bioorg Chem*. 2018;80(June):204-211. doi:10.1016/j.bioorg.2018.06.012

43. Singh S, Agarwal D, Sharma K, Sharma M, Nielsen MA, Alifrangis M, Singh AK, Gupta RD, Awasthi SK.4-Aminoquinoline derivatives: Synthesis, in vitro and in vivo antiplasmodial activity against chloroquine-resistant parasites. *Eur J Med Chem*. 2016;122:394-407. doi:10.1016/j.ejmech.2016.06.033

Chapter 2

2. Literature Review

2.1. Life Cycle
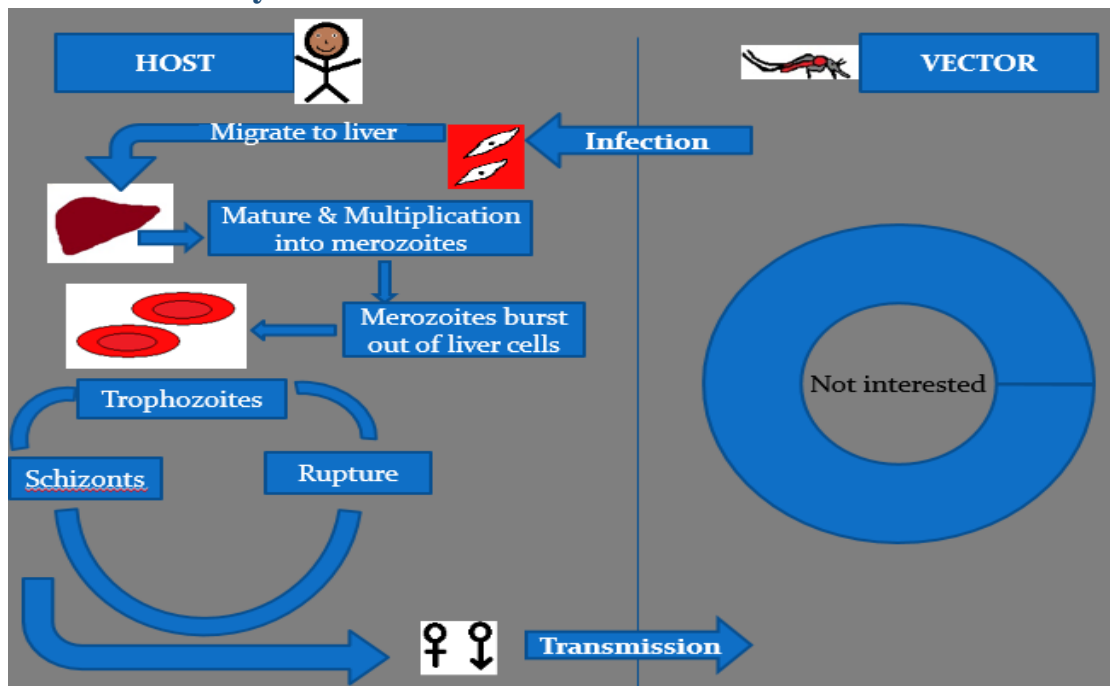
Figure 1: Shows life cycle of malaria parasite inside the host

Malaria life cycle involves two life forms the human (host) and the mosquito (vector). The cycle starts with the infected mosquito that bears sporozoites in its salivary gland when it feeds on humans it injects the saliva containing those sporozoites[1]. Malaria life cycle undergoes multiple stages of asexual reproduction within the human host. Inside the human bloodstream, these sporozoites migrate into the liver[2] within few minutes, and at this stage, there are no visible symptoms observed for about a week or two[3]. Inside the liver cells, these sporozoites mature and reproduce asexually in thousands of forms merozoites[4] and this stage is referred to as the pre-erythrocytic stage. Merozoites multiply asexually inside hepatocytes and burst out invading the blood cells erythrocytes[4]. Symptoms of malaria start to appear at this stage[5] such as fever, organ failure, and anaemia[6]. Inside the erythrocytes, the parasites evolve into different forms and some mature into gametocytes[2] and some evolve from trophozoites into schizonts then again into merozoites which causes the erythrocytes to rupture infecting more blood cells.

The parasites that developed into gametocytes carry on the life cycle of the parasite in the mosquito when it feeds on an infected human. Inside the mosquito, these gametocytes reproduce sexually into zygote that develops into ookinetes and then later into oocysts.[7] Oocysts grow and divide into sporozoites which invade mosquito's salivary gland[8].

2.2.   Classes of antimalarials

Malaria is a global threat which has led to researchers discovering different classes of antimalarials. The classes are characterized based on their activity against the parasite strains and can control the infections via prophylaxis, clinical cure, and radical cure. Each class of antimalarial targets a specific malarial life stage[9] within the human host, as some target liver and blood stage infections. Some of these classes suffer from short half-life[10] in terms of bioavailability within the human body. Most of them have severe side effects and *P. falciparum* has developed resistance to all of them. Presently, the focus is currently based on hybridizing these classes in order to enhance their therapeutic efficacy and bioavailability. Hybridization of these antimalarials with metals-based compounds is also a novel and excellent approach according to some recent research reports[9]. These classes of antimalarials used in hybridization include compounds on scheme 1.
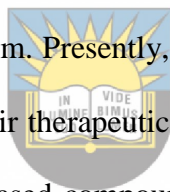
Aminoquinoline examples
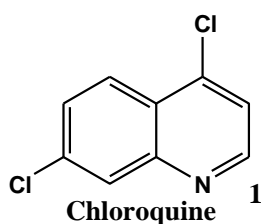
Chloroquine
Active against the blood stage parasite.
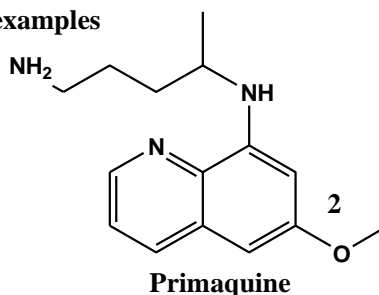
Primaquine
Active against the liver stage and also hinders reproduction of the gametocytes in the mosquito's digestive tract when it feeds from its host.

Diaminopyrimethamine example
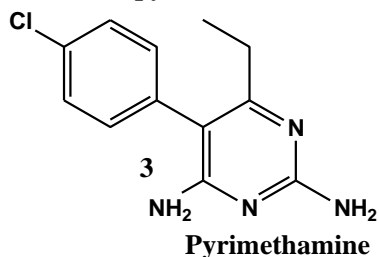
Pyrimethamine
Targets blood form of parasite and hinders the development of oocyst.

Cinchona alkoids example
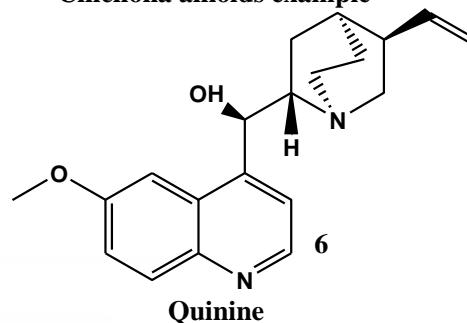
Quinine
Prevent gametocyte forms in the blood.

Biguanide example

Proguanil
Inhibit dihydrofolate reductase pathway used by the parasite for its survival.
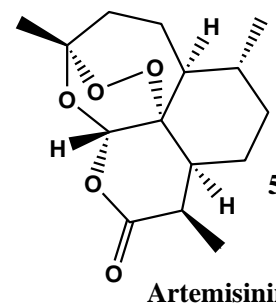
Artemisinin

Blood active schizontocidal drug which eliminates clinical attacks of malaria.

sulfonamides & salfones

Salfadoxine
Act similar to pyrimethamine blocking oocyst development.

Scheme 1: Antimalarial classes categorized according to their structure and activity against parasite's life stages

Each class of the antimalarials has its own exclusive mechanism of action and that of resistance against the *P. falciparum*. The focus of this research is on 4-aminoquinolines.

2.3.   4-aminoquinoline as antimalarial drugs

Quinoline-containing drugs especially 4-aminoquinoline have a successful history mostly in malaria treatment. 4-aminoquinolines like chloroquine, are weakly basic compounds with pKa ranged from 8-10, and reviews have stated that they can exist as protonated and unprotonated forms. The unprotonated forms of chloroquine easily traverse the biological membranes of the infected blood cells thus adjusting the pH to accumulate the parasites acidic food vacuole where they become protonated and diffuse out of the parasites food vacuole, whereas protonated form is less permeable and so diffusion across membrane is reduced, resulting in its accumulation in the digestive vacuole[11,12]. This indicates that chloroquine disturbs the parasites metabolism or feeding system as its site of action. Chloroquine has been widely used globally in places where malaria is endemic, but the resistance of malaria parasites to chloroquine has become the challenge for malaria treatment.

2.4.   Chloroquine mechanism of action

Many hypotheses have been reported in terms of chloroquine's mechanism of action. Some are associated with DNA binding, interference with hemoglobin detoxification by parasite, and the inhibition of various enzymes etc.[13] Chloroquine acts only in the erythrocyte stage of P. *falciparum* life cycle and is not active against liver and mature gametocyte stages[14]. With chloroquine being active solely on the erythrocyte stage indicates that its site of action is the disturbance of parasites metabolism. Chloroquine is a basic molecule which makes it accumulate in the permeable membrane of the parasites acid food vacuole[15]. Inside the food vacuole, chloroquine is protonated making it unable to diffuse out of the food vacuole, where it is believed to inhibit *P. falciparum* Export Protein1 (*Pf*EXP1) mediated by hematin degradation and also inhibit hemozoin formation[16–20]. Heme produced is the main target for chloroquine and its accumulation result in prolonged starvation of the parasite because it is

unable to feed on red blood cells. Chloroquine is also believed to form a complex with ferriprotoporphyrin IX (FPIX) allowing it to accumulate in the membrane fraction of infected cells, and this leads to disruption of cation homeostasis and parasite death[20].

2.5. Mechanism of resistance in Chloroquine

Mechanism of action for chloroquine is not fully understood[21]. Erythrocytes contain hemoglobin which contains heme responsible for its pigment (red color) and it is toxic to malaria parasites. The malaria parasite digests hemoglobin, polymerizing and detoxifying heme thereby converting it into hemozoin[18,22]. Chloroquine acts on the parasites digestive system by disturbing its metabolisms of hemoglobin degradation. Chloroquine resistance is linked with increased levels of drug efflux in which the parasite release the drug out of its digestive system at a faster rate in resistant strains[11,14,23,24]. Resistance to chloroquine is accompanied by multiple gene mutations. Many researchers have also linked chloroquine resistance with mutations in the gene encoding the protein (*PfCRT*), *P. falciparum* chloroquine resistant transporter, a member of the drug transporter, resulting in a decreased in drug accumulation inside the parasites digestive system, the site of action for chloroquine[10,17,25–27]. Lack of access for chloroquine to the targeted binding site is also assumed to be another cause of resistance[28]. Moreover, charge-loss mutation K76T, frequently presented as 2 single mutations (K76N & K76I) also affect drug accumulation into the parasite[26].
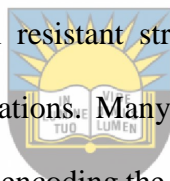
2.6. Modes of action of hybrid compounds containing 4-aminoquinoline
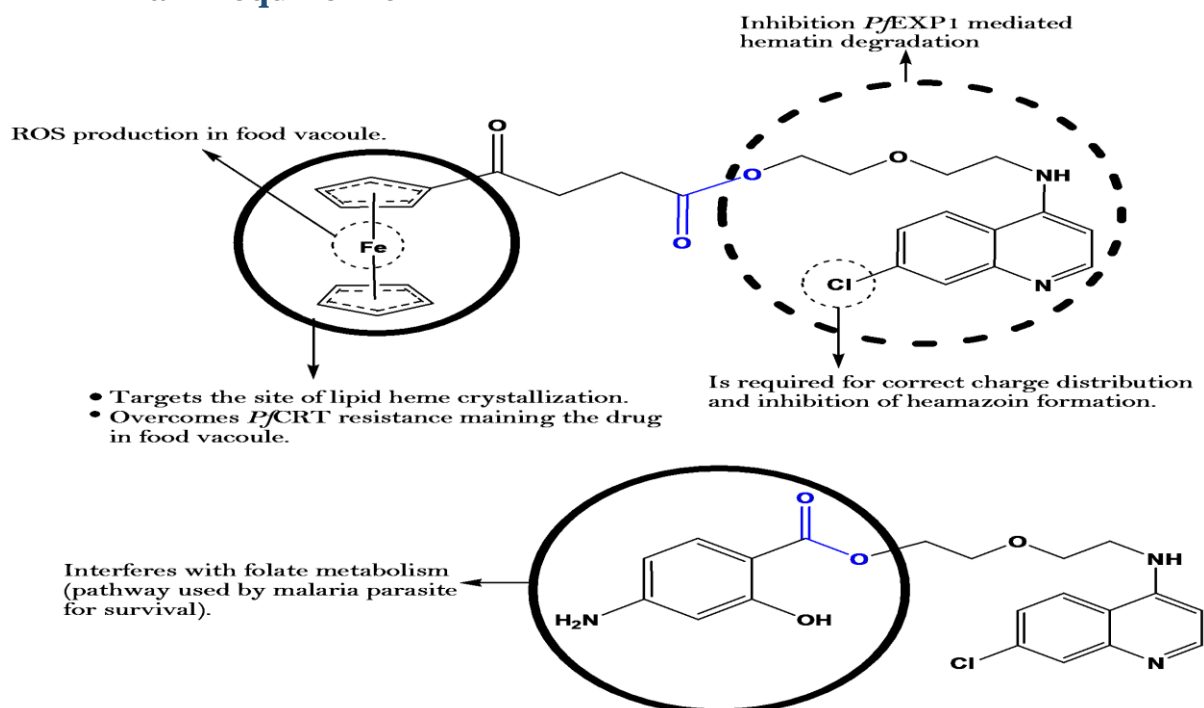
Scheme 2: Modes of action for the selected molecules.

Reactive oxygen species (ROS) is produced by human bodies with innate immunity to fight and attack foreign components within the body. ROS effect in malaria is not well understood and some reports have illustrated its pathology and benefit which is determined by its amount and region of production[30,31]. During host infection by the malarial parasite, causes oxidative stress resulting in increased production of ROS[32], which eventually cause an imbalance between the activity of antioxidants and oxidizing species formation, activated during hemoglobin degradation[33] in the parasite and host's neutrophils[34]. The imbalance causes oxidative stress which is an important immunity used by the host when responding to foreign attack or infections, and in malaria, it leads to parasite death[30]. Regardless of ROS being beneficial in clearance of the parasite, it is also toxic to the host's cells[35]. However, antioxidants enzymes such as catalase and superoxide dismutase (SOD) play an important role in detoxifying hydrogen peroxide (H_2O_2) into water and oxygen and also in the transformation of superoxides (O_2^-) into H_2O_2[30,35]. Dihydrofolate reductase (*dhfr*), an enzyme responsible for the

reduction of dihydrofolate to tetrahydrofolate in the folate pathway is a target of many antimalarials[36–38]. *Dhfr* inhibition is essential in blocking DNA synthesis and amino acid metabolism important for parasite's survival, and this results in cell death[39]. *Pfcrt,* as explained before*,* is a resistant transport protein used by the parasite to efflux drugs out of its system.

2.7. Hybrid compounds

Combination therapy has shown great effectiveness against drug resistance, which is common in most antimalarials and is undoubtedly the best therapy[40,41]. The design of hybrid compounds with antimalarial activity has many benefits such as reduced risk of drug-drug interaction, patient compliance, decreased toxicity, better absorption and distribution inside the body, and they are metabolized and eliminated as a waste product at a single rate. Muregi and Ishih classified them as "conjugates in which the pharmacophores are separated by a linker group that is distinct; cleavage conjugates in which the pharmacophores are separated by a metabolized linker; fused hybrid molecules with reduced linker between the pharmacophores, resulting in the closeness of the pharmacophores and merged hybrid in which the framework is merged"[10,23]. In addition, the hybrid compounds pharmacophores are joined covalently giving them the advantage of multiple stage activity against malarial parasite inside the host[18,42,25]. M. Lodige and L. Heirsch concluded that "hybrid molecules can offer the advantages of a combination therapy together with improved pharmacokinetic profiles and potential enhanced antimalarial activity against resistant strains, however, they have less flexibility when administered orally"[43]. This statement can be proved or supported by Lipinski's rule of five where he states that molecules with a molecular mass greater than 500 g/mol are hardly administered orally.

2.8. Ferrocene and quinoline-ferrocene-based hybrids as antimalarials
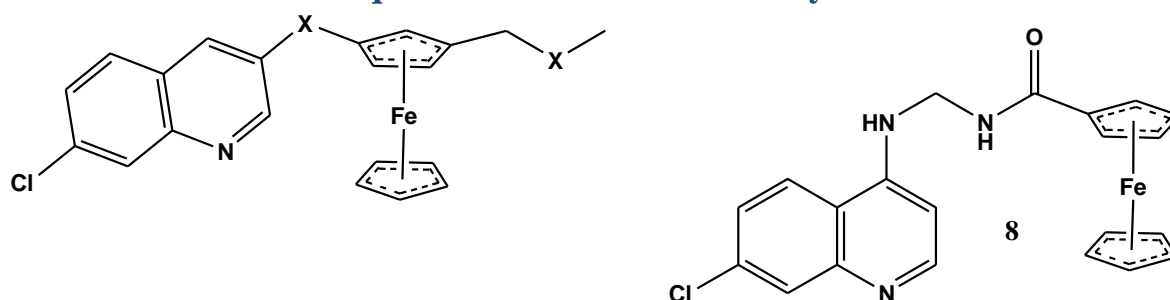
7-X= Amine
9-X= Thiosemicarbazones
11-X= 1,2,3,5-diisopropylidene glucofuranose moiety
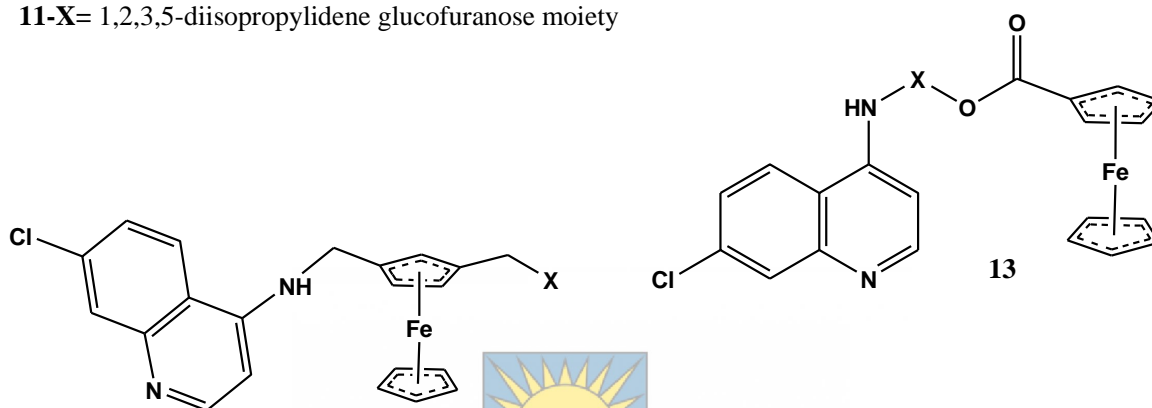
10-X= 1,2,4-Trioxane
12a-X= Diisopropylidede-protected d 6-amino-6-deoxyglucofuranose
12b-X= 6-amino-6-deoxygalactopyranose

Scheme 3: Ferrocene-quinoline hybrids

Hybrid molecules having quinoline and ferrocene moiety have been reported as potent antimalarials. One example of a quinoline-ferrocene hybrid is ferroquine, **7** which was reported to be potent-and active against *P. falciparum* isolates when compared to other antimalarial such as piperaquine, chloroquine etc.[44]. Nonetheless, artesunate was more potent when compared to ferroquine[44]. Ferroquine mechanism of action is via the blockage *Pfcrt* and it acts as an agent reversing resistance because of its lipophilic properties[44,45]. Domarle et al. synthesized analogs of quinoline-ferrocene and they inhibited the parasite resistance this was linked to the covalent bonding of ferrocene to chloroquine. Analogs of tartaric acid compared to chloroquine drug were reported to be very effective at low concentrations[46]. Mechanism of action of ferrocene

18

moiety in the hybrid compound is to inhibit resistance against chloroquine without increasing the activity of chloroquine[46]. Biot et al. prepared an analog of quinoline-ferrocene from aminoquinoline and ferrocene. These analogs exhibited an effective antimalarial activity against chloroquine-resistant strains Dd2 *in vitro*[47]. N'Da et al. synthesized quinoline–ferrocene hybrid, **8** with selected linkers between 4-aminoquinolines and ferrocene carboxaldehyde. These hybrid compounds were prepared via amination reaction of 4,7-dichloroquinolines and selected diamines[48]. Hybrid compounds containing rigid linkers were reported to be inactive biologically when compared to hybrid compounds containing flexible linkers against Dd2 and D10 strains of the malarial parasite. It was observed that the hybrid compound with a 3-aminopropyl methylamine linker was the most effective antimalarial compound with $IC_{50} = 0.008$ vs. 0.148 μM, i.e., 19-fold higher than the equimolar chloroquine–ferrocene combination with $IC_{50} = 3.7$ vs. 41 ng/mL, and tenfold more active against the Dd2 strain[48]. Biot et al. synthesized ferroquine derivatives that mimic hydroxychloroquine[49]. These derivatives were 6-fold more effective when compared to that of chloroquine and 1.5 fold less effective when compared to ferroquine against all isolates and strains of malarial parasite *in vitro*[49]. These hybrid compounds were also reported to be potential antimalarials in regions with co-infection of malaria with SARS and HIV [49]. Biot et al. also synthesized ferrocene-quinoline hybrid molecules that contain thiosemicarbazones, **9**[50]. Aminoquinoline structure was found to improve the delivery of the hybrid drug into the parasite's digestive system over the parasitic cysteine protease falcipain-2 and *in vitro* assay on *P. falciparum.* The ferrocene moiety preserved the activity of the 4-aminoquinoline in the hybrid molecule[50]. Chavain et al. prepared ferroquine-quinoline hybrids linked to glutathione reductase inhibitor via an amide bond. The activity of antimalarial hybrid compounds was significant when compared to chloroquine and ferroquine[51]. *In vitro* evaluation on K1 and NF54, parasite's chloroquine resistant and sensitive strains revealed a reduced antimalarial activity of the hybrids. The

decrease in activity of the hybrid compounds was attributed to the amide bond cleavage of the hybrid compounds and the side chain when they react in the parasite's digestive system, revealing that the design of hybrid molecules has an effect on their antimalarial activity[51]. Bellot et al. prepared trioxaferroquines containing ferroquine covalently bonded to 1,2,4-trioxane **10**[52]. The compound, **10** exhibited well *in vitro* antiplasmodial activity against chloroquine-resistant strains of *P. falciparum*[52]. Herrmann et al. prepared hybrid molecule, **11** from chloroquine derivative, ferrocene scaffold and a 1,2,3,5-(diisopropylidene)-α-D-glucofuranose moiety with good *in vitro* antiplasmodial activity against K1 and Dd2 strains of *P. falciparum*[53]. In another research reported by Herrmann et al. conjugated ferrocene scaffolds via ether linker with either 7-chloroquinoline followed by incorporation of diisopropylidene-protected 6-amino-6-deoxyglucofuranose or 6-amino-6-deoxygalactopyranose by reductive amination to produce hybrid compounds **12a** and **12b**[54]. The carbohydrate moiety improved the antimalarial activity of the molecule with an $IC_{50} = 0.77$ µM[54]. The activity of antimalarials was effective against chloroquine-resistant Dd2 strains when compared with chloroquine sensitive D10 strains[54]. Sallas et al. prepared ferrocenophane derivatives of ferroquine with a significant potent antimalarial activity against chloroquine-resistant strain and sensitive strain. The advantage of these derivatives resulting from their solubility in fats, non-polar solvents and lipids enhanced their potential to overcome drug resistance[55]. Ferroquine is known by its unique conformation resulting from the presence of intramolecular hydrogen bond under non-polar conditions which increases its permeability through the *P. falciparum* membrane, causing an increased level of the drug inside the parasite's digestive system, high lipophilicity at pH 7.4, and weak base properties. It is responsible for the inhibition of self-assembly of the hemozoin crystal which also generates ROS, making lipid peroxidation and the alteration of food vacuole[56]. The presence of the intra-molecular hydrogen bond gives ferroquine the capability to overcome resistance mechanisms by avoiding cross-resistance[56]. David et al. also

prepared 4-aminoquinoline compound, **13** conjugated to ferrocene molecule by the use of ester bonding. The compounds with a ferrocenylformic acid moiety presented good activity against chloroquine-resistant and sensitive strains of the malarial parasite. Nonetheless, chloroquine showed superior antimalarial activity against chloroquine-sensitive strains. The compound that presented a better antimalarial activity exhibited $IC_{50} = 0.13$ mM in chloroquine-resistant strains as well as 2.5-folds greater when compared to chloroquine with $IC_{50} = 0.34$ mM[57].

2.9. Examples of previously prepared hybrid compounds

For a compound to be considered as potent or effective, it must show less IC_{50} values compared to that of chloroquine[58–60]. "The low value of resistance index indicates the activity of the compound regardless of the susceptibility to the parasite strains, whereas the large values indicate the loss of activity due to drug resistance", as shown in **Table 1**[61]. Most of the chloroquine-based hybrid compounds showed great results both *in vitro* and *in vivo*, but Compound B presented better results *in vitro* only [18,40,62].

University of Fort Hare
Together in Excellence
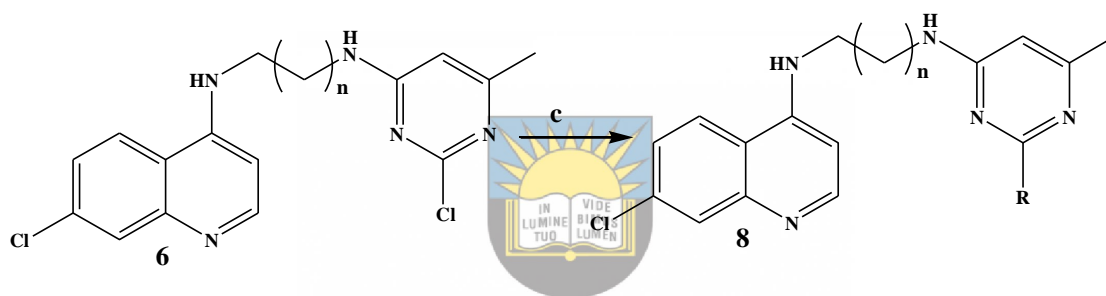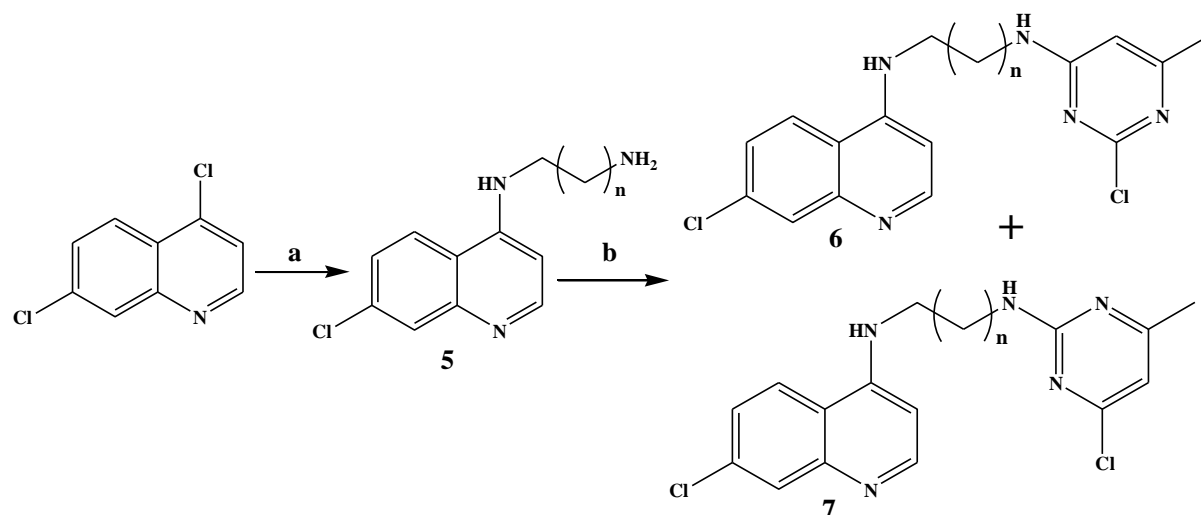
n= 1
 = 2
 = 5
R= piperidine
a= Diaminoalkanes
b= 2,4-Dichloro-6-methyl-pyrimidine

Scheme 4: Synthesis of 4-aminoquinoline pyrimidine-based hybrids[63].

Table 1: in vitro antimalarial activity of 4-aminoquinoline-pyrimidine hybrids[63].

Entry		P. falciparum D6		P. falciparum W2		Vero Cells
		$IC_{50}\,(\mu M)^b$	(S.I)	$IC_{50}\,(\mu M)$	(S.I)	
6	n=1	0.16 ± 0.05	$>3.70 \times 10^2$	0.5 ± 0.2	$>1.20 \times 10^2$	NC
	n=2	0.33 ± 0.02	$>1.84 \times 10^2$	0.70 ± 0.04	>85	NC
	n=5	0.44 ± 0.02	74.3	0.54 ± 0.00	60.6	32.7 ± 1.8

7	n=1	0.21 ± 0.06	2.05×10^2	0.81 ± 0.10	53.1	43.0 ± 0.0
	n=2	0.24 ± 0.03	$>2.50 \times 10^2$	1.17 ± 0.07	>51.3	NC
	n=5	0.14 ± 0.03	3.53×10^2	0.58 ± 0.01	85.2	49.4 ± 6.2
8	n=1	ND	ND	ND	ND	ND
	n=2	0.02 ± 0.001	$>3.00 \times 10^3$	0.21 ± 0.003	$>2.85 \times 10^2$	NC
	n=5	0.06 ± 0.01	1.46×10^2	0.10 ± 0.02	88	8.8 ± 0.5
Chloroquine		0.04 ± 0.004	$>1.50 \times 10^3$	0.39 ± 0.04	$>1.52 \times 10^2$	NC

ND; not determined, [b]; mean of two independent experiment values ± standard deviation, SI; selectivity index and IC_{50}; the concentration that causes growth inhibition of 50%.

Synthesis of "Siamese-twin hybrid" compound A at 120◦C (82%). Compound A
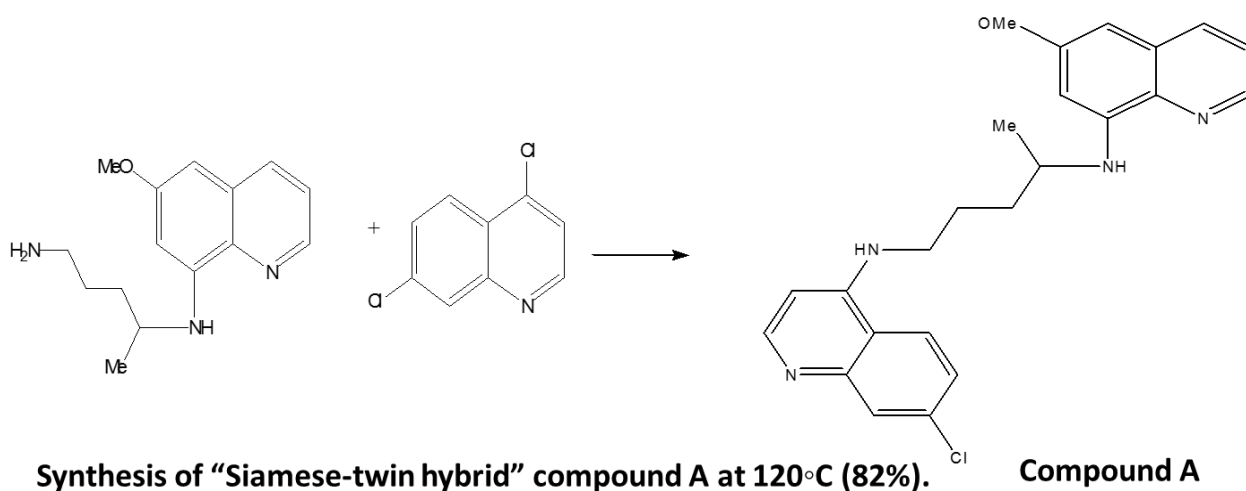
Scheme 5: Synthesis of "Siamese-twin hybrid" compound A at 120°C (82%).

The above hybrid molecule was examined for its antimalarial activity at all the life stages of the parasite within the host *in vitro* and *in vivo*. According to (lodge M 2013), Compound A showed significant inhibitory effects against *Plasmodium* liver and blood stage parasites *in vitro* and *in vivo*.
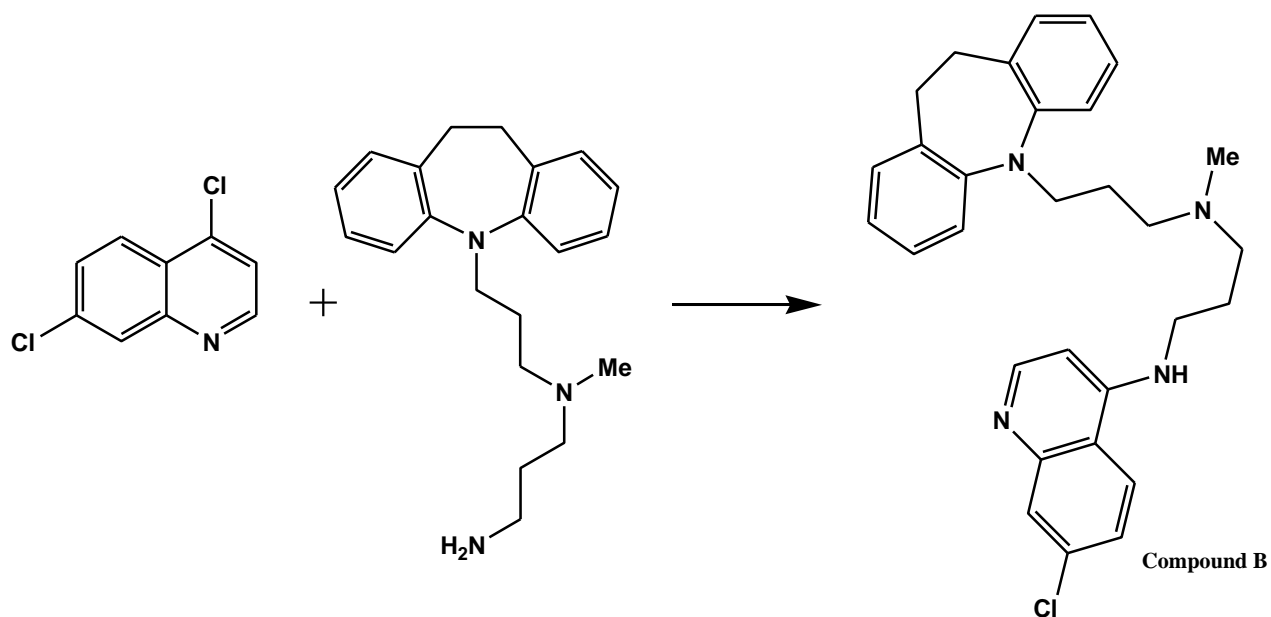
Scheme 6: Synthesis of aminoquinoline-imipramine

Synthesis of aminoquinoline-imipramine hybrid compound B was successful. According to (Pretorius I.S, Prof Breytenbach J.C 2013), the structure of the synthesized compound was validated by means of NMR and MS spectroscopy. The antiplasmodial activity screening showed that all the hybrid compounds were active against the chloroquine-sensitive D10 strain of *P. falciparum*. None of the synthesized compounds showed better activity than chloroquine in chloroquine-resistant strains.
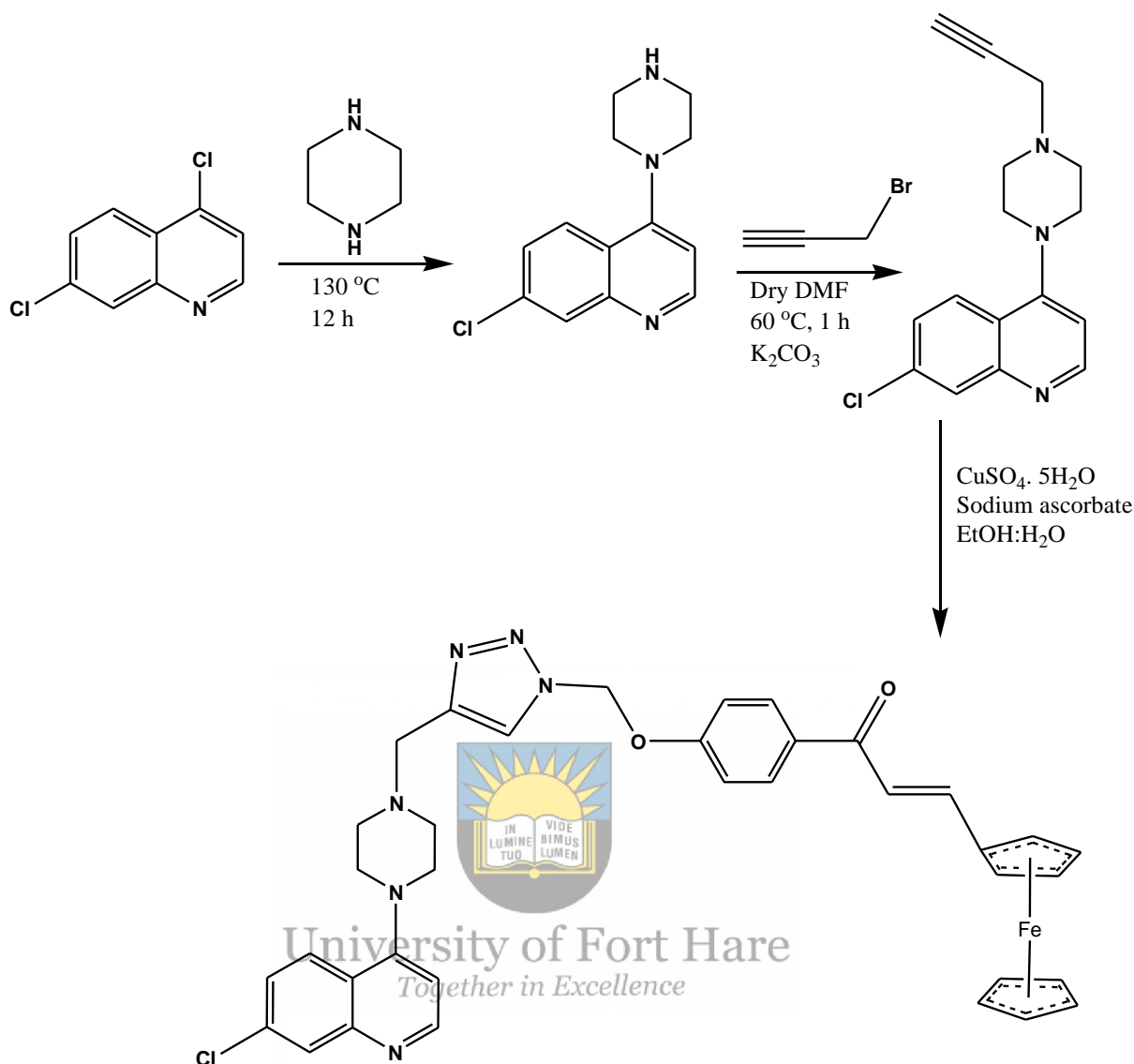
Scheme 7: Synthesis of piperazine-linked 7-chloroquinoline-ferrocenylchalcone conjugates[64].

The activity of the above compound was tested using *in vitro* antiplasmodial analysis and was compared with chloroquine activity. The compound showed good antimalarial activity with IC_{50} values ranging between 2.55-5.08µM. "The compound exhibited a molecular ion peak at 686.1849 in its high-resolution mass spectrum (HRMS). Its ^{1}H NMR spectrum showed the presence of a singlet at 4.18 ppm corresponding to 5H (cyclopentadiene ring of ferrocene) along with singlets at 4.50 ppm (4H) and 4.59 ppm (2H) due to the presence of ferrocene ring and methylene protons. The presence of two singlets at 2.86 ppm (4H) and 3.29 ppm (4H)

corresponding to the piperazine ring protons and a characteristic singlet at 8.07 ppm (1H)

corresponding to the triazole ring proton supported the assigned structure"[64].

References

1. Molina-Cruz A, Canepa GE, Barillas-Mury C. Plasmodium P47: a key gene for malaria transmission by mosquito vectors. *Curr Opin Microbiol*. 2017;40:168-174. doi:10.1016/j.mib.2017.11.029

2. Cowman AF, Tonkin CJ, Tham WH, Duraisingh MT. The Molecular Basis of Erythrocyte Invasion by Malaria Parasites. *Cell Host Microbe*. 2017;22(2):232-245. doi:10.1016/j.chom.2017.07.003

3. Hoffman SL, Vekemans J, Richie TL, Duffy PE. The march toward malaria vaccines. *Vaccine*. 2015;33:D13-D23. doi:10.1016/j.vaccine.2015.07.091

4. Farrow RE, Green J, Katsimitsoulia Z, Taylor WR, Holder AA, Molloy JE. The mechanism of erythrocyte invasion by the malarial parasite, Plasmodium falciparum. *Semin Cell Dev Biol*. 2011;22(9):953-960. doi:10.1016/j.semcdb.2011.09.022

5. Cowman AF, Crabb BS. Invasion of red blood cells by malaria parasites. *Cell*. 2006;124(4):755-766. doi:10.1016/j.cell.2006.02.006

6. Flammersfeld A, Lang C, Flieger A, Pradel G. International Journal of Medical Microbiology Phospholipases during membrane dynamics in malaria parasites. *Int J Med Microbiol*. 2018;308(1):129-141. doi:10.1016/j.ijmm.2017.09.015

7. Ashley EA, Pyae Phyo A, Woodrow CJ. Malaria. *Lancet*. 2018;391. doi:10.1016/S0140-6736(18)30324-6

8. Khan SM, Waters AP. Malaria parasite transmission stages: An update. *Trends Parasitol*. 2004;20(12):575-580. doi:10.1016/j.pt.2004.10.001

9. Wu L, Rathi B, Singh S, Rawat M, Chhikara BS. Multistage inhibitors of the malaria parasite : Emerging hope for chemoprotection and malaria eradication.

2018;(September 2017):1-25. doi:10.1002/med.21486

10. Muregi FW, Ishih A. Next-generation antimalarial drugs: Hybrid molecules as a new strategy in drug design. *Drug Dev Res*. 2010;71(1):20-32. doi:10.1002/ddr.20345

11. Foley M, Tilley L. Quinoline Antimalarials : Mechanisms of Action and Resistance and Prospects for New Agents. *Pharmacol. Ther.* 1998;79(1):55-87.

12. Hawley SR, Bray PG, Neill PMO, Park BK, Ward SA. The Role of Drug Accumulation in + Aminoquinoline Antimalarial Potency The structures. 1996;52(January):723-733.

13. Stoli I, Juki M, Opa T, Star K. European Journal of Medicinal Chemistry New quinoline-arylamidine hybrids : Synthesis, DNA / RNA binding and antitumor activity Luka Krstulovi. 2017;137:196-210. doi:10.1016/j.ejmech.2017.05.054

14. Asia S, Pacific S, America L, Atlas WM. 2008:1-152.

15. Bray PG, Saliba KJ, Davies JD, Spiller DG, White RH, Kirk K, Ward SA. Distribution of acridine orange fluorescence in Plasmodium falciparum -infected erythrocytes and its implications for the evaluation of digestive vacuole pH. *Mol Biochem Parasitol.* 2002;119:301-304.

16. Lisewski AM, Quiros JP, Mittal M, Putluri N, Sreekumar A, Haeggström JZ, Lichtarge O. Potential role of Plasmodium falciparum exported protein 1 in the chloroquine mode of action. *Int J Parasitol Drugs Drug Resist*. 2018;8(1):31-35. doi:10.1016/j.ijpddr.2017.12.003

17. Kumar S, Bhardwaj TR, Prasad DN, Singh RK. Drug targets for resistant malaria: Historic to future perspectives. *Biomed Pharmacother*. 2018;104(March):8-27. doi:https://doi.org/10.1016/j.biopha.2018.05.009

18. Oliveira R, Miranda D, Magalhães J, Capela R, Perry MJ, O'Neill PM, Moreira R, Lopes F. From hybrid compounds to targeted drug delivery in antimalarial therapy. *Bioorganic Med Chem*. 2015;23(16):5120-5130. doi:10.1016/j.bmc.2015.04.017

19. Lehane AM, McDevitt CA, Kirk K, Fidock DA. Degrees of chloroquine resistance in Plasmodium - Is the redox system involved? *Int J Parasitol Drugs Drug Resist*. 2012;2:47-57. doi:10.1016/j.ijpddr.2011.11.001

20. Ginsburg H, Krugliak M. Chloroquine - Some open questions on its antimalarial mode of action and resistance. *Drug Resist Updat*. 1999;2(3):180-187. doi:10.1054/drup.1999.0085

21. Bray PG, Ward SA, O'Neill PM. Quinolines and Artemisinin: Chemistry, Biology and History. *Malar Drugs, Dis Post-genomic Biol*. 2005;1:3-38. doi:10.1007/3-540-29088-5_1

22. Foley M, Tilley L. Quinoline antimalarials: Mechanisms of action and resistance. *Int J Parasitol*. 1997;27(2):231-240. doi:10.1016/S0020-7519(96)00152-X

23. Nqoro X, Tobeka N, Aderibigbe BA. Quinoline-based hybrid compounds with antimalarial activity. *Molecules*. 2017;22(12). doi:10.3390/molecules22122268

24. Griffin CE, Hoke JM, Samarakoon U, Duan J, Mu J, Ferdig MT, Warhurst DC, Cooper RA. Mutation in the Plasmodium falciparum CRT protein determines the stereospecific activity of antimalarial Cinchona alkaloids. *Antimicrob Agents Chemother*. 2012;56(10):5356-5364. doi:10.1128/AAC.05667-11

25. Hu YQ, Gao C, Zhang S, Xu L, Xu Z, Feng LS, Wu X, Zhao F. Quinoline hybrids and their antiplasmodial and antimalarial activities. *Eur J Med Chem*. 2017;139:22-47. doi:10.1016/j.ejmech.2017.07.061

26. Lynch D. 4-aminoquinolines as Antimalarial Drugs. *Trinity Student Sci Rev*.

2016;2(September 2015):196-210. https://trinityssr.files.wordpress.com/2016/06/4th-chem.pdf.

27.   Salem M, Ahmedou O, Lekweiry KM, Bouchiba H, Pascual A, Pradines B, Ould A, Salem, M, Briolant S, Basco LK. Characterization of Plasmodium falciparum genes associated with drug resistance in Hodh Elgharbi, a malaria hotspot near Malian – Mauritanian border. *Malar J*. 2017:1-9. doi:10.1186/s12936-017-1791-2

28.   Olliaro P. Mode of action and mechanisms of resistance for antimalarial drugs. 2001;89.

29.   Soni R, Sharma D, Rai P, Sharma B, Bhatt TK. Signaling strategies of malaria parasite for its survival, proliferation, and infection during erythrocytic stage. *Front Immunol*. 2017;8(MAR). doi:10.3389/fimmu.2017.00349

30.   Percário S, Moreira DR, Gomes BAQ, Ferreira MES, Gonçalves ACM, Laurindo PSOC, Vilhena TC, Dolabela MF, Green MD.Oxidative stress in Malaria. *Int J Mol Sci*. 2012;13(12):16346-16372. doi:10.3390/ijms131216346

31.   Postma NS, Mommers EC, Eling WM, Zuidema J. Oxidative stress in malaria; implications for prevention and therapy. *Pharm World Sci*. 1996;18(4):121-129. http://www.ncbi.nlm.nih.gov/pubmed/8873227. Accessed October 15, 2018.

32.   Akanbi OM, Odaibo AB, Olatoregun R, Ademowo AB. Role of malaria induced oxidative stress on anaemia in pregnancy. *Asian Pac J Trop Med*. 2010;3(3):211-214. doi:10.1016/S1995-7645(10)60011-9

33.   Rahbari M, Rahlfs S, Jortzik E, Bogeski I, Becker K. H 2 O 2 dynamics in the malaria parasite Plasmodium falciparum. 2017:1-23. doi:10.1371/journal.pone.0174837

34.   Cui L, Miao J, Cui L. Cytotoxic Effect of Curcumin on Malaria Parasite Plasmodium falciparum: Inhibition of Histone Acetylation and Generation of Reactive Oxygen

Species. *Antimicrob Agents Chemother*. 2007;51(2):488-494. doi:10.1128/AAC.01238-06

35.   Bahia AC, Oliveira JHM, Kubota MS, Araújo HRC, Lima JBP, Ríos-Velásquez CM, Lacerda MVG, Oliveira PL, Traub-Csekö YM, Pimenta PFP. The Role of Reactive Oxygen Species in Anopheles aquasalis Response to Plasmodium vivax Infection. *PLoS One*. 2013;8(2):e57014. doi:10.1371/journal.pone.0057014

36.   Bilsland E, Van Vliet L, Williams K, Feltham J, Carrasco MP, Fotoran WL, Cubillos EFG, Wunderlich G, Grøtli M, Hollfelder F, Jackson V, King RD, Oliver SG. Plasmodium dihydrofolate reductase is a second enzyme target for the antimalarial action of triclosan. *Sci Rep*. 2018;8(1):1-8. doi:10.1038/s41598-018-19549-x

37.   Talisuna AO, Nalunkuma-Kazibwe A, Langi P, Mutabingwa, TK, Watkins, WW, Marck EV, Egwang TG, D'Alessandro U. Two mutations in dihydrofolate reductase combined with one in the dihydropteroate synthase gene predict sulphadoxine-pyrimethamine parasitological failure in Ugandan children with uncomplicated falciparum malaria. *Infect Genet Evol*. 2004;4(4):321-327. doi:10.1016/j.meegid.2004.04.002

38.   Tran PN, Tate CJ, Ridgway MC, Saliba KJ, Kirk K, Maier AG. Human dihydrofolate reductase influences the sensitivity of the malaria parasite Plasmodium falciparum to ketotifen – A cautionary tale in screening transgenic parasites. *Int J Parasitol Drugs Drug Resist*. 2016;6(3):179-183. doi:10.1016/j.ijpddr.2016.09.003

39.   Hecht D, Tran J, Fogel GB. Structural-based analysis of dihydrofolate reductase evolution. *Mol Phylogenet Evol*. 2011;61(1):212-230. doi:10.1016/j.ympev.2011.06.005

40.   Singh S, Agarwal D, Sharma K, Sharma M, Nielsen MA, Alifrangis M, Singh AK, Gupta RD, Awasthi SK.4-Aminoquinoline derivatives: Synthesis, in vitro and in vivo

antiplasmodial activity against chloroquine-resistant parasites. *Eur J Med Chem*. 2016;122:394-407. doi:10.1016/j.ejmech.2016.06.033

41. Srivastava V, Lee H. Chloroquine-based hybrid molecules as promising novel chemotherapeutic agents. *Eur J Pharmacol*. 2015;762:472-486. doi:10.1016/j.ejphar.2015.04.048

42. Chopra R, Chibale K, Singh K. Pyrimidine-chloroquinoline hybrids: Synthesis and antiplasmodial activity. *Eur J Med Chem*. 2018;148:39-53. doi:10.1016/j.ejmech.2018.02.021

43. Lodige M, Hiersch L. Design and Synthesis of Novel Hybrid Molecules against Malaria. *Int J Med Chem*. 2015;2015:458319. doi:10.1155/2015/458319

44. Barends M, Jaidee A, Khaohirun N, Singhasivanon P, Nosten F. In vitro activity of ferroquine (SSR 97193) against Plasmodium falciparum isolates from the Thai-Burmese border. *Malar J*. 2007;6(1):81. doi:10.1186/1475-2875-6-81

45. Christophe B, Donatella T, Isabelle FB, Lucien AM, Mlandzeni B, Guy N, Jacques SB, Nicoletta B, Piero O, Timothy JE. Insights into the Mechanism of Action of Ferroquine. Relationship between Physicochemical Properties and Antiplasmodial Activity. 2005. doi:10.1021/MP0500061

46. Domarle O, Blampain G, Agnaniet H, Nzadiyabi T, Lebibi J, Brocard J, Maciejewski L, Biot C, Georges AJ, Millet P. In vitro antimalarial activity of a new organometallic analog, ferrocene-chloroquine. *Antimicrob Agents Chemother*. 1998;42(3):540-544. http://www.ncbi.nlm.nih.gov/pubmed/9517929. Accessed October 11, 2018.

47. Biot C, Dessolin J, Ricard I, Dive D. Easily synthesized antimalarial ferrocene triazacyclononane quinoline conjugates. 2004;689:4678-4682. doi:10.1016/j.jorganchem.2004.04.036

48. N'Da DD, Smith PJ. Synthesis, in vitro antiplasmodial and antiproliferative activities of a series of quinoline–ferrocene hybrids. *Med Chem Res*. 2014;23(3):1214-1224. doi:10.1007/s00044-013-0748-4

49. Biot C, Daher W, Chavain N, Fandeur T, Khalife J, Dive D, De Clercq, E. Design and Synthesis of Hydroxyferroquine Derivatives with Antimalarial and Antiviral Activities. *J Med Chem*. 2006;49(9):2845-2849. doi:10.1021/jm0601856

50. Biot C, Pradines B, Ne Sergeant M-H, Gut J, Rosenthal PJ, Chibale K. Design, synthesis, and antimalarial activity of structural chimeras of thiosemicarbazone and ferroquine analogues. 2007. doi:10.1016/j.bmcl.2007.10.003

51. Chavain N, Davioud-Charvet E, Trivelli X, Mbeki L, Rottmann M, Brun R, Biot C. Antimalarial activities of ferroquine conjugates with either glutathione reductase inhibitors or glutathione depletors via a hydrolyzable amide linker. 2009. doi:10.1016/j.bmc.2009.10.008

52. Bellot F, Coslédan F, Vendier L, Brocard J, Meunier B, Robert A. Trioxaferroquines as New Hybrid Antimalarial Drugs. *J Med Chem*. 2010;53(10):4103-4109. doi:10.1021/jm100117e

53. Herrmann C, Salas PF, Cawthray JF, de Kock C, Patrick, BO, Smith PJ, Adam MJ, Orvig C. 1,1′-Disubstituted Ferrocenyl Carbohydrate Chloroquine Conjugates as Potential Antimalarials. *Organometallics*. 2012;31(16):5736-5747. doi:10.1021/om300354x

54. Herrmann C, Salas PF, Patrick BO, de Kock C, Smith PJ, Adam MJ, Orvig C. Modular Synthesis of 1,2- and 1,1′-Disubstituted Ferrocenyl Carbohydrate Chloroquine and Mefloquine Conjugates as Potential Antimalarial Agents. *Organometallics*. 2012;31(16):5748-5759. doi:10.1021/om300392q

55. Salas PF, Herrmann C, Cawthray JF, Nimphius C, Kenkel A, Chen J, de Kock C, Smith PJ, Patrick BO, Adam MJ, Orvig C. Structural Characteristics of Chloroquine-Bridged Ferrocenophane Analogues of Ferroquine May Obviate Malaria Drug-Resistance Mechanisms. *J Med Chem*. 2013;56(4):1596-1613. doi:10.1021/jm301422h

56. Biot C, Nosten F, Fraisse L, Ter-Minassian D, Khalife J, Dive D. The antimalarial ferroquine: from bench to clinic. *Parasite*. 2011;18(3):207-214. doi:10.1051/parasite/2011183207

57. N'Da DD, Breytenbach JC, Smith PJ, Lategan C. Synthesis and in vitro antiplasmodial activity of quinoline-ferrocene esters. *Arzneimittelforschung*. 2011;61(6):358-365. http://www.ncbi.nlm.nih.gov/pubmed/21827047. Accessed October 11, 2018.

58. Murugan K, Raichurkar A V, Rahman F, Khan N, Iyer PS. Bioorganic & Medicinal Chemistry Letters Synthesis and in vitro evaluation of novel 8-aminoquinoline – pyrazolopyrimidine hybrids as potent antimalarial agents. *Bioorg Med Chem Lett*. 2015;25(5):1100-1103. doi:10.1016/j.bmcl.2015.01.003

59. Lombard MC, N'Da DD, Breytenbach JC, Smith PJ, Lategan CA. Synthesis, in vitro antimalarial and cytotoxicity of artemisinin- aminoquinoline hybrids. *Bioorganic Med Chem Lett*. 2011;21(6):1683-1686. doi:10.1016/j.bmcl.2011.01.103

60. Terzić N, Konstantinović J, Tot M, Burojević J, Djurković-Djaković O, Srbljanović J, Štajner T, Verbić T, Zlatović M, Machado M, Albuquerque IS, Prudêncio M, Sciotti RJ, Pecic S, D'Alessandro S, Taramelli D, Šolaja BA. Reinvestigating Old Pharmacophores: Are 4-Aminoquinolines and Tetraoxanes Potential Two-Stage Antimalarials? *J Med Chem*. 2016;59(1):264-281. doi:10.1021/acs.jmedchem.5b01374

61. Maurya SS, Khan SI, Bahuguna A, Kumar D, Rawat DS. Synthesis, antimalarial activity, heme binding and docking studies of N-substituted 4-aminoquinoline-

pyrimidine molecular hybrids. *Eur J Med Chem*. 2017;129:175-185. doi:10.1016/j.ejmech.2017.02.024

62.   Reddy PL, Khan SI, Ponnan P, Tripathi M, Rawat DS. European Journal of Medicinal Chemistry Design, synthesis and evaluation of 4-aminoquinoline-purine hybrids as potential antiplasmodial agents. *Eur J Med Chem*. 2017;126:675-686. doi:10.1016/j.ejmech.2016.11.057

63.   Manohar S, Rajesh UC, Khan SI, Tekwani BL, Rawat DS. Vitro and in Vivo Antimalarial Activity. 2012:6-10.

64.   Singh A, Gut J, Rosenthal PJ, Kumar V. European Journal of Medicinal Chemistry 4-Aminoquinoline-ferrocenyl-chalcone conjugates : Synthesis and anti-plasmodial evaluation. *Eur J Med Chem*. 2017;125:269-277. doi:10.1016/j.ejmech.2016.09.044
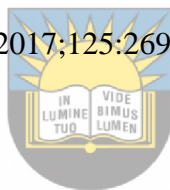
University of Fort Hare

Together in Excellence

Chapter 3
3. Experimental

3.1. Materials

All the starting materials and reagents used are 2-(2-(2-aminoethoxy)ethoxy)ethanamine (EDDA), ethanolamine (EA), 2(2-Aminoethoxy)ethanol (AEE), 1,3-diaminopropane (PDA), ethyldiamine (EDA), hydrazine hydrate (HZN), dimethylsulfoxide (DMSO), N,N'-Dicyclohexylcarbodiimide (DCC), N-Hydroxysuccinimide (HSU), 4-Dimethylaminopyridine (DMAP) and the solvents used are dichloromethane (DCM), ethyl acetate (EtOAc), chloroform (CHCl$_3$), methanol (MeOH), ethanol (EtOH), Hexane, dimethylformide (DMF), acetone and acetonitrile. The solvents used were of high grade and were dried over a molecular sieve, 4 Å beads 4-8 mesh purchased from Merck Millipore, before usage for the organic synthesis. The starting materials were supplied by Merck Millipore and were used as obtained without further purification. Thin layer chromatography was performed using silica gel plates (TLC Silica gel 60 F254) purchased from Merck Millipore and the spots were visualized under MiniMax UV lamp (254 nm) by spectroline model UV-4NFW 365 nm/254 nm white light. Column chromatography was performed using silica gel (technical grade, pore size 60 A, 230-400 mesh particle size, 40-63 µm particle size) bought from Sigma Aldrich. NMR spectra for ^{1}H NMR (400 MHz) and ^{13}C NMR (600 MHz) were recorded using either CD$_3$OD, DMSO-d_6 or CDCl$_3$ solvents on Bruker\TopSpin3.5pl5. Chemical shifts are expressed in parts per million (ppm) using the solvent peak as a reference. FTIR spectra were recorded on Perkin Elmer spectrum 100 Hz and it was recorded between 4000-400 cm^{-1}

3.2. Characterization
3.2.1. FTIR

FTIR was performed in order to determine the functional groups on the 4-aminoquinoline derivatives and the hybrid compounds. It was performed in a range of 4000-400 cm^{-1} using Perkin Elmer model 100 Hz.

3.2.2. NMR

NMR was used to determine the types of carbons and protons on the hybrid compounds with the solvent signal used as a reference peak. It was performed on Bruker Nuclear Magnetic Resonance (NMR) Spectrometer 400MHz for proton & 600MHz for carbon using a deuterated solvent (DMSO, CDCl$_3$, and CD$_3$OD).

3.2.3. LC-MS

LC-MS was used to determine the molecular weight of the isolated hybrid compounds. It was performed on Bruker Compact Liquid Chromatography Mass Spectrometry (LC-MS/MS), with the use of a C18 column with a gradient elution of acetonitrile (with formic acid 0.1%) and water (with formic acid 0.1%). LC-MS was performed on the prepared 4-aminoquinoline-based hybrid compounds.

3.3. Methodology for *in vitro* assay

Compounds were assayed using the Malaria SYBR Green I based assay, which quantifies parasite DNA content to account for compound diversity in the mode of action. Malaria parasite proliferation can be directly monitored in their intra-erythrocytic environment through detecting and monitoring DNA replication (without background forthcoming from erythrocytes, which lack DNA). SYBR Green I is a fluorescent dye that interacts with DNA, therefore a correlation between DNA content (SYBR Green I signal) and parasitaemia can be used to monitor a decrease in parasitaemia as a measurement of the inhibition of parasite proliferation

P. falciparum parasites were kept at a temperature of 37˚C in human blood cells types (O$^+$/A$^+$) suspended in complete culture medium [RPMI 1640 medium (Sigma-Aldrich) supplemented with 25 mM HEPES (Sigma-Aldrich), 20 mM D-glucose (Sigma-Aldrich), 200 μM hypoxanthine (Sigma-Aldrich), 0.2% sodium bicarbonate, 24 μg/ml Gentamicin (Sigma-Aldrich) and 0.5% AlbuMAX II] in a gaseous environment of 90% N$_2$, 5% O$_2$, and 5% CO$_2$ as described by Verlinden et al[1]. *In vitro* ring-stage intra-erythrocytic *P. falciparum* parasite

cultures (genotyped drug sensitive strain) NF54 (200 µl at 1% haematocrit, 1% parasitaemia) were treated with the compounds. The controls for this assay included chloroquine diphosphate (1 µM, as positive control) and complete RPMI media (as negative control) and grown for 96 h at 37˚C under the 90% N_2, 5% O_2, and 5% CO_2 gas mixture in 96-well plates. At the conclusion of the 96 h growth period, equal volumes (100 µl each) of the *P. falciparum* parasite cultures were combined with SYBR Green I lysis buffer (0.2 µl/ml 10 000x SYBR Green I, Invitrogen; 20 mM Tris, pH 7.5; 5 mM EDTA; 0.008% (w/v) saponin; 0.08% (v/v) Triton X-100). The samples were incubated for 1 h at room temperature after which the fluorescence was measured using a GloMax®-Explorer Detection System with Instinct® Software (Promega, excitation at 485 nm and emission at 538 nm). The 'background' fluorescence (i.e. that measured in the samples derived from chloroquine-treated infected erythrocytes in which parasite proliferation was completely inhibited) was subtracted from the total fluorescence measured for each sample to provide a measure of parasite proliferation. Data obtained were analyzed in Excel, and graphs determined using GraphPad 7 and experiments are performed in technical triplicate for a single biological repeat (n=1).

SELECTION CRITERIA
Compound activity is classified as indicated below for selection for full dose-response determination:

1) **Good activity** (IC_{50} expected to be below 1 µM)

   Inhibition greater than 70% at 5 µM and 50% at 1 µM

2) **Moderate activity** (IC_{50} expected to be between 1 and 5 µM)

   Inhibition greater than 70% at 5 µM and less than 50% at 1 µM

   Inhibition less than 70% at 5 µM and greater than 50% at 1 µM

   Inhibition of at least 50% and at most 70% at 5 µM and inhibition of greater than 50% at 1 µM

3) **No/ minimal activity** (IC$_{50}$ expected to be above 5 μM)

Inhibition of less than 50% at 5 μM and at 1 μM

- Compounds with **good activity** will be prioritized for full IC$_{50}$ determination (n=3).
- Compounds with **moderate activity** will undergo a single IC$_{50}$ determination (n=1) as confirmation of dual-point results.

REFERENCE ACTIVITIES:

Reference compound, Chloroquine (CQ) typically produce the following average % inhibition of asexual parasite proliferation at 1 and 5 μM:

|	Conc. (μM)	Asexual inhibition (%)
CQ	1	100%
	5	100%

3.4. General Methodology

4-Aminoquinoline derivatives were prepared from amination reaction of either amines or amino alcohols with 4.7-dichloroquinoline resulting in compounds with targeted functional groups. These derivatives were prepared and refluxed at 120°C and the reaction was monitored by TLC. After the completion of the reaction, work up process was performed in order to isolate the expected compounds followed by column chromatography. The hybrid compounds were prepared from the reaction of the isolated 4-aminoquinoline derivatives with selected compounds via either esterification or amidation reactions. The reactions were performed at room temperature overnight and monitored by TLC. Column chromatography was used to purify the isolated hybrid compounds followed by characterization using NMR, MS, LCMS.

3.4.1. Synthesis of 4.7-dichloroquinoline derivatives

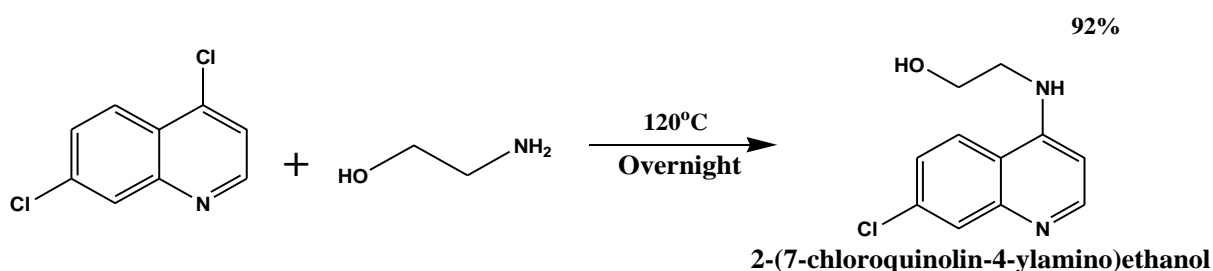#### 3.4.1.1. Synthesis of 1-(-7-chloroquinolin-4yl)hydrazine

4.7-dichloroquinoline (1.00 g, 50.50 mmol) was refluxed in absolute ethanol with hydrazine hydrate (1.5 mL, 30.30 mmol) at 120°C overnight. The reaction was then cooled to room temperature and the resulting solid was filtered, dried and recrystallized with 10 mL ethanol. After recrystallization, it was again filtered, dried and collected followed by TLC using solvents (6:2:2 methanol/TEA/hexane. Rf = 0.31). (5.09 g), Yield: 87%, melting point (272-274°C) FTIR (cm^{-1}): N−H stretch at 3450, C=C stretch at 1659, and C−Cl stretch at 756.5[2].
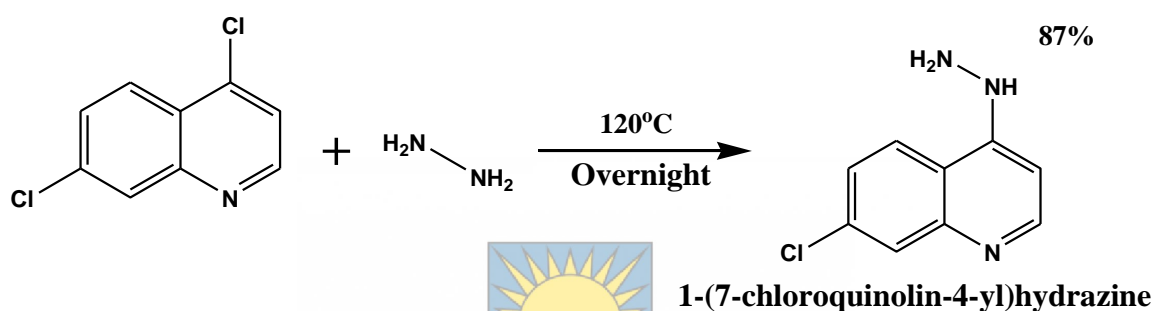
Scheme 8: Synthesis of 1-(-7-chloroquinolin-4yl)hydrazine at 120°C overnight

3.4.1.2. Synthesis of 2(7-chloroquinolin-4-ylamino)ethanol

4.7-dichloroquinoline (1.00 g, 5.05 mmol) was refluxed with ethanolamine (3.05 mL, 50.50 mmol) at 120°C overnight. The reaction was then poured into 30 mL distilled water and filtered, dried and recrystallized with 20 mL methanol. The cream white crystals were filtered and dried. TLC was performed using (6:2:2 methanol/ TEA/ hexane, Rf = 0.73). (1.03 g), Yield: 76%, melting point (229-231°C), IR (cm^{-1}): N−H stretch at 3316 cm^{-1}, C−H stretch at 2951, C=C at 1580, C−O stretch at 1063 and C−Cl stretch at 756.5[3].

Scheme 9: Synthesis of 4.7-dichloroquinoline with ethanolamine at 120°C overnight

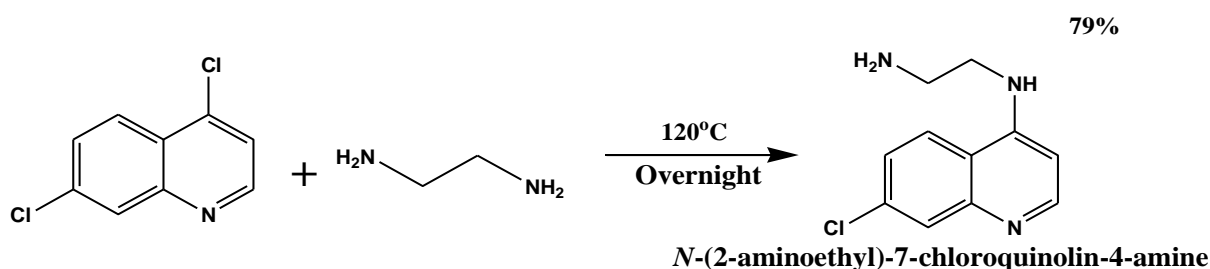### 3.4.1.3. Synthesis of 2-(2-(7-chloroquinolin-4-ylamino)ethoxy)ethanol

4.7-dichloroquinoline (50 mg, 2.25 mmol) was refluxed with 2-(2-aminoethoxy)ethanol (1 mL, 10.1 mmol) at 120°C overnight. The reaction was then poured into 30 mL distilled water and filtered, dried and recrystallized with 20 mL methanol. The cream white crystals formed were filtered and dried. TLC was performed using (6:2:2 methanol/TEA/Hexane, Rf = 0.54). (0.56 g), Yield: 84%, melting point (210-212°C), IR (cm^{-1}): N−H stretch at 3446, C−H stretch at 2901, C=C stretch at 1577, C−O−C stretch at 1124 and C−Cl stretch at 756.5[3].
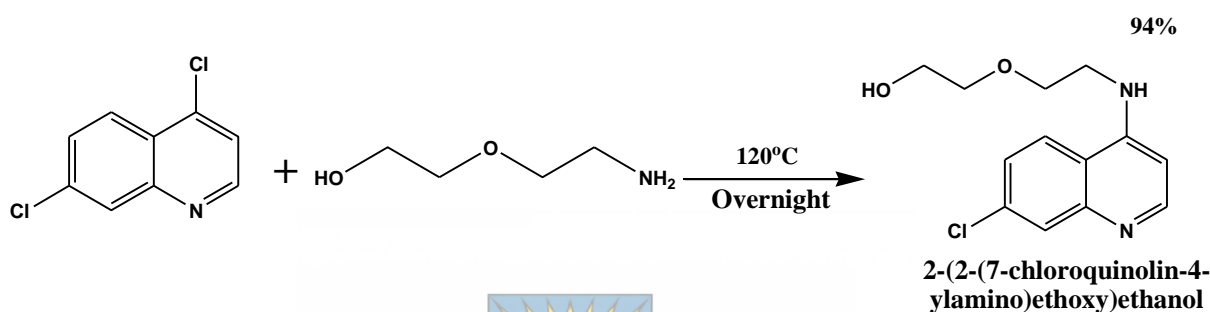
Scheme 10: synthesis of 4.7-dichloroquinoline with 2-(2-aminoethoxy)ethanol at 120°C overnight

3.4.1.4. Synthesis of *N*-(2-aminoethyl)-7-chloroquinolin-4-amine

A mixture of 4.7-dichloroquinoline (50 mg, 2.52 mmol) and *N*-(2-aminoethyl)-7-chloroquinoline-4-amine (1.7 mL, 25.25 mmol) was refluxed at 120°C overnight. The reaction was then extracted three times with 20 mL DCM and sodium hydroxide (1M, 10 mL). The organic layer was concentrated on a roti-evaporator. TLC was performed (6:2:2 methanol/TEA/hexane, Rf = 0.27). cream white solid (0.44 g), Yield: 79%, melting point (157-161°C), IR (cm$^{-1)}$: N−H stretch at 3366, C−H stretch at 2901, C=C stretch at 1587 and C−Cl stretch at 756.5[3].

3.4.1.5.   Synthesis of *N*-(2-(2-(2-aminoethoxy)ethoxy)ethyl)-7-chloroquinolin-4-amine

A mixture of 4.7-dichloroquinoline (50 mg, 2.52 mmol) and crude 2-(2-(2-aminoethoxy)ethoxy)ethanamine (3.7 mL, 25.25 mmol) was heated at reflux over a temperature of 120°C overnight. The reaction was then extracted three times with 20 mL DCM and 20 mL distilled water. The organic layer was dried over anhydrous sodium sulphate followed by filtration and concentration on roti-evaporator. TLC was performed using (6:3:1 methanol/TEA/hexane, Rf = 0.44). dark brown viscous oil (0.6 g), Yield: 77%, IR (cm^{-1}): N−H stretch 3269, C−H stretch at 2869, C=C stretch at 1577, C−O stretch at 1102 and C−Cl stretch at 796.6[4].
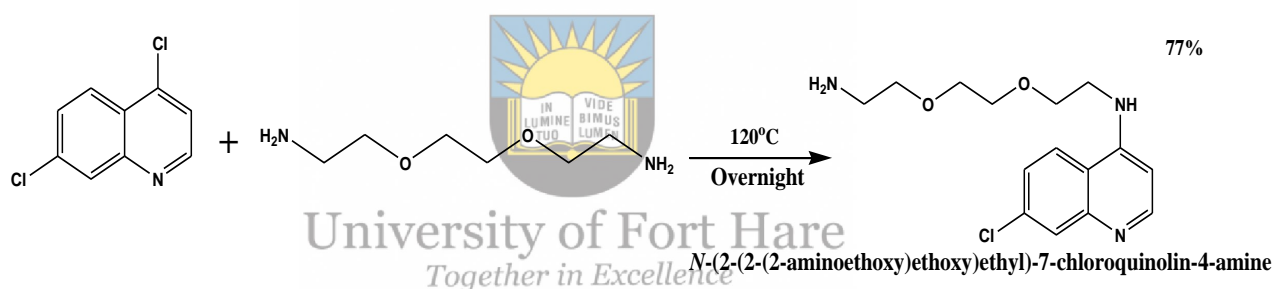
Scheme 12: Synthesis of 4.7-dichloroquinoline with N-(2-(2-(2-aminoethoxy)ethoxy)ethyl)-7-chloroquinolin-4-amine at 120°C overnight

3.4.1.6.   Synthesis of *N*-(3aminopropyl)-7-chloroquinolin-4-amine

A mixture of 4.7-dichloroquinline (1.00 g, 5.05 mmol) and 1.3-diaminopropane (1.9 mL, 22.7mmol) was refluxed at 120°C overnight. The reaction was then extracted three times with 20 mL DCM and sodium hydroxide (1M, 10 mL). The organic layer was dried over sodium sulphate anhydrous, filtered and concentrated on a roti-evaporator. TLC was performed using (6:3:1 methanol/TEA/hexane, Rf = 0.41), cream/yellow solid, (1.03 g), Yield: 87%, melting point (130-135°C), IR (cm^{-1}): N−H stretch 3248, C−H stretch at 2961, C=C stretch at 1577 and C−Cl stretch at 796.6[4].

87%

N-(3-aminopropyl)-7-chloroquinolin-4-amine
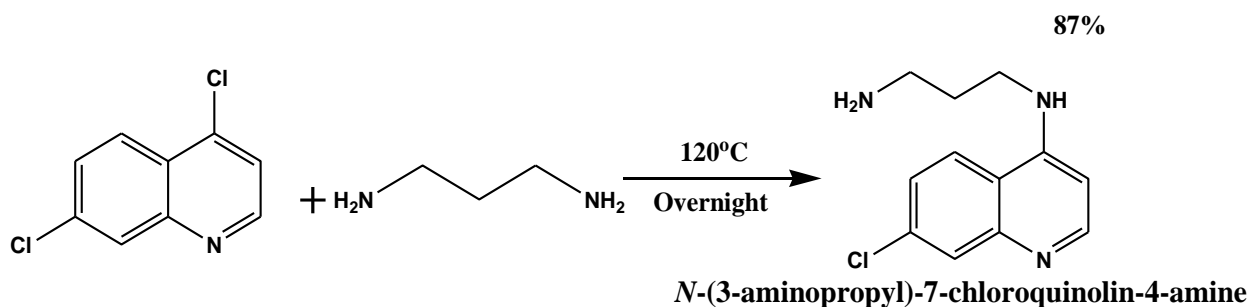
Scheme 13: Synthesis of 4.7-dichloroquinoline with 1.3-diaminopropane at 120°C overnight

3.4.2. Synthesis of Hybrid compounds

3.4.2.1.   2-(7-Chloroquinolin-4-ylamino)ethyl 4-amino-2-hydroxybenzoate
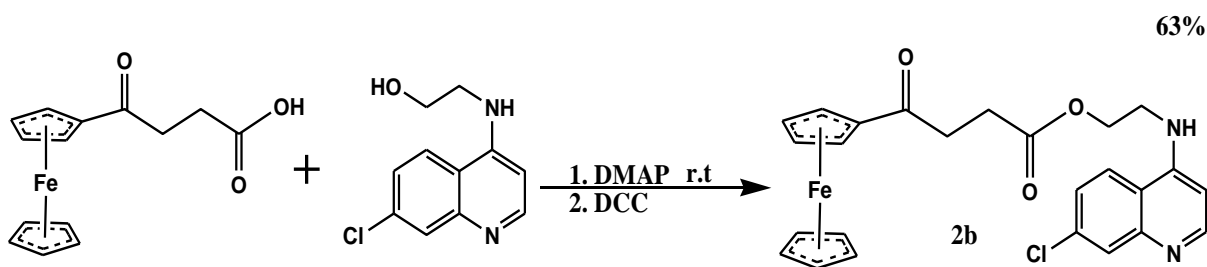
4-aminosalicylic acid (70 mg, 0.45 mmol) was dissolved in 5 mL DMSO followed by the addition of 2-(7-chloroquinolin-4-ylamino)ethanol (100 mg, 0.45 mmol). The reaction was allowed to stir for approximately 10 minutes until all the solute were completely dissolved followed by the addition of DMAP (55 mg, 0.45 mmol). The reaction was allowed to stir for 10 minutes followed by the addition of DCC (103 mg, 0.50 mmol) in portions within a period of 5 minutes. The reaction was allowed to stir overnight at room temperature. It was monitored by TLC using (6:4 toluene/ethyl acetate, and Rf = 0.24). The obtained product was extracted three times using 20 mL dichloromethane and 20 mL cold distilled water. The organic layer was dried over anhydrous sodium sulphate, filtered and then concentrated on the roti-evaporator. A viscous liquid was obtained which was further purified by column chromatography (6:4:1 Toluene/Ethyl acetate/Methanol). (0.108 g), Yield: (68%), MS: expected 357 g/mol: found 358 g/mol ratio (1:1), ^{1}HNMR (CD$_3$OD): 9.15 ppm (d, 1H, J= 4Hz), 9.06 ppm (d, 1H, J= 8Hz), 9.02 ppm (d, 1H, J= 8Hz), 8.86 ppm (d, 1H, J= 4Hz), 8.10 ppm (s, 1H), 7.37 ppm (d, 1H, J= 4Hz), 7.27 ppm (d, 1H, J= 4Hz), 6.33 ppm (d, 1H), 4.31 ppm (t, 2H, J= 4Hz), 3.72 ppm (s, 1H), 2.77 ppm (s, 2H). ^{13}CNMR (CD$_3$OD): 169.19 ppm, 160.10 ppm, 159.08 ppm, 149.88 ppm, 139.72 ppm, 134.77 ppm, 125.38 ppm, 107.99 ppm, 99.99 ppm, 64.04 ppm, and 48.95 ppm. FTIR (cm^{-1}): 3382 (N−H), 2981 (C−H), 15621 (C=C aromatic), 1695 (C=O), 1288 (N−H bending) and 1176 (C−O).
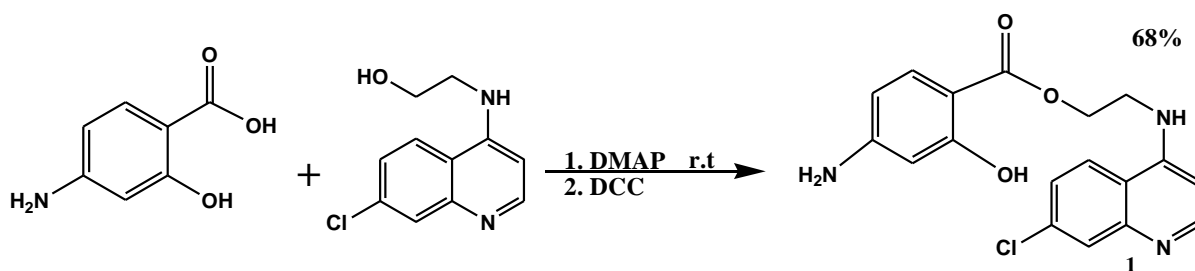
Scheme 14: Synthesis of 4-aminosalicylic acid with 2(7-chloroquinolin-4-ylamino)ethanol at R.T overnight

3.4.2.2.   Synthesis of ferrocene butanoic acid + 2(7-chloroquinolin-4-ylamino)ethanol
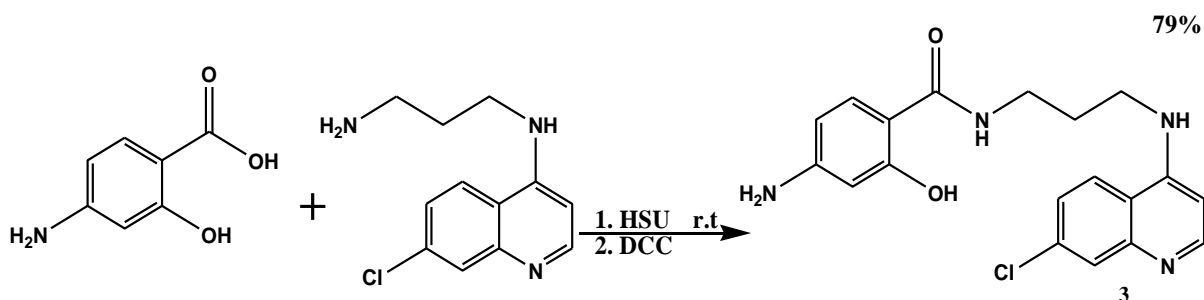
Ferrocene butanoic acid (129 mg, 0.45 mmol) was dissolved in 5 mL dry DCM followed by 2(7-chloroquinolin-4-ylamino)ethanol (100 mg, 0.45 mmol), the reaction was allowed to stir for approximately 10 minutes or at least solute has completely dissolved then DMAP (55 mg, 0.45 mmol) was added. The reaction was then again allowed to stir for about 10 minutes in an ice bath then DCC (103 mg, 0.50 mmol) was added in portions within a time range of 3-5 minutes and the reaction was allowed to run overnight at room temperature. The reaction was monitored by TLC. The obtained product was extracted three times using 20 mL DCM and 20 mL distilled water, the organic layer was dried over anhydrous sodium sulphate, filtered then concentrated on the roti-evaporator. An orange-like precipitate was obtained. TLC (7:2:1 ethyl acetate/hexane/methanol, Rf = 0.60). The obtained product was further purified using column chromatography (ethyl acetate/hexane/Methanol, 8:2:2). (0.14 g), Yield: 63%, melting point (116-124°C), MS: expected 490 g/mol: found 491 g/mol ratio (1:1), ^{1}HNMR (CDCl$_3$): 8.09 ppm (s, 1H), 4.23, 4.54 and 4.77 ppm (s, 4H, 2H and 1H)[5,6]. ^{13}CNMR (CDCl$_3$): 201.37 ppm, 156.87 ppm, 153.72 ppm, 148.87 ppm, 125.54 ppm, 121.81 ppm, 109.33 ppm, 98.75 ppm, (70,01 and 69.23 ppm) [5,6], 58.43 ppm, 33.94 ppm, 25.61 ppm, and 24.94 ppm. FTIR (cm^{-1}): 3357 (N−H)[7], 2912 (C−H), 1518 (C=C), 1705 (C=O), 1082 (C−O), 1201 (N−H bending) and 440 (Cp).

63%

Scheme 15: Synthesis of ferrocene butanoic acid with 2(7-chloroquinolin-4-ylamino)ethanol at R.T overnight

3.4.2.3. Synthesis of 4-aminosalicylic acid + *N*-(3-aminopropyl)-7-chloroquinolin-4-amine

The compound was prepared by amidation reaction. 4-aminosalicylic acid (60 mg, 0.40 mmol) was dissolved in 5 mL DMSO followed by *N*-(3-aminopropyl)-7-chloroquinolin-4-amine (100 mg, 0.40 mmol), the reaction was allowed to stir for approximately 10 minutes or at least solute has completely dissolved then HSU (50 mg, 0.40 mmol) was added. The reaction was then again allowed to stir for about 10 minutes then DCC (91 mg, 0.44 mmol) was added in portions within a time range of 3-5 minutes and the reaction was allowed to stir overnight at room temperature and it was monitored by TLC. The obtained product was extracted three times using 20 mL DCM and 20 mL cold distilled water. The organic layer was dried over anhydrous sodium sulphate, filtered and then concentrated on the roti-evaporator. A brown solid precipitate obtained. TLC (7:4 toluene/ethyl acetate, Rf = 0.33). The obtained product was further purified using column chromatography (Toluene/Ethyl acetate). (0.12 g), Yield: (79%), melting point (87-95°C), MS: expected 371 g/mol: found 371 g/mol ratio (1:1), ^{1}HNMR (DMSO): 8.54 ppm (s, 1H), 8.29 ppm (d, 1H, J= 8Hz), 8.14 ppm (d,1H, J= 4Hz), 2.40 ppm (dt, 2H, J= 8, 4Hz)[8]. ^{13}C NMR (DMSO): 33.8 ppm, 25.75 ppm, and 24.93 ppm. FTIR (cm^{-1}): 3320 (N−H)[7], 2938 (C−H), 1577 (C=C), 1619 (C=O), 1082 (C−O).

Scheme 16: Synthesis of 4-aminosalicylic acid with N-*(3aminopropyl)-7-chloroquinolin-4-amine at R.T overnight*

3.4.2.4. Synthesis of ferrocene butanoic acid + *N*-(3-aminopropyl)-7-chloroquinolin-4-amine

Ferrocene butanoic acid (114 mg, 0.4 mmol) was dissolved in 5 mL dry DCM followed by the addition of *N*-(3-aminopropyl)-7-chloroquinolin-4-amine (100 mg, 0.4 mmol), the reaction was allowed to stir for approximately 10 minutes or at least solute has completely dissolved then HSU (50 mg, 0.4 mmol) was added. The reaction was then again allowed to stir for about 10 minutes in an ice bath and DCC (90 mg, 0.44 mmol) was added in portions over a period of 3-5 minutes followed by continuous stirring overnight at room temperature. The reaction was monitored by TLC. The obtained product was extracted three times using 20 mL dichloromethane and 20 mL distilled water. The organic layer was dried over anhydrous sodium sulphate, filtered and then concentrated on the roti evaporator. An orange precipitate was obtained. TLC (6:4 toluene/ethyl acetate, Rf = 0.6). The obtained product was further purified using column chromatography (6:4:1 toluene/ethyl acetate/methanol). (0.13 g), Yield: (63%), melting point (110-115°C), MS: expected 502 g/mol: found 493 g/mol ratio (1:1), ^{1}HNMR (CDCl$_3$): 7.63 ppm (s, 1H), 3.11 and 3.73 ppm (s, 2H and 3H)[5]. ^{13}C NMR (CDCl$_3$): 203.60 ppm, 167.21 ppm, 148.43 ppm, 139.34 ppm, 128.36 ppm, 124.93 ppm, 122.73 ppm, 115.70 ppm, 103.80 ppm, 102.93 ppm, (69.93 ppm and 68.89 ppm)[5], 58.41 ppm, 45.82 ppm, 33.94 ppm, 25.62 ppm, and 18.43 ppm. FTIR (cm^{-1}): 3396 (N−H), 2978 (C−H), 1573 (C=C), 1628 (C=O), 1303 (N−H bending)[7], 1152 (C−O) and 478 (Cp).
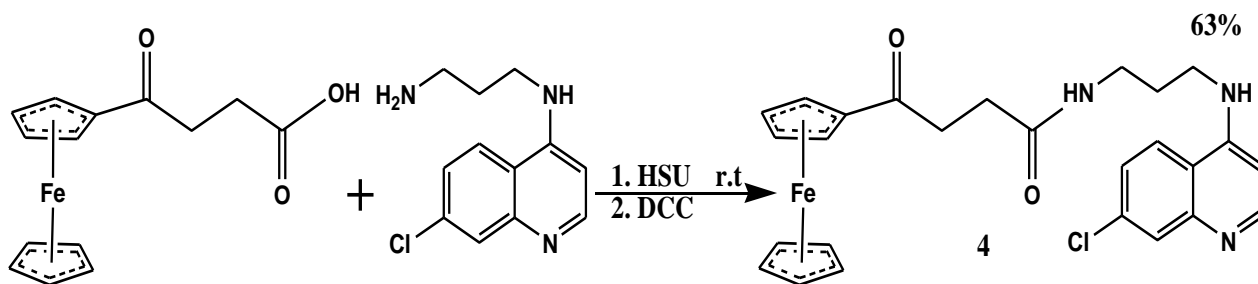
*Scheme 17: Synthesis of ferrocene butanoic acid with **N-***(3aminopropyl)-7-chloroquinolin-4-amine at R.T*
overnight

3.4.2.5.   Synthesis of 4-aminosalicylic acid + 2-(2-(7-chloroquinolin-4-ylamino)ethoxy)ethanol

4-aminosalicylic acid (50 mg, 0.35 mmol) was dissolved in 5 mL dry DCM followed by 2-(2-(7-chloroquinolin-4-ylamino)ethoxy)ethanol (100 mg, 0.35 mmol). The reaction was allowed to stir for approximately 10 minutes or at least solute has completely dissolved then DMAP (40 mg, 0.35 mmol) was added. The reaction was then again allowed to stir for about 10 minutes in an ice bath followed by the addition of DCC (80 mg, 0.39 mmol) in portions over a period of 3-5 minutes and the reaction was allowed to run overnight at room temperature. The obtained product was extracted three times using 20 mL DCM and 20 mL cold distilled water. The organic layer was dried over anhydrous sodium sulphate, filtered and then concentrated on the roti-evaporator. A viscous liquid was obtained. TLC (7:4 toluene/ethyl acetate, Rf = 0.54). The obtained product was further purified using column chromatography (7:4:2 toluene/ethyl acetate/methanol). (0.105 g), Yield: (75%), MS: expected 401 g/mol: found 402 g/mol ratio (1:1), ^{1}HNMR (DMSO): 8.37 ppm (d, 2H, J= 8Hz), 8.24 ppm (d, 1H, J= 8Hz), 7.79 ppm (d, 1H, J= 4Hz), 4.63 ppm (s, 1H), 3.76 ppm (t, 6H, J= 4Hz). ^{13}C NMR (DMSO): 154.47 ppm, 152.38 ppm, 150.57 ppm, 149.51 ppm, 133.89 ppm, 127.94 ppm, 124.54 ppm, 117.89 ppm, 107.17 ppm, 72.73 ppm, 68.48 ppm, and 60.68 ppm. FTIR (cm^{-1}): 3581 (OH), 3440 (NH), 2984 (CH) sp^3, 1678 (C=O), 1593 (C=C), 1156 (CO).
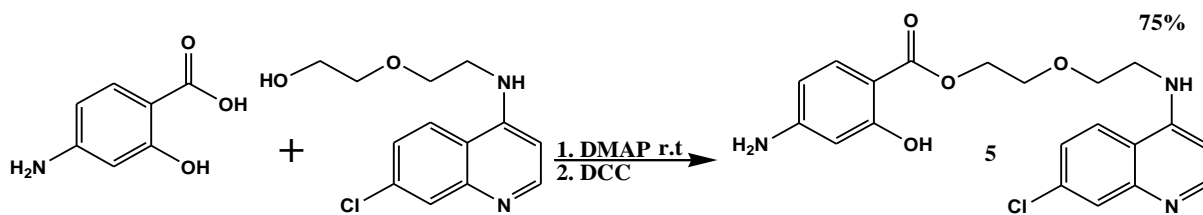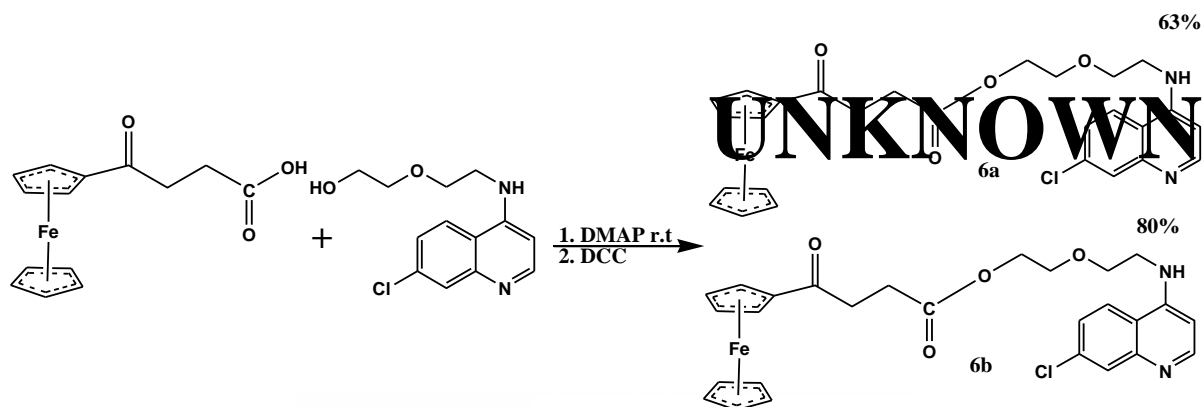
Scheme 18: Synthesis of 4-aminosalicylic acid with 2-(2-(7-chloroquinolin-4-ylamino)ethoxy)ethanol at R.T overnight
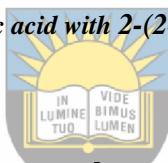
3.4.2.6. Synthesis of ferrocene butanoic acid + 2-(2-(7-chloroquinolin-4-ylamino)ethoxy)ethanol

Ferrocene butanoic acid (50 mg, 0.35 mmol) was dissolved in 5 mL DMSO followed by 2-(2-(7-chloroquinolin-4-ylamino)ethoxy)ethanol (100 mg, 0.35 mmol), the reaction was allowed to stir for approximately 10 minutes or at least solute has completely dissolved then DMAP (86 mg, 0.7 mmol) was added. The reaction was again allowed to stir for another 10 minutes then DCC (159 mg, 0.77 mmol) was added in portions within the time range of 3-5 minutes and the reaction was allowed to run overnight at room temperature monitored by TLC. The obtained product was extracted three times using 20 mL dichloromethane and 20 mL distilled water, the organic layer was dried with anhydrous sodium sulphate, filtered then concentrated on the roti evaporator. An orange precipitate 6a and viscous liquid 6b and were obtained. TLC (6:4 toluene/ethyl acetate, Rf = **6a:** 1, **6b:** 0.74). The obtained mixture of products was further purified using column chromatography (6:4 toluene/ethyl acetate). Two product were separated from column chromatography **6a :** (0.12 g), Yield 63%, melting point (100-107°C), MS: expected 535 g/mol: found 535 g/mol ratio (1:1), ^{1}HNMR (DMSO): 8.28 ppm (d, 1H, J= 8Hz), 7.38 ppm (d, 1H, J= 12Hz), 7.31 ppm (s, 1H), 5.59 ppm (d, 1H, J= 8Hz), 4.27 ppm (s, 4H) and 4.56 and 4.81 ppm (t, 2H, 1H)[5,6], 3.03 ppm (t, 2H, J= 8Hz). ^{13}C NMR (DMSO): 154.02 ppm, 72.44, 70.13 and 69.47, 32.20 ppm, 30.82 ppm, 25.92 ppm, 24.84 ppm. FTIR (cm^{-1}): 3332 (N−H), 2939 (C−H), 1577 (C=C), 1689 (C=O), 1062 (C−O).

6b: (0.152 **g**), Yield: 80%, MS: expected 535 g/mol: found 528 g/mol ratio (1:1), ^{1}HNMR (DMSO): 8.41 ppm (d, 1H, J= 4Hz), 8.28 ppm (d, 1H, J= 4Hz), 7.80 ppm (s, 1H), 6.84 ppm (d, 1H, J= 8Hz), 6.56 ppm (d, 1H, J= 4Hz). FTIR (cm^{-1}): 3332 (N−H), 2939 (C−H), 1577 (C=C), 1689 (C=O), 1062 (C−O).
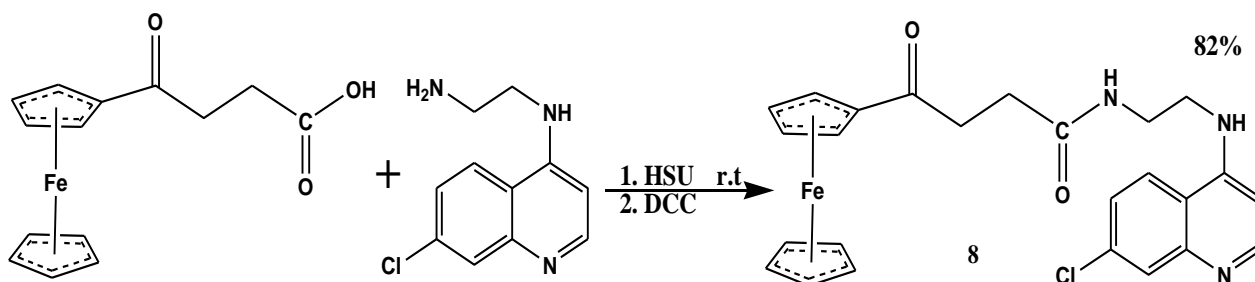

Scheme 19: Synthesis of ferrocene butanoic acid with 2-(2-(7-chloroquinolin-4-ylamino)ethoxy)ethanol at R.T overnight

3.4.2.7.   Synthesis of ferrocene butanoic acid + *N*-(2-aminoethyl)-7-chloroquinolin-4-amine

Ferrocene butanoic acid (130 mg, 0.45 mmol) was dissolved in 5mL dry DCM followed by the addition of *N*-(2-aminoethyl)-7-chloroquinolin-4-amine (100 mg, 0.45 mmol). The reaction was allowed to stir for approximately 10 minutes or at least solute has completely dissolved, then HSU (0.52 mg, 0.45 mmol) was added. The reaction was then again allowed to stir for about 10 minutes in an ice bath then DCC (90 mg, 0.5 mmol) was added in portions over a time range of 3-5 minutes and the reaction was allowed to run overnight at room temperature. The obtained product was extracted three times using 20 mL DCM and 20 mL distilled water. The organic layer was dried over anhydrous sodium sulphate, filtered then concentrated on the roti evaporator. A dark orange precipitate was obtained. TLC (7:3 ethyl acetate/toluene, Rf = 0.66). The obtained product was further purified using column chromatography (6:4 ethyl acetate/toluene). (0.18 g), Yield: 82%, melting point (145-153°C), MS: expected 489 g/mol: found 490 g/mol ratio (1:1), ^{1}HNMR (CDCl$_3$): 8.22 ppm (d, 1H, J= 48Hz), 7.99 ppm (s, 1H),

4.60, 4.44 and 4.12 ppm (s, 1H, 1H and 4H)[5,6], 3.66 ppm(s, 1H). ^{13}C NMR (CDCl$_3$): 203.67

ppm linked, 156.87 ppm, 149.70 ppm, 127.10 ppm, 124.91 ppm, 122.77 ppm, 113.13 ppm,

108.01 ppm, 72.55, 69.96 and 69.19 ppm[5,6], 49.16 ppm, 33.94 ppm, 25.61 ppm, and 24.94 ppm.

FTIR (cm^{-1}): 3368 (N−H)[7], 2882 (C−H), 1528 (C=C aromatic), 1685 (C=O) and 1208 (N−H
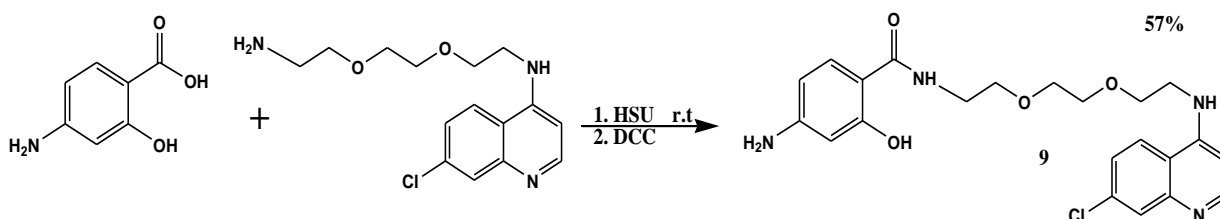
bending).

Scheme 20: Synthesis of ferrocene butanoic acid with N-(2-aminoethyl)-7-chloroquinolin-4-amine at R.T overnight

3.4.2.8. Synthesis of 4-aminosalicylic acid + N-(2-(2-(2-aminoethoxy)ethoxy)ethyl)-7-chloroquinolin-4-amine

This reaction of 4-aminosalicylic acid (50 mg, 0.32 mmol) was dissolved in 5mL dry DMSO

followed by N-(2-(2-(2-aminoethoxy)ethoxy)ethyl)-7-chloroquinolin-4-amine (100 mg, 0.32

mmol), the reaction was allowed to stir for approximately 10 minutes or at least solute has

completely dissolved then HSU (40 mg, 0.32 mmol) was added. The reaction was then again

allowed to stir for another 10 minutes then DCC (70 mg, 0.36 mmol) was added in portions

over a period of 3-5 minutes and the reaction was allowed to run overnight at room temperature.

The obtained product was extracted three times using 20 mL DCM and 20 mL cold distilled

water, the organic layer was dried over anhydrous sodium sulphate, filtered then concentrated

on the roti evaporator. A dark brown viscous liquid was obtained. TLC (6:4:1 toluene/ethyl

acetate/methanol, Rf = 0.8). The obtained product was further purified using column

chromatography (6:4 toluene/ethyl acetate). (0.08 g), Yield: 57%, MS: expected 444 g/mol:

found 445 g/mol ratio (1:1), ^{1}HNMR (CDCl$_3$): 4.40 ppm (s, 1H), 3.72 ppm (q, 4H, J= 4Hz),

2.99 ppm (s, 1H). ^{13}C NMR (CDCl$_3$): 157.03 ppm, 120.99 ppm, 119.20 ppm, 106.45 ppm,

98.63 ppm, 97.33 ppm, 58.33, 40.96 ppm and 33.83 ppm. FTIR (cm^{-1}): 3386 (OH), 2921 (C−H)

[9], 1645 (C=C aromatic), 1735 (C=O), 1023 (C−O), 1438 (N−H bending)[7].
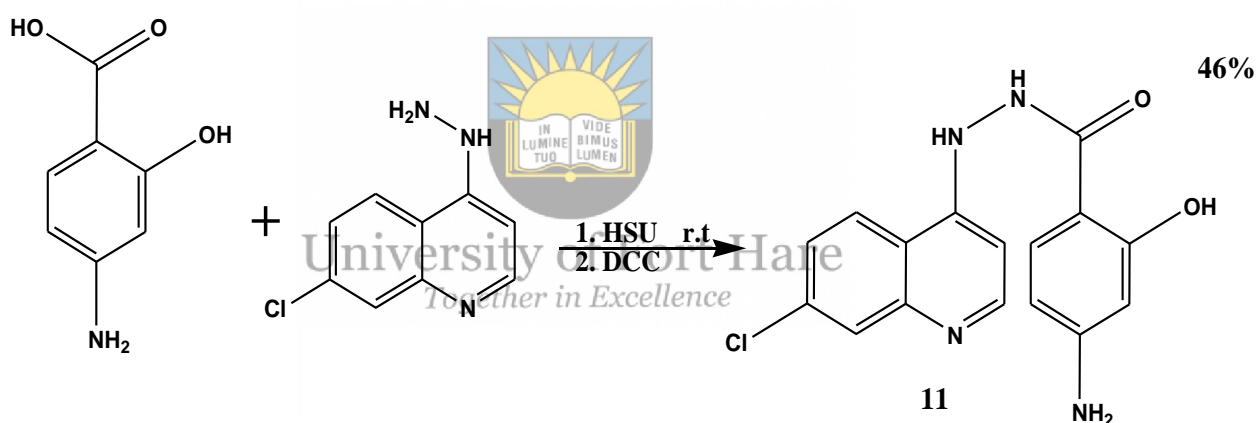

Scheme 21: Synthesis of 4-aminosalicylic acid with N-(2-(2-(2-aminoethoxy)ethoxy)ethyl)-7-chloroquinolin-4-amine at R.T overnight

3.4.2.9.   Synthesis of ferrocene butanoic acid + N-(2-(2-(2-aminoethoxy)ethoxy)ethyl)-7-chloroquinolin-4-amine

Ferrocene butanoic acid (100 mg, 0.35 mmol) was dissolved in 5 mL dry DCM followed by

the addition of N-(2-(2-(2-aminoethoxy)ethoxy)ethyl)-7-chloroquinolin-4-amine (110 mg,

0.35 mmol). The reaction was allowed to stir for approximately 10 minutes or at least solute

has completely dissolved, then HSU (40 mg, 0.35 mmol) was added. The reaction was then

again allowed to stir for about 10 minutes in an ice bath then DCC (80 mg, 0.4 mmol) was

added in portions over a time range of 3-5 minutes and the reaction was allowed to run

overnight at room temperature. The obtained product was extracted three times using 20 mL

DCM and 20 mL distilled water. The organic layer was dried over anhydrous sodium sulphate,

filtered then concentrated on the roti evaporator. A dark brown solid and a sticky black solid

precipitate were obtained and again was checked under TLC (6:4:1 toluene/ethyl

acetate/methanol, Rf = 10a: 0.41 10b: 0.67). The obtained product was further purified using

column chromatography (6:4 then later 6:4:1 Toluene: Ethyl acetate: Methanol). **10a**: (0.11 g),

Yield 56%, (90-100°C), MS: expected 560 g/mol: found 578 g/mol ratio (1:1), ^{1}HNMR

(CDCl$_3$): 4.74, 4.44 and 4.16 ppm (s, 1H, 1H and 3H)[5,6], 3.44 ppm (s, 1H). ^{13}CNMR (CDCl$_3$):

203.43 ppm, 152.42 ppm, 139.99, 136.03, 114.67 ppm, 104.43 ppm, 102.48 ppm, 72.39, 69.99

and 69.32 ppm[5,6], 58.51 ppm, 29.70 ppm, 25.63 ppm. FTIR (cm^{-1}): 3327 (N−H)[7], 2921 (C−H), 1557 (C=C aromatic), 1627 (C=O)[7], 1300 (N−H bending), 1082 (C−O) and 415 (Cp).

10b: (0.14 g), Yield: 71%, MS: expected 560 g/mol: found 578 g/mol ratio (1:1), ^{1}HNMR (CDCl$_3$): 8.25 ppm (d, 1H, J= 4Hz), 8.14 ppm (d, 1H, J= 12Hz), 7.95 ppm (s, 1H), 7.30 ppm (d, 1H, J= 8Hz), 4.70, 4.43 and 4.14 ppm (s, 1H, 1H and 3H)[5,6], 3.84 ppm (t, 4H, J= 4Hz), 3.52 ppm (t, 4H, J= 4Hz), 3.05 ppm (t, 4H, J= 4Hz). ^{13}C NMR (CDCl$_3$): 203.71 ppm, 172.65 ppm, 166.18 ppm, 142.90 ppm, 126.77 ppm, 123.68 ppm, 116.05 ppm, 72.47, 69.98 and 69.25 ppm[5,6], 58.45 ppm, and 39.34 ppm. FTIR (cm^{-1}): 3327 (N−H)[7], 2921 (C−H), 1557 (C=C), 1627 (C=O), 1082 (C−O) and 467 (Cp).

Scheme 22: Synthesis of ferrocene butanoic acid with N-(2-(2-(2-aminoethoxy)ethoxy)ethyl)-7-chloroquinolin-4-amine at R.T overnight

3.4.2.10.   Synthesis of 4-aminosalicylic acid + *1-(-7-chloroquinolin-4yl)hydrazine*

4-aminosalicylic acid (100 mg, 0.65 mmol) was dissolved in 5 mL DMSO followed by 1-(-7-chloroquinolin-4yl)hydrazine (140 mg, 0.65 mmol), then the reaction was allowed to stir for approximately 10 minutes at least solute has completely dissolved then HSU (70 mg, 0.65 mmol) was added. The reaction was then again allowed to stir for about 10 minutes then DCC (150 mg, 0.72 mmol) was added in portions over a period of 3-5 minutes then the reaction was allowed to run overnight at room temperature monitored by TLC. The obtained product was

extracted three times using 20 mL DCM and 20 mL cold distilled water. The organic layer was dried over anhydrous sodium sulphate, filtered then concentrated on the roti evaporator. A dark precipitate was obtained. TLC (7:4 toluene/ethyl acetate, Rf = 0.73). The obtained product was further purified using column chromatography (6:4:1 toluene/ethyl acetate/methanol). (0.96 g), Yield: (46%), melting point (176-187 °C), MS: expected 329 g/mol: found 317 g/mol ratio (1:1), ^{1}HNMR (DMSO): 7.39 ppm (d, 1H, J= 8Hz), 7.32 ppm (d, 1H, J=8Hz), 7.08 ppm (d, 1H, J=4Hz), 6.71 ppm (s, 1H), 6.25 ppm (d, 1H, J= 8Hz), 3.96 ppm (s, 1H). ^{13}C NMR (DMSO): 163.15 ppm, 156.99 ppm, 147.64 ppm, 128.58 ppm, 125.70 ppm, 116.98 ppm, 115.81 ppm, 106.33 ppm, 104.37 ppm, 101.55 ppm, and 97.65 ppm. FTIR (cm^{-1}): 3437 (N−H), 2921 (C−H) sp^3, 1557 (C=C), 1617 (C=O), 1300 (N−H bending) and 1182 (C−O)[10].

Scheme 23: Synthesis of 4-aminosalicylic acid with **1-(-7-chloroquinolin-4yl)hydrazine** *at R.T overnight*

Reference

1. Verlinden BK, Niemand J, Snyman J, Sharma SK, Beattie RJ, Woster, PM, Birkholtz LM. Discovery of Novel Alkylated (bis)Urea and (bis)Thiourea Polyamine Analogues with Potent Antimalarial Activities. *J Med Chem*. 2011;54(19):6624-6633. doi:10.1021/jm200463z

2. Khalil W.K.B, Ghaly I.S DKA. International Journal of Pharmacy Practice. *Conf 5*. 2010;4(3):68-82. doi:10.1016/j.ijpharm.2010.06.045

3. Pretorius IS. Synthesis, characterization and antimalarial activity of quinoline-pyrimidine hybrids. 2012.

4. Smit F. Synthesis and in vitro antimalarial activity of novel chalcone derivatives. 2014;(May).

5. Singh A, Gut J, Rosenthal PJ, Kumar V. European Journal of Medicinal Chemistry 4-Aminoquinoline-ferrocenyl-chalcone conjugates : Synthesis and anti-plasmodial evaluation. *Eur J Med Chem*. 2017;125:269-277. doi:10.1016/j.ejmech.2016.09.044

6. Carbon Synthesis and Reactions of Ferrocene.

7. Chapter 5 Synthesis and Biological Evaluation of Some Thiazolylhydrazinomethylideneferrocenes as Antimicrobial Agents CHAPTER 5. Synthesis and Biological Evaluation of Some Thiazolylhydrazinomethylideneferrocenes as Antimicrobial Agents.

8. Gamov GA, Kuranova NN, Pogonin AE, Aleksandriiskii V V., Sharnin VA. Hydrogen bonds determine the signal arrangement in13C NMR spectra of nicotinate. *J Mol Struct*. 2018;1154:565-569. doi:10.1016/j.molstruc.2017.10.086

9. Njogu EM, Omondi B, Nyamori VO. Synthesis, Physical and Antimicrobial Studies of Ferrocenyl-N-(pyridinylmethylene) anilines and Ferrocenyl-N-(pyridinylmethyl) anilines. *South African J Chem*. 2016;69:51-66. doi:10.17159/0379-4350/2016/v69a7

10.   Yong J, Jiang X, Wu X, Huang S, Zhang Q, Lu C. Synthesis and Characterization of Ferrocene Derivatives and Preliminarily Electrocatalytic Oxidation of L-Cysteine at Nafion-Ferrocene Derivatives Modified Glassy Carbon Electrode. *Adv Chem.* 2014;2014(Scheme 1):1-7. doi:10.1155/2014/987481

University of Fort Hare
Together in Excellence

Chapter 4

4. Results and Discussion

4.1. FTIR results for 4-aminoquinoline derivatives

Table 2: FTIR results of 4.7-dichloroquinoline derivatives

Functional groups	N−H	C=C	C−O	OH	C−Cl	C−H	
Compounds							*Figures*
1-(7-chloroquinolin-4-yl)hydrazine	3450 cm^{-1}	1659 cm^{-1}	_	_	756.5 cm^{-1}	_	*3* [1]
2-(2-(7-chloroquinolin-4-ylamino)ethoxy)ethanol	3446 cm^{-1}	1577 cm^{-1}	1124 cm^{-1}	3544 cm^{-1}	756.5 cm^{-1}	2901 cm^{-1}	*4* [2]
2-(7-chloroquinolin-4-ylamino)ethanol	3316 cm^{-1}	1580 cm^{-1}	1063 cm^{-1}	3535 cm^{-1}	756.5 cm^{-1}	2951 cm^{-1}	*5* [2]
N-(2-aminoethyl)-7-chloroquinolin-4-amine	3366 cm^{-1}	1587 cm^{-1}	_		756.5 cm^{-1}	2901 cm^{-1}	*6* [2]
N-(2-(2-(2-aminoethoxy)ethoxy)ethyl)-7-chloroquinolin-4-amine	3269 cm^{-1}	1577 cm^{-1}	1102 cm^{-1}	_	796.6 cm^{-1}	2869 cm^{-1}	*7* [3]
N-(3-aminopropyl)-7-chloroquinolin-4-amine	3248 cm^{-1}	1577 cm^{-1}	_	_	796.6 cm^{-1}	2961 cm^{-1}	*8* [3]

The table above presents a successful linkage of two reagents in the formation of 4.7-dichloroquinoline derivatives. The observed functional group peaks are within the expected

region on the spectra for all the derivatives. Characteristic peaks for N−H were within the range of 3446-3248 cm⁻¹, C−H 2961-2869 cm⁻¹, C=C 1659-1577 cm⁻¹, OH 3544-3535 cm⁻¹, C−O 1124-1063 cm⁻¹ and C−Cl from 796.6-756.5 cm⁻¹ this confirms the successful isolation of pure molecules.

4.2. FTIR results for Hybrid compounds

Table 3: FTIR results of hybrid compounds

Functional groups	O−H	N−H	C−H	C=O	C=C	C−O	Cp	
Compounds								*Figures*
9	3516 cm⁻¹	_	2921 cm⁻¹	1735 cm⁻¹	1645 cm⁻¹	1023 cm⁻¹	_	*9*
10a	_	3327 cm⁻¹	2921 cm⁻¹	1687 cm⁻¹	1557 cm⁻¹	1082 cm⁻¹	415 cm⁻¹	*10*
10b	_	3327 cm⁻¹	2921 cm⁻¹	1697 cm⁻¹	1567 cm⁻¹	1082 cm⁻¹	467 cm⁻¹	*11*
11	_	3437 cm⁻¹	2921 cm⁻¹	1687 cm⁻¹	1557 cm⁻¹	1182 cm⁻¹	_	*12*
3	_	3320 cm⁻¹	2938 cm⁻¹	1719 cm⁻¹	1577 cm⁻¹	1082 cm⁻¹	_	*13*
4	_	3396 cm⁻¹	2978 cm⁻¹	1701 cm⁻¹	1573 cm⁻¹	1152 cm⁻¹	478 cm⁻¹	*14*

6	_	3332 cm^{-1}	2939 cm^{-1}	1718 cm^{-1}	1647 cm^{-1}	1126 cm^{-1}	440 cm^{-1}	*15*
8	_	3368 cm^{-1}	2882 cm^{-1}	1685 cm^{-1}	1528 cm^{-1}	_	476 cm^{-1}	*16*
2	_	3357 cm^{-1}	2912 cm^{-1}	1705 cm^{-1}	1518 cm^{-1}	1082 cm^{-1}	440 cm^{-1}	*17*

According to the results obtained from the spectra, we can conclude and discuss that the desired hybrid compounds were successfully hybridized and isolated during column chromatography. During hybridization of compound 10, a mixture of products was observed under thin layer chromatography and both compounds were isolated, FTIR confirms that both compounds contain similar or the same functional groups which were observed at almost the same regions. The important peaks were clearly observed and were those of secondary amine found at the range of 3396-3320 cm^{-1} respectively for all the hybrid compounds synthesized via amidation reaction, and that of the ester at 1126-1082 cm^{-1}.

4.3. NMR Results for hybrid compound

H^1 NMR (400 MHz, CDCl$_3$) spectra of compound **2a** (**figure 30**) showed visible signals at (s) at 7.48 ppm, (s) at 4.25, 4.50 and 4.78 ppm for (3H, 1H, 1H) are due to cyclopentadiene ring of ferrocene, (t) at 0.81 ppm (2H, J= 8) linked to **n**. ^{13}C NMR (600 MHz, CDCl$_3$), (**figure 18**) presented signals at 154.53 ppm related to **l**, 131.83 ppm due **f**, 115.13 ppm linked **a** & **c**, 104.38 ppm allied to **d**, 100.33 ppm linked to **h**, 70.50 and 69.62 ppm are characteristic signals to C$_5$H$_5$, 50.02 ppm resultant to **k**, 35.33 ppm linked to **j**, 31.94 ppm corresponding to **m**, 26.17 ppm linked to **o** and 22.71 ppm corresponding **n**. During the synthesis of this compound two products, 2a & 2b were formed, separated and characterized NMR was able to confirm that compound 2a is less of our desired compound, making compound 2b our desired compound.

H^1 NMR (400 Hz, CDCl$_3$) spectra for compound **2b** (**figure 31**) presented signals for aromatic protons (s) at 8.09 ppm (1H) linked to **a**, (s) at 4.23, 4.54 and 4.77 ppm (5H, 2H, and 1H) correspond to cyclopentadiene ring of ferrocene. ^{13}C NMR was able to peak the alkyl carbons. ^{13}C NMR (600 Hz, CDCl$_3$), (**figure 19**) presented signals at 201.37 ppm due to **o**, 156.87 ppm linked to **l**, 153.72 ppm related to **i**, 148.87 ppm linked to **g**, 125.54 ppm characteristic signal for **a** and **c**, 121.81 ppm due to **e**, 109.33 ppm corresponding to **d**, 98.75 ppm allied to **h**, 70,01 and 69.23 ppm are characteristic signals for Cp, 58.43 ppm linked to **k**, 33.94 ppm related to **j** and 25.61 ppm resultant to **m** and 24.94 ppm linked to **n**. ^{13}C NMR was clear and able to confirm the expected number of carbons. The compound was a result of a simple esterification reaction and was successfully isolated as the NMR results presented the expected number of carbon and protons.
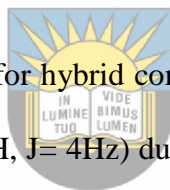
H^1 NMR (400 Hz, CD$_3$OD) spectra for hybrid compound **1** (**figure 32**) presented signals for aromatic protons (d) at 9.15 ppm (1H, J= 4Hz) due to **g**, (d) at 9.06 ppm (1H, J= 8Hz) linked to **c**, (d) at 9.02 ppm (1H, J= 8Hz) related to **r**, (d) at 8.86 ppm (1H, J= 4Hz) resultant to **d**, (s) at 8.10 ppm (1H) corresponding to **a**, (d) at 7.37 ppm (1H, J= 4Hz) linked to **h**, (d) at 7.27 ppm (1H, J= 4Hz) characteristic signal to **q**, (d) at 6.33 ppm (1H) corresponds to **o**, (t) at 4.31 ppm (2H, J= 4) linked to **k**. ^{13}C NMR (600 Hz, CD$_3$OD), (**figure 20**) presented signals at 169.19 ppm related to **l**, 160.10 ppm due to **n**, 159.08 ppm resultant to **p**, 153.12 ppm corresponding to **g**, 149.88 ppm linked to **f**, 139.72 ppm corresponds to **b**, 134.77 ppm due to **r**, 128.69 ppm linked to **a** & **c**, 125.38 ppm characteristic signal to **d**, 107.99 ppm related to **e**, 99.99 ppm linked to **o**, 94.88 ppm due to **m**, 64.04 ppm allied to **k** and 48.95 ppm due to **j**. NMR was able to confirm the successful formation of a hybrid compound.

^{1}H NMR (400 Hz, CD$_3$OD) spectra for hybrid compound **4** (**figure 33**) presented signals (s) at 7.63 ppm (1H) linked to **a**, (s) at 3.11 and 3.73 ppm (2H and 3H) corresponds to cyclopentadiene ring of ferrocene. ^{13}C NMR (600 Hz, CD$_3$OD), (**figure 21**) presented signals

at 203.60 ppm as a result to **p**, 167.21 ppm due to **m**, 148.43 ppm related to **i**, 139.34 ppm due to **g**, 128.36 ppm corresponds to **f**, 124.93 ppm resultant to **b**, 122.73 ppm due to **a & c**, 115.70 ppm characteristic signal to **d**, 103.80 ppm due to **e**, 102.93 ppm corresponds to **h**, 69.93 ppm and 68.89 ppm resultant to cyclopentadiene ring of ferrocene, 58.41 ppm due to **l**, 45.82 ppm corresponding to **j**, 33.94 ppm due to **n**, 25.62 ppm related to **o** and 18.43 ppm due to **k** position.

^{1}H NMR spectra (400 Hz, CDCl$_3$) for hybrid compound **8** (**figure 34**) presented signals (d) at 8.22 ppm position **c** (1H, J= 44Hz), (s) at 8.16 ppm (1H) arise due to position **a**, (s) at 4.60, 4.44 and 4.12 ppm (1H, 1H and 4H) corresponds to cyclopentadiene ring of ferrocene. ^{13}C NMR (600 Hz, CDCl$_3$) (**figure 22**), presented signal peaks at 203.67 ppm due to **o**, 156.87 ppm resultant to **l**, 149.70 ppm related to **i**, 127.10 ppm corresponding to **b**, 124.91 ppm due to **a** and **c**, 122.77 ppm linked to **e**, 113.13 ppm corresponds to **d**, 108.01 ppm due to **h**, 72.55, 69.96 and 69.19 ppm characteristic signal to the cyclopentadiene ring of ferrocene, 49.16 ppm related to **k**, 33.94 ppm due to **j**, 25.61 ppm linked to **m** and 24.94 ppm corresponding to **n.**

^{1}H NMR spectra (400 Hz, DMSO) for hybrid compound **11** (**figure 35**) presented signals (d) at 7.39 ppm (1H, J= 8Hz) due to **c**, (d) at 7.32 ppm (1H, J=8Hz) linked **p**, (d) at 7.08 ppm (1H, J=4Hz) related to **h**, (s) at 6.71 ppm (1H) due to **m** and a (d) at 6.25 ppm (1H, J= 8Hz) resultant to **o**. ^{13}C NMR (600 Hz, DMSO) (**figure 23**), presented signal peaks at 163.15 ppm **j**, 156.99 ppm **n**, 147.64 ppm **f**, 128.58 ppm **b**, 125.70 ppm **a** and **c**, 116.98 ppm **d**, 115.81 ppm **e**, 106.33 ppm **h**, 104.37 ppm **k**, 101.55 ppm **o** and 97.65 ppm **m**.

^{1}H NMR spectra (400 Hz, CDCl$_3$) for hybrid compound **9** (**figure 36**) presented signals (s) at 4.40 ppm (1H) due to Ar-OH, (q) at 3.72 ppm (4H, J= 4Hz) characteristic signals to **j** and **o**, (s) at 2.99 ppm related to Ar-NH. ^{13}C NMR (600 Hz, CDCl$_3$) (**figure 24**), presented signal peaks at 157.03 ppm due to **p**, 120.99 ppm resultant to **a** and **c**, 119.20 ppm due to **d**, 106.45

ppm corresponding to **h**, 98.63 ppm linked to **u**, 97.33 ppm corresponds to **s**, 58.33 ppm characteristic signal to positions **k**, **l**, **m** and **n**, 40.96 ppm linked to **j** and 33.83 ppm due to **o**.

^{1}H NMR spectra (400 Hz, CDCl$_3$) for hybrid compound **10a** (**figure 37**) presented signals (s) at 4.74, 4.44 and 4.16 ppm (1H, 1H, and 3H) are due to cyclopentadiene ring of ferrocene, (t) at 3.55 ppm (4H, J= 16Hz) corresponds to **j** and **o**. ^{13}C NMR (600 Hz, CDCl$_3$) (**figure 25**), presented signal peaks at 203.43 ppm due to **s**, 152.42 ppm related to **p**, 139.99 linked to **b**, 136.03 ppm corresponding to **a** and **c**, 114.67 ppm resultant to **d**, 104.43 ppm due to **e**, 102.48 ppm related to **h**, 72.39, 69.99 and 69.32 ppm characteristic signals to cyclopentadiene ring of ferrocene, 58.51 ppm linked to **k, l, m** and **n**, 29.70 ppm corresponding **q**, 25.63 ppm due to **r**. A mixture of products was obtained during the synthesis of a compound leading to compounds 10a and 10b, NMR was convincing enough that compound 10b rather than 10a is the expected compound.

^{1}H NMR spectra (400 Hz, CDCl$_3$) for hybrid compound **10b** (**figure 38**) presented signals (d) at 8.25 ppm (1H, J= 4Hz) due to **g**, (d) at 8.14 ppm (1H, J= 12Hz) corresponds to **d**, (s) at 7.95 ppm (1H) related to **a**, (d) at 7.30 ppm (1H, J= 8Hz) corresponding to **c**, (d) at 6.39 ppm (1H, J= 8Hz) linked to **h**, (s) at 4.70, 4.43 and 4.14 ppm (1H, 1H and 3H) due to cyclopentadiene ring of ferrocene, (t) at 3.84 ppm (4H, J= 4Hz) characteristic signal to **l** and **m**, (q) at 3.66 ppm (4H, J= 8Hz) related to **j** and **o**, (t) at 3.52 ppm (4H, J= 4Hz) resultant to **k** and **n**, (t) at 3.05 ppm (2H, J= 4Hz) positions **q** and **n**. ^{13}C NMR (600 Hz, CDCl$_3$) (**figure 26**), presented signal peaks at 203.71 ppm due to **s**, 172.65 ppm related to **p**, 166.18 ppm corresponding to **i**, 142.90 ppm related to **f**, 126.77 ppm due to **b**, 123.68 ppm corresponds to **a** and **c**, 116.05 ppm linked to **d**, 109.24 ppm characteristic signal to **e**, 98.35 ppm due to **h**, 72.47, 69.98 and 69.25 ppm are related to cyclopentadiene ring of ferrocene, 58.45 ppm resultant to **k, l, m** and **n**, 39.34 ppm due to **j**, 34.88 ppm corresponding to **o**, 30.05 ppm related to **r** and 18.44 ppm due to **q**.

^{1}H NMR spectra (400 Hz, DMSO) for hybrid compound **3** (**figure 39**) signals (s) at 8.54 ppm (1H) due to **a**, (d) at 8.29 ppm (1H, J= 8Hz) related to **c**, (d) at 8.14 ppm (1H, J= 4Hz) corresponds to **s**, (s) at 6.78 ppm (1H) due to **p**, (s) at 5.75 (2H) linked to OCNH, (s) 4.36 (1H) Ar-NH, (dt) at 2.40 ppm (2H, J= 8, 4Hz). ^{13}C NMR (600 Hz, DMSO) (**figure 27**), presented signal peaks at 33.8 ppm linked to **l**, 25.75 ppm related to **j** and 24.93 ppm due to **k**.

^{1}H NMR spectra (400 Hz, DMSO) for hybrid compound **6a** (**figure 40**) signals (d) at 8.28 ppm (1H, J= 8Hz) due to **g**, (d) at 7.38 ppm (1H, J= 12Hz) related to **c**, (s) at 7.31 ppm (1H) corresponds to **a**, (d) at 5.59 ppm (1H, J= 8Hz) related to **h**, (s) at 4.27 ppm and (t) at 4.56 and 4.81 ppm characteristic signals to cyclopentadiene ring of ferrocene, (t) at 3.03 ppm (2H, J= 8Hz) related to **j**, (t) at 2.61 ppm (2H, J= 8Hz) due to **o**. ^{13}C NMR (600 Hz, DMSO) (**figure 28**) presented signal peaks at 154.02 ppm corresponding to **n**, 72.44, 70.13 and 69.47 due to cyclopentadiene ring of ferrocene, 32.20 ppm related to **k** and **l**, 30.82 ppm linked to **j** and **m**, 25.92 ppm due to **p** and 24.84 ppm linked to **o**. During synthesis of the compound a mixture of products was observed and separated accordingly to **6a** and **6b** and hybrid compound **6a** presented significant results to confirm the expected hybrid compound.

^{1}H NMR spectra (400 Hz, DMSO) for hybrid compound **6b** (**figure 41**) signals (d) at 8.41 ppm (1H, J= 4Hz) due to **g**, (d) at 8.28 ppm (1H, J= 4Hz) related to **c**, (s) at 7.80 ppm (1H) linked to **a**, (d) at 6.84 ppm (1H, J= 8Hz) corresponds to **d**, (d) at 6.56 ppm (1H, J= 4Hz) related to **h**. NMR results did not present clear signals for this compound mostly for carbon spectra this could be related to compounds not being soluble during analysis, however, compounds are still to be analyzed to confirm any personal or technical errors.

^{1}H NMR spectra (400 MHz, DMSO) for hybrid compound **5** (**figure 42**) signals (d) at 8.37 ppm (2H, J= 8Hz) linked to **c**, (d) at 8.24 ppm (1H, J= 8Hz) due to **d**, (d) at 7.79 ppm (1H, J= 4Hz) corresponding to **s**, (d) at 6.53 ppm (1H, J= 8Hz) related to **t**, (s) at 4.63 ppm (1H) due to

Ar-NH. ^{13}C NMR (600 MHz, DMSO) (**figure 29**), presented signal peaks at 154.47 ppm corresponding to **n**, 152.38 ppm related to **p**, 150.57 ppm corresponds to **r**, 150.30 ppm due to **i**, 149.51 ppm related to **g**, 133.89 ppm due to **f**, 129.87 ppm corresponding to **b**, 127.94 ppm related to **t**, 124.60 ppm due to **a** and **c**, 124.54 ppm resultant to **d**, 117.89 ppm related to **e**, 107.17 ppm linked to **h**, 108.71 ppm corresponding to **s**, 101.38 ppm due to position **o** and 99.25 related to **q**, 72.73 ppm linked **k** and **l**, 68.48 ppm corresponds to **m** and 60.68 ppm due to **j**.

4.4. LC-MS results for hybrid compounds

Table 4: LC-MS results of hybrid compounds

Compounds	Molecular formula	Molecular weight(g/mol)		Possible molecular formula	Figures
		Expected	Found		
1	$C_{18}H_{16}N_3ClO_3$	357	358	[M+H]	43
2a	$C_{25}H_{23}N_2ClFeO_3$	490	474	$C_{25}H_{23}N_2ClFeO_2$	44
2b	$C_{25}H_{23}N_2ClFeO_3$	490	491	[M+H]	45
3	$C_{19}H_{19}N_4O_2$	371	371	−	46
4	$C_{26}H_{26}N_3ClFeO_2$	503	493	−	47
5	$C_{20}H_{20}N_3ClO_4$	402	402	−	48
6a	$C_{27}H_{27}N_2ClFeO_4$	534	528	−	49
6b	$C_{27}H_{27}N_2ClFeO_4$	534	535	[M+H]	50
8	$C_{25}H_{24}N_3ClFeO_2$	489	490	[M+H]	51
9	$C_{22}H_{25}N_4ClO_4$	445	445	−	52
10a	$C_{29}H_{32}N_3ClFeO_4$	560	578	$C_{28}H_{30}N_3ClFeO_5$	53
10b	$C_{29}H_{32}N_3ClFeO_4$	560	578	$C_{28}H_{30}N_3ClFeO_5$	54
11	$C_{16}H_{13}N_4ClO_2$	329	317	$C_{16}H_{13}N_3ClO_2$	55

4.5. *In vitro* assay

Table 5: Shows alphabets as corresponding to Hybrid compounds

Compound	2a	1	4	8	FeC₄H₅O₃	9	C₇H₇NO₃	10b	3	6a	6b	5
Relevant alphabet	A	C	D	E	F	H	I	J	K	L	M	N

Dual-point analysis

The selected compounds were screened for *in vitro* asexual activity using the SYBR Green I-based assay on the NF54 strain of *P. falciparum* parasites. Each compound was tested at concentrations of 5 and 1 µM. Figure 29 indicates the percentage inhibition obtained against asexual parasites for compound concentrations of 1 µM and 5 µM for each series. Actual values are provided in Table 6 below.
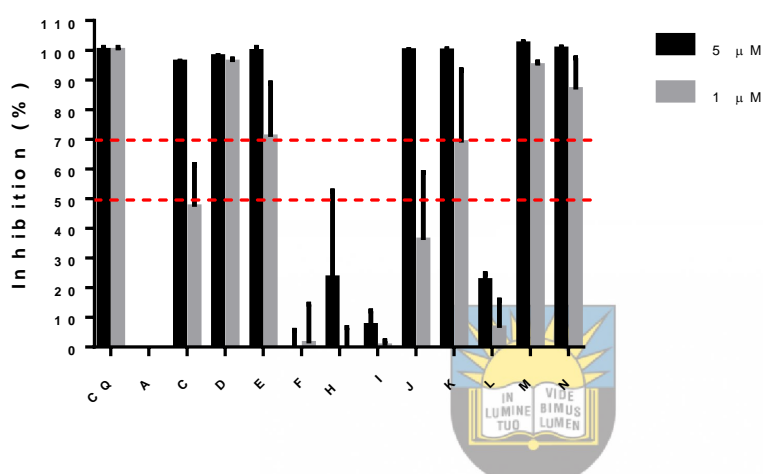
Figure 2: In vitro activity of compounds at 1 µM and 5 µM concentrations, against asexual stages of P. falciparum (n=1, one biological assay with technical triplicates). Negligible compound activity was obtained where there are no bars shown on the table.

Table 6: *In vitro* **activity of compounds o against asexual n** *P. falciparum* **parasites, obtained at concentrations of 1 µM and 5 µM (n=1, one biological assay with technical triplicates). CQ was used as a control compound. Compounds highlighted in dark grey indicate compounds with good activity, compounds highlighted in light grey indicate compounds with moderate activity.**

Dual Screens		
Compound name	**Asexual parasites, SYBR Green**	
	1 µM	**5 µM**
	% Inhibition	% Inhibition

z-factor	0.80	0.80
CQ (1 μM)	100	100
2a	0.0	0.0
1	47.2	96.0
4	96.0	97.9
8	70.8	99.6
Ferrocene butanoic acid	1.2	0.0
11	0.0	23.4
4-aminosalicylic acid	0.4	7.3
10b	36.0	99.9
3	68.9	99.8
6a	6.5	22.4
6b	94.8	102.2
5	86.7	100.4

4.6. Discussion

FTIR results for the synthesized hybrid compounds confirmed successful linkage of 4-aminoquinoline derivatives to the desired drugs to form hybrid compounds and the significant peaks were visible at (3320-3396 cm^{-1}) amides, (1082-1152 cm^{-1}) ester, (1619-1735 cm^{-1})

carbonyl carbons, (1518-1677 cm^{-1}) aromatic carbons and (478 cm^{-1}) cyclopentadiene ring of ferrocene moiety this is in agreement with results reported by (MacMillan *et al.*, 2013; Mahesh Bhata, 2014; Njogu, Omondi and Nyamori, 2016)[4–6].

NMR results presented positive and successful isolation of hybrid compounds with the number of carbons and protons found between (8.53-6.33 ppm) doublets, (8.10-6.71 ppm) singlets for aromatic protons, at (9.12-8.32) doublets and at (7.03-6.63 ppm) singlets for 4-aminosalicylic acid, at (2.77-3.66 ppm) amino group protons, at (4.12-4.81 ppm) singlet from cyclopentadiene ring of the ferrocene moiety, and the alkyl linkers triplet and quartet at (2.4-3.8 ppm). ^{13}C NMR (97.56-164.19 ppm) aromatic carbons, at (129.87-167 ppm) 4-aminosalicylic acid carbons, (154.02-156.87 ppm) ester carbons, at (152.47-172.65 ppm) amide carbons, at (201.37-203.71) ppm ketone and at (68.89-72.47 ppm) cyclopentadiene ring of the ferrocene moiety (Yong *et al.*, 2014; 'Supporting informations 1.1 General 1', 2016) reported similar results[7–9].

LC-MS was able to confirm the successful isolation of hybrid compounds thereby confirming the expected molecular weight and some of the compounds were visible as isotopes. Compounds with complete different molecular weight were analyzed to check the possible molecular weight and it is presented in the form of a molecular formula in table 2. The difference in expected molecular weight compared to the found molecular weight can be linked to impurities or fragmentation of the compound during separation via column chromatography.

Melting points and the yields of ferrocene hybrids were in the range of 90-153°C and 63-82%, respectively when compared to 4-aminosalicylic acid hybrids which were in the range of 87-187°C and 46-79%. Yong *et al.*, 2014; and Njogu, Omondi and Nyamori, 2016, reported ferrocene hybrids with melting points ranged from 88-174°C and yield between 75-94% and these are similar to the ones reported in this work[6,7]. The melting point of the hybrids increased with a decrease in the linker between the parent compounds (**10b** < **6b** < **4** < **8**), respectively.

Sheng *et al.*, 2008; and Dhaneshwar *et al.*, 2009 reported the melting points of 4-aminosalicylic acid hybrids in the range of 105-200°C and the yields in the range of 75-90%, respectively. Their findings are similar to those reported in this research[10,11]. The ferrocene containing hybrids were isolated in good yield when compared to hybrids containing 4-aminosalicylic acid scaffold (**8** < **6b**< **3**), respectively. *In vitro* assay on selected hybrids was also performed.

Singh *et al.*, 2017 prepared a series of hybrid compounds containing chloroquine and ferrocene moiety with a different linker and they reported them to be potent against asexual *P. falciparum* parasites *in vitro.* Their results can be compared with the findings obtained in this work in which ferrocene hybrids exhibited significant antimalarial activity **6a** (94.8% at 1µM and 102.2% at 5 µM), **8** (70.8 at 1 µM and 99.6 at 5 µM), **4** (96% at 1 µM and 97.9% at 5 µM) and it is evident that the percentage inhibition is influenced by concentration[12,13]. They further stated that amino alcohol linkers decreased the antimalarial activity of the compounds, however from this research, amino alcohols presented percentage inhibition of 86.7 to 94.8% at 1µM which is a significant antimalarial activity. The poor antimalarial activity can be linked to the length of the alky chain[14]. Manohar *et al.*, 2012 prepared hybrid compounds containing chloroquine with different alkyl linkers and they reported that the length of the linkers had no significant effect on the antimalarial activity of the hybrids prepared[15]. In this research, hybrid compounds with short linkers between both organic scaffolds (**1**, **2a** and **11**) and hybrid compounds with long linkers (**9** and **10b**) exhibited poor to moderate activity. Hu *et al*., 2017 further stated that bulky substituents linked to the amino group terminal may decrease the potency *in vitro*. However, their antimalarial activity was significant *in vivo* resulting from their decreased rate of efflux by the parasite[14]. (Biot *et al.*, 2007) reported that the antimalarial activity of the aminoquinoline compounds is influenced by the amino groups on the alkyl linkers[16] this can be supported by our findings where compounds (**3**, **4** and **8**) containing amino groups on the alkyl linkers exhibited good antimalarial activity with percentage inhibition

effect of 98%, 97%, 99.6% at 5 µM, respectively. The aforementioned findings indicate that the hybrid compounds may promote a high accumulation of the drug into the parasite food vacuole. Hybrid compounds **5** and **6** contain amino alcohol linkers and their percentage inhibition effect against asexual parasite was 100.4 and 102.2% which was higher than chloroquine. (Huang *et al.*, 2012; Bilsland *et al.*, 2018) reported that dihydrofolate compounds exhibit enhanced inhibition effect against asexual parasite[17,18]. 4-aminosalicylic acid (7.3% at 5 µM) and ferrocene butanoic acid (0.0% at 5 µM) were not effective against the asexual parasite. However, hybridizing 4-aminosalicylic acid or ferrocene butanoic acid with 4-aminoquinoline derivatives resulted in hybrid compounds with significant antimalarial activity. This finding suggests that ferrocene butanoic acid and 4-aminosalicylic acid act as potentiating agents. However, more studies are required in order to understand the mode of action of these hybrid compounds.
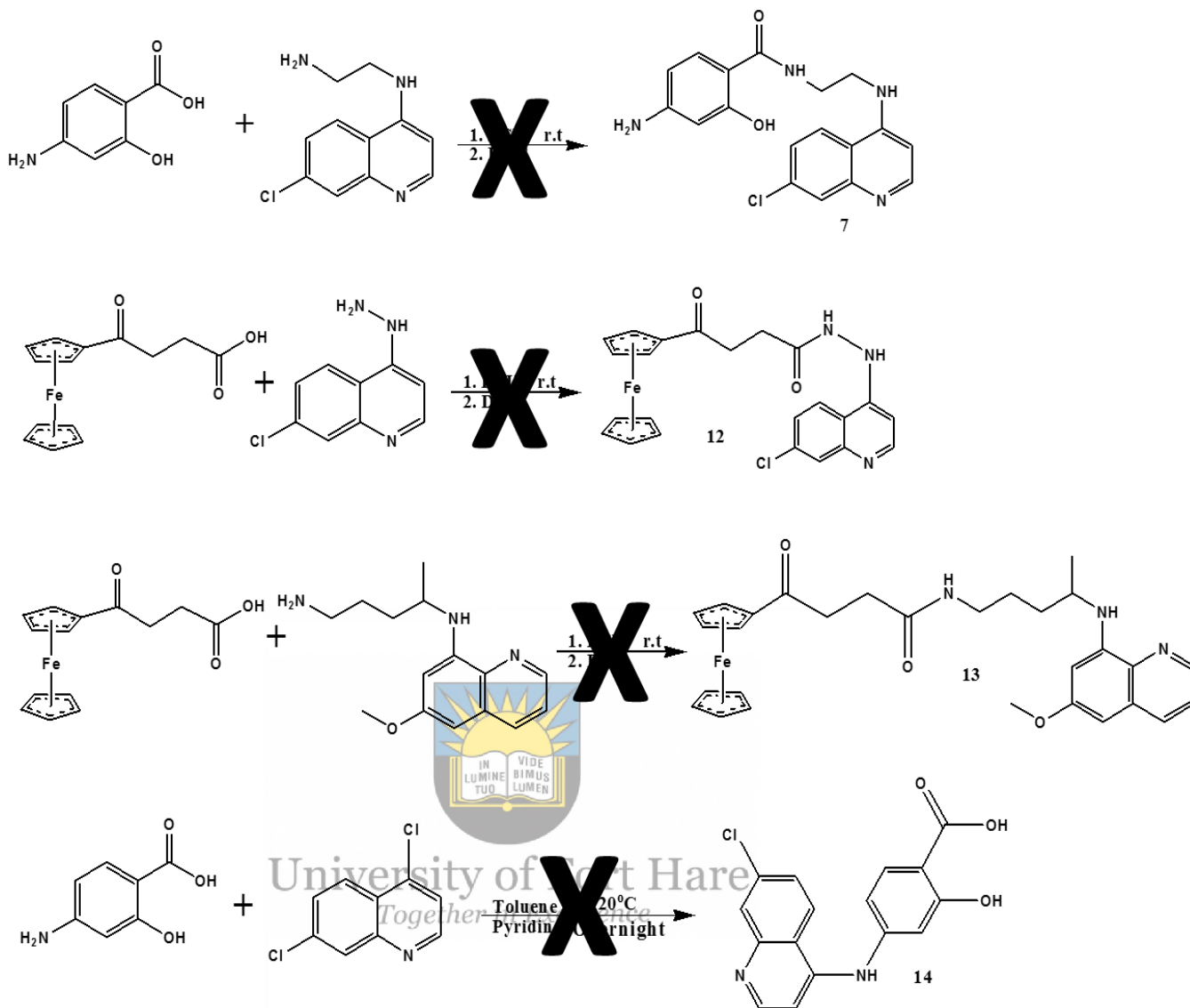
Scheme 24: Unsuccessful hybrid compounds

A series of hybrid compounds that were not successfully isolated were not characterized and challenges leading to poor isolation are still to be done as future work. Thin layer chromatography presented or revealed decomposed compounds. However, further modifications to their procedure are still to be done.

References

1. Khalil W.K.B, Ghaly I.S DKA. International Journal of Pharmacy Practice. *Conf 5*. 2010;4(3):68-82. doi:10.1016/j.ijpharm.2010.06.045

2. Pretorius IS. Synthesis, characterisation and antimalarial activity of quinoline-pyrimidine hybrids. 2012.

3. Smit F. Synthesis and in vitro antimalarial activity of novel chalcone derivatives. 2014;(May).

4. MacMillan DS, Murray J, Sneddon HF, Jamieson C, Watson AJB. Evaluation of alternative solvents in common amide coupling reactions: Replacement of dichloromethane and N,N-dimethylformamide. *Green Chem*. 2013;15(3):596-600. doi:10.1039/c2gc36900a

5. Mahesh Bhata BSL. Synthesis of Azo-Bridged Benzothiazole-Phenyl Ester Derivatives via Steglich Esterification. *Int J Curr Eng Technol*. 2014;4(4):2711-2715.

6. NJOGU EM, OMONDI B, NYAMORI VO. Synthesis, Physical and Antimicrobial Studies of Ferrocenyl-N-(pyridinylmethylene) anilines and Ferrocenyl-N-(pyridinylmethyl) anilines. *South African J Chem*. 2016;69:51-66. doi:10.17159/0379-4350/2016/v69a7

7. Yong J, Jiang X, Wu X, Huang S, Zhang Q, Lu C. Synthesis and Characterization of Ferrocene Derivatives and Preliminarily Electrocatalytic Oxidation of L-Cysteine at Nafion-Ferrocene Derivatives Modified Glassy Carbon Electrode. *Adv Chem*. 2014;2014(Scheme 1):1-7. doi:10.1155/2014/987481

8. Carbon Synthesis and Reactions of Ferrocene.

9. Supporting informations 1.1 General 1. 2016;4(3).

10. Dhaneshwar SS, Chail M, Patil M, Naqvi S, Vadnerkar G. Colon-specific mutual amide prodrugs of 4-aminosalicylic acid for their mitigating effect on experimental colitis in rats. *Eur J Med Chem*. 2009;44(1):131-142. doi:10.1016/j.ejmech.2008.03.035

11. Sheng SF, Zheng HX, Liu J, Zhao ZB. Synthesis of phenol-class azo derivatives of 4-aminosalicylic acid. *Chinese Chem Lett*. 2008;19(4):419-422. doi:10.1016/j.cclet.2008.01.042

12. Wani WA, Jameel E, Baig U, Mumtazuddin S, Hun LT. Ferroquine and its derivatives: New generation of antimalarial agents. *Eur J Med Chem*. 2015;101:534-551. doi:10.1016/j.ejmech.2015.07.009

13. Singh A, Gut J, Rosenthal PJ, Kumar V. European Journal of Medicinal Chemistry 4-Aminoquinoline-ferrocenyl-chalcone conjugates : Synthesis and anti-plasmodial evaluation. *Eur J Med Chem*. 2017;125:269-277. doi:10.1016/j.ejmech.2016.09.044

14. Hu YQ, Gao C, Zhang S, Xu L, Xu Z, Feng LS, Wu X, Zhao F. Quinoline hybrids and their antiplasmodial and antimalarial activities. *Eur J Med Chem*. 2017;139:22-47. doi:10.1016/j.ejmech.2017.07.061

15. Manohar S, Rajesh UC, Khan SI, Tekwani BL, Rawat DS. Vitro and in Vivo Antimalarial Activity. 2012:6-10.

16. Biot C, Pradines B, Ne Sergeant M-H, Gut J, Rosenthal PJ, Chibale K. Design, synthesis, and antimalarial activity of structural chimeras of thiosemicarbazone and ferroquine analogues. 2007. doi:10.1016/j.bmcl.2007.10.003

17. Huang H, Lu W, Li X, Cong X, Ma H, Liu X, Zhang Y, Che P, Ma R, Li H, Shen X, Jiang H, Huang J, Zhu J. Design and synthesis of small molecular dual inhibitor of falcipain-2 and dihydrofolate reductase as antimalarial agent. *Bioorganic Med Chem Lett*. 2012;22(2):958-962. doi:10.1016/j.bmcl.2011.12.011

18. Bilsland E, Van Vliet L, Williams K, Feltham J, Carrasco MP, Fotoran WL, Cubillos EFG, Wunderlich G, Grøtli M, Hollfelder F, Jackson V, King RD, Oliver SG. Plasmodium dihydrofolate reductase is a second enzyme target for the antimalarial action of triclosan. *Sci Rep*. 2018;8(1):1-8. doi:10.1038/s41598-018-19549-x

University of Fort Hare

Together in Excellence

Chapter 5
5. Conclusion

FTIR results for the synthesized hybrid compounds confirmed successful linkage of 4-aminoquinoline derivatives to the desired drugs to form hybrid compounds and the significant peaks were visible at (1082-1152 cm^{-1}) for ester linkers, (3320-3396 cm^{-1}) for amides linkers, at (1619-1735 cm^{-1}) for the carbonyl carbons and at (1518-1677 cm^{-1}) for the aromatic C=C stretch.

NMR results presented positive and successful isolation of hybrid compounds with signals for aromatic protons between (9.15-6.33 ppm) for doublets and at (8.10-6.71 ppm) for singlets, (9.12-8.32) doublets, (7.03-6.63 ppm) singlets for 4-aminosalicylic acid, the amino protons were visible at (2.77-3.66 ppm) and at (4.12-4.81 ppm) peaks of the cyclopentadiene ring of the ferrocene moiety was significant. The protons on the linkers were visible as triplets and quartets between (2.4-3.8 ppm). On the ^{13}C NMR spectra of the hybrid compounds, at (97.56-164.19 ppm) the aromatic carbons signals were found, at (129.87-167 ppm) 4-aminosalicylic acid carbons, at (154.02-156.87 ppm) the ester carbons were visible, at (152.47-172.65 ppm) the amide carbons were visible, and at (201.37-203.71 ppm) and (68.89-72.47 ppm) ketone and cyclopentadiene ring of the ferrocene moiety carbons were visible, respectively.

LC-MS was able to confirm successful isolation of hybrid compounds thereby confirming the expected molecular weight and some of the compounds were visible as isotopes. Compounds with complete different molecular weight were analyzed to check the possible molecular weight and it is presented in a form of molecular formula in table 2. The difference in expected molecular weight compared to found can be linked to impurities or fragmentation of the compound during separation via column chromatography.

Ferrocene hybrids were isolated in good yields and low melting points of 63-82% and 90-153°C, respectively when compared to 4-aminosalicylic acid hybrids with a melting point in

the range of 87-187°C and yields of 46-79%. The melting point trend increases from the longer linkers to the short linkers (**10b** < **6b** < **4** < **8**), respectively. The hybrids with good yield were those of ferrocene compared with 4-aminosalicylic acid, compound **8** < **6b** < **3** respectively, apart from the yield *in vitro* assay on selected hybrids was performed.

Selected compounds were screened for in vitro assay against the asexual parasite and compounds with ferrocene butanoic acid presented percentage inhibition in the range of 22.4-102.2% at 5μM, 4-aminosalicylic acid from 23.4% to 98.9% at 5μ respectively regardless of the ester or amide bond. The hybrid compounds containing the same 4-aminoquinoline derivatives presented similar antimalarial activity when hybridized with either ferrocene butanoic acid or 4-aminosalicylic acid. The inhibition effect of compound **3** was (99.8% at 5μM), **4** (97.9% at 5μM), **5** (100.4% at 5μM) and **6b** (102.2% at 5μM). This indicates that the nature of the alkyl linkers used in the design of the hybrids plays a significant role in the antimalarial activity of the hybridized compounds. We can conclude that hybrid compounds containing a combination of 4-aminoquinoline derivatives with either ferrocene or 4-aminosalicylic acid scaffolds are promising antimalarials which can be modified into potent compounds, that can overcome drug resistance which is common in the currently used antimalarials. From these findings, it can be said that hybrid compounds containing an alkyl linker of 3 to 5 carbon positions from the aminoquinoline moiety are a promising approach for the designing of potent antimalarials. Regardless of these compounds showing antimalarial activity, further clinical studies are still to be performed including the evaluation of the mode of action of the hybrid compounds.

5.1. Future work

Compounds showing **good activity** will be prioritized for full IC_{50} determination (n=3) against asexual drug sensitive NF54 and K1 and W2 drug-resistant *P. falciparum* parasites.

Compounds showing **moderate activity** will be prioritized for a single IC_{50} determination (n=1) against asexual NF54 and K1 and W2 drug-resistant *P. falciparum* parasites followed by *in vivo* studies.

The synthetic approach will be reviewed for the synthesis of compounds **7**, **12**, **13**, **14** which were not successfully isolated. The structures for hybrids **6a** and **10a** were not fully elucidated. More studies will be performed to fully elucidate the structures of these compounds.

5.2. Appendix

5.2.1. FTIR spectra's of 4.7-dichloroquinoline derivatives
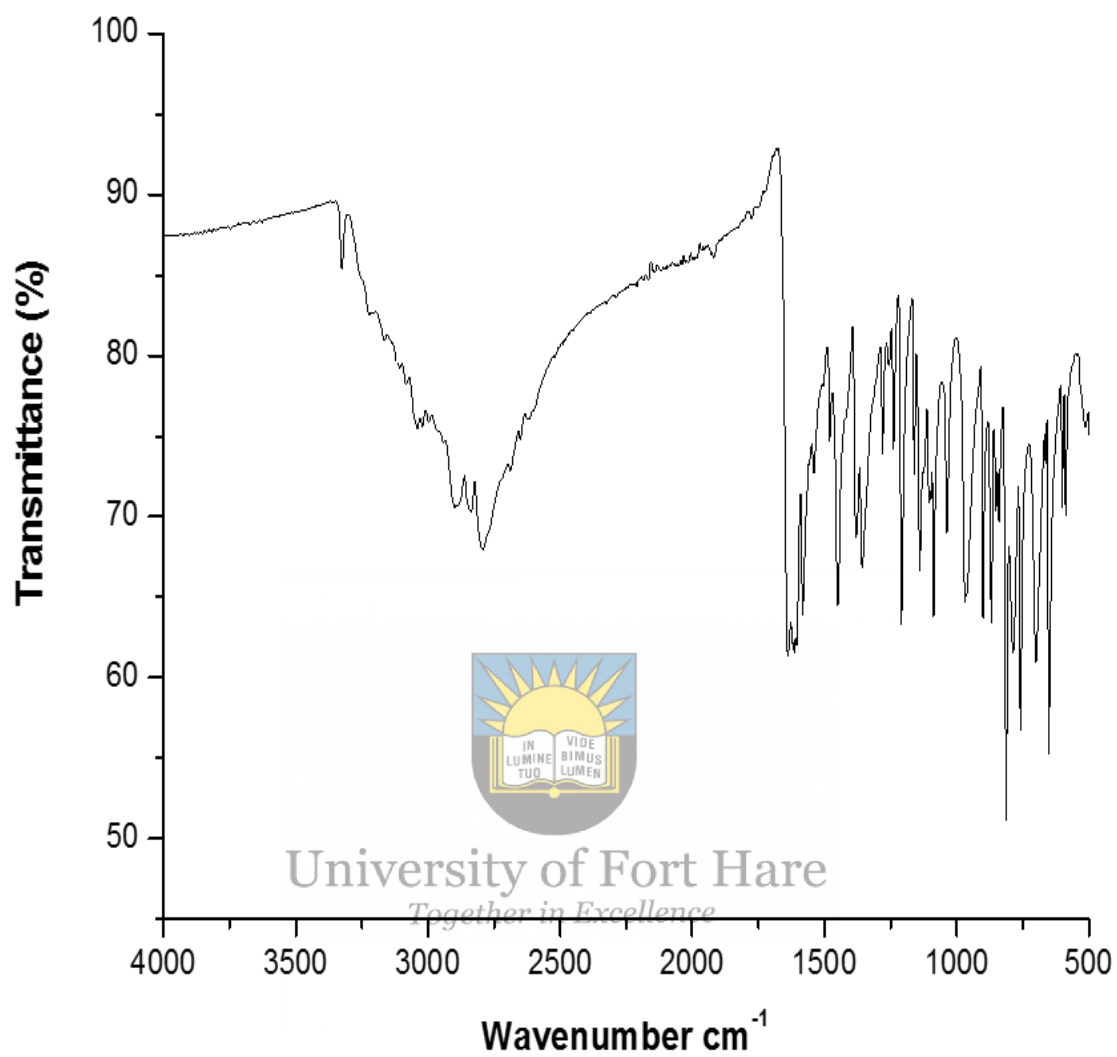
Figure 3: FTIR results for 1-(7-chloroquinolin-4-yl)hydrazine
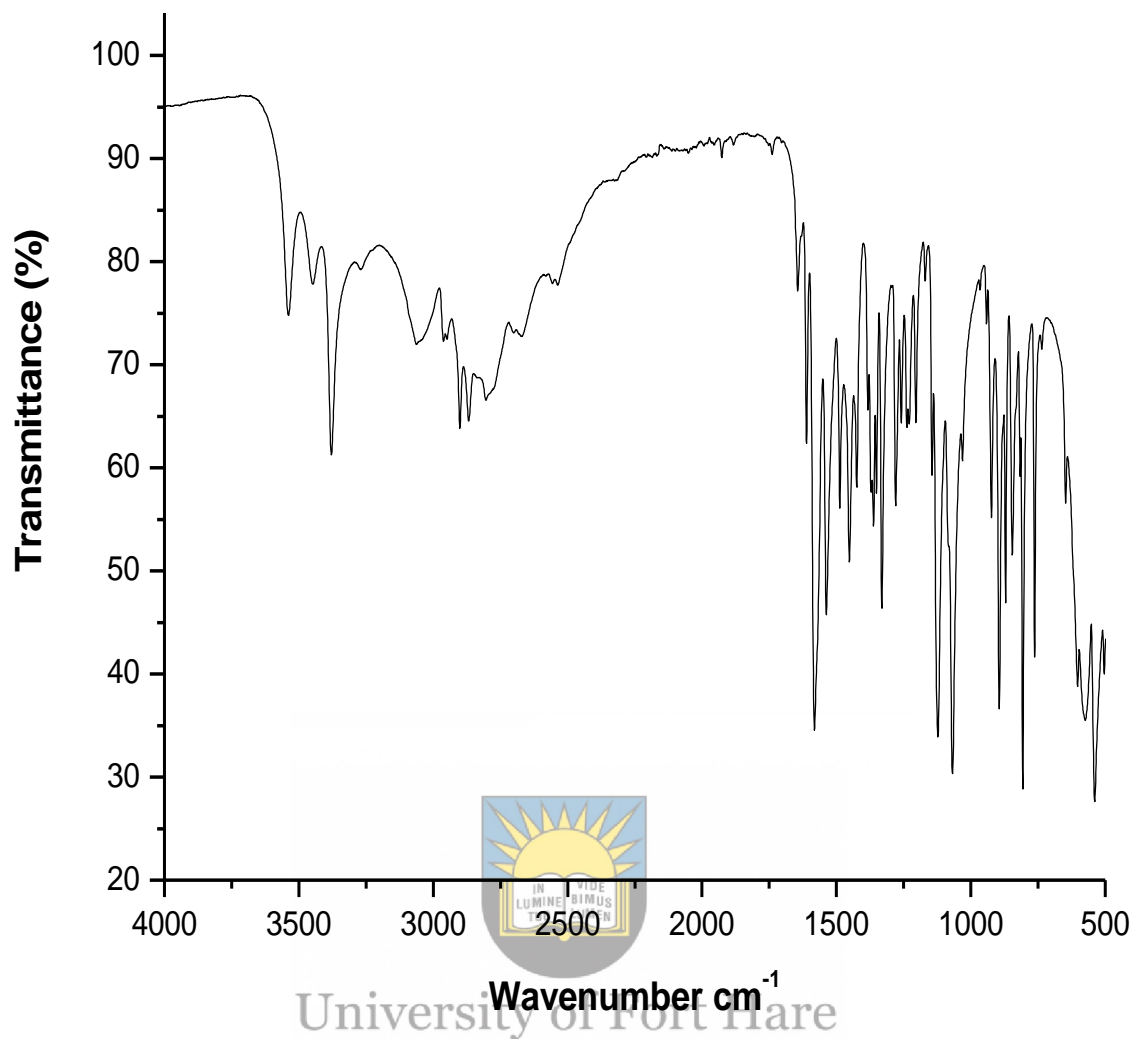
Figure 4: FTIR results of 2-(2-(7-chloroquinolin-4-ylamino)ethoxy)ethanol
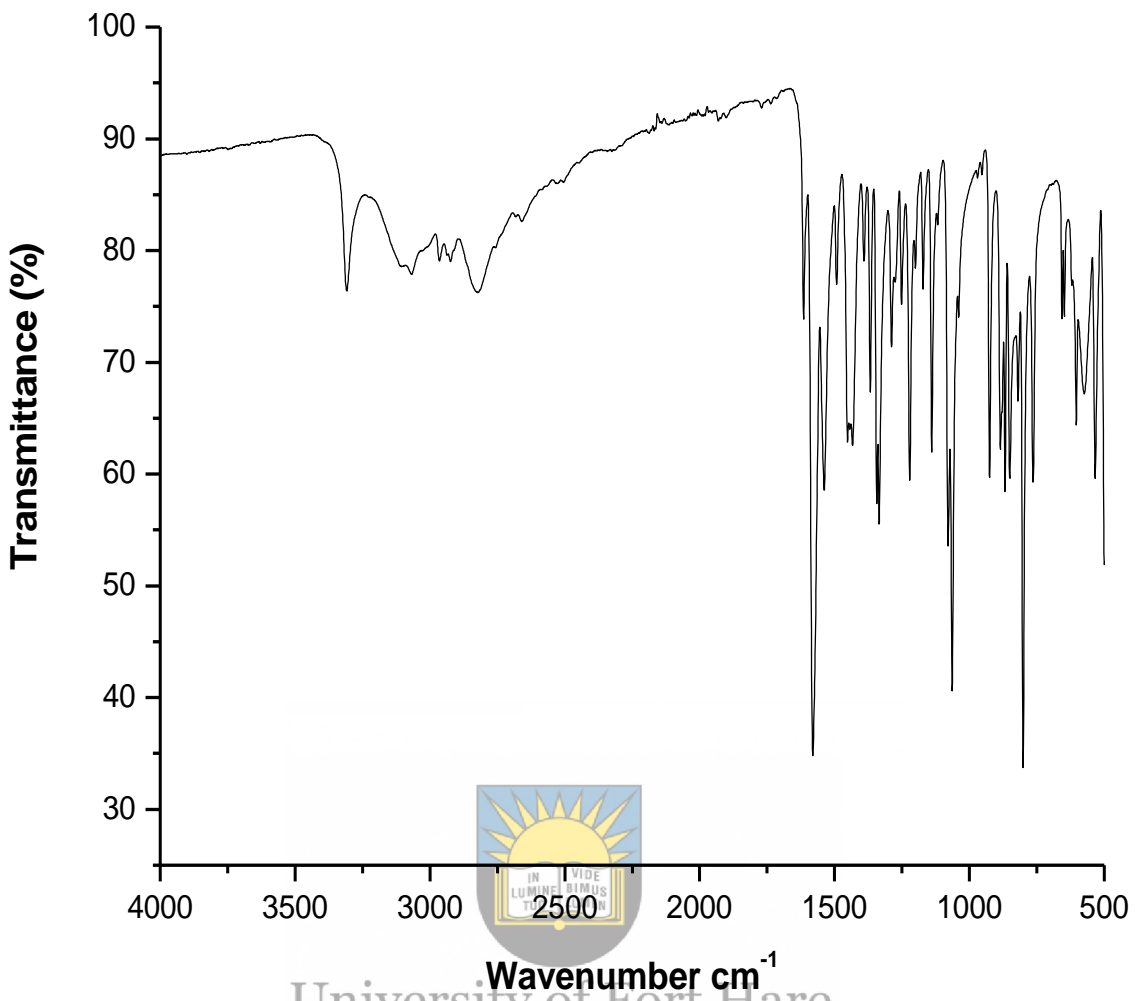
Figure 5: FTIR results of 2-(7-chloroquinolin-4-ylamino)ethanol
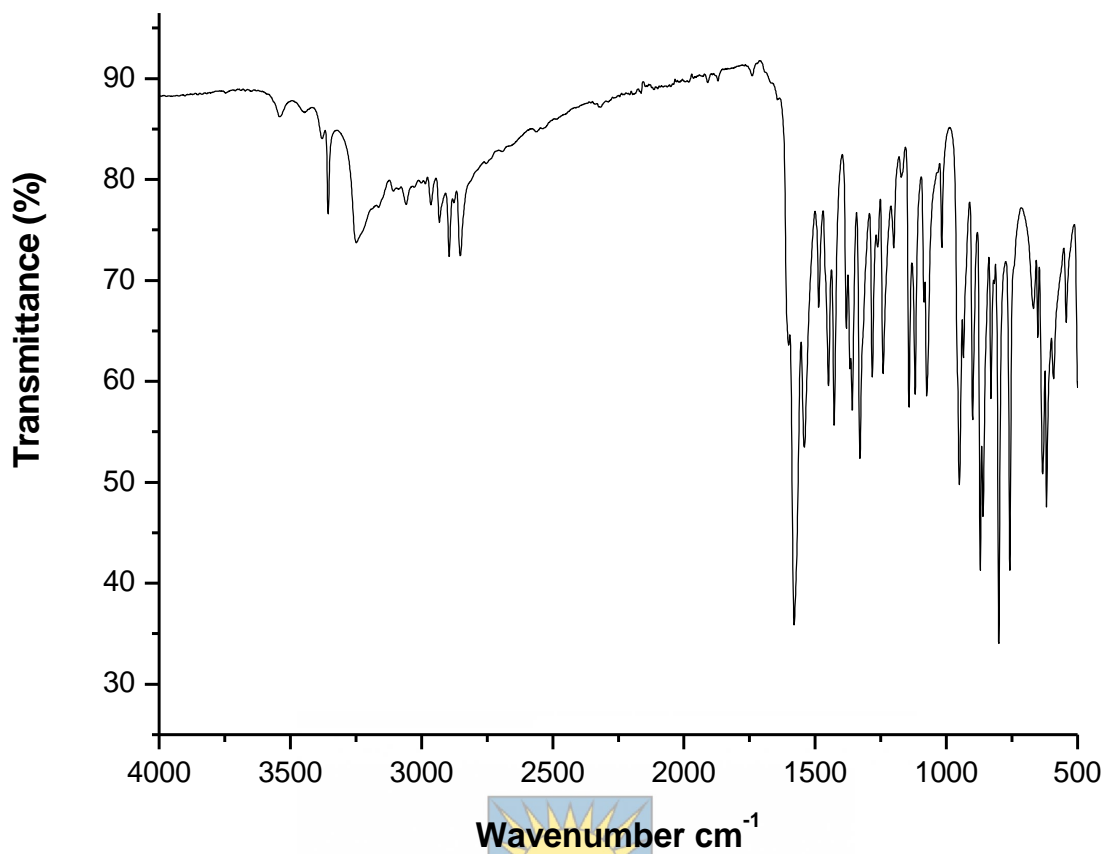
Figure 6: FTIR results of N-(2-aminoethyl)-7-chloroquinolin-4-amine
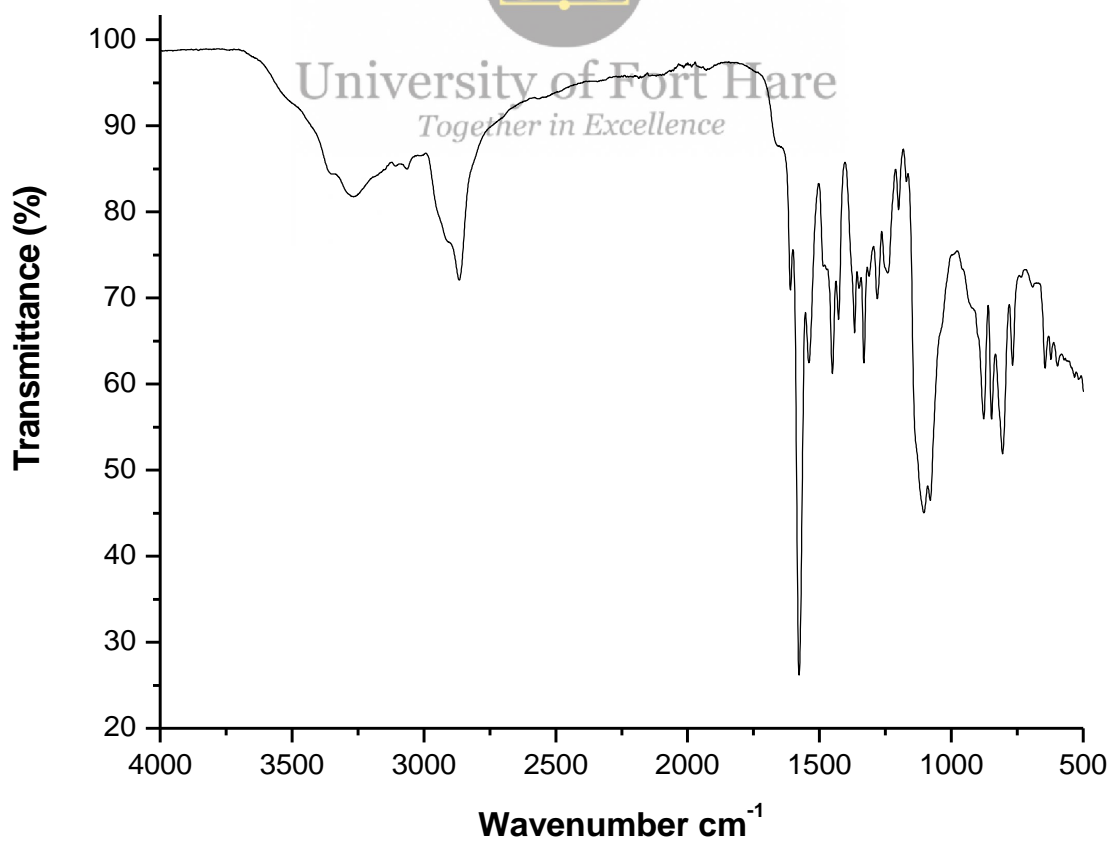
Figure 7: FTIR results of N-(2-(2-(2-aminoethoxy)ethoxy)ethyl)-7-chloroquinolin-4-amine
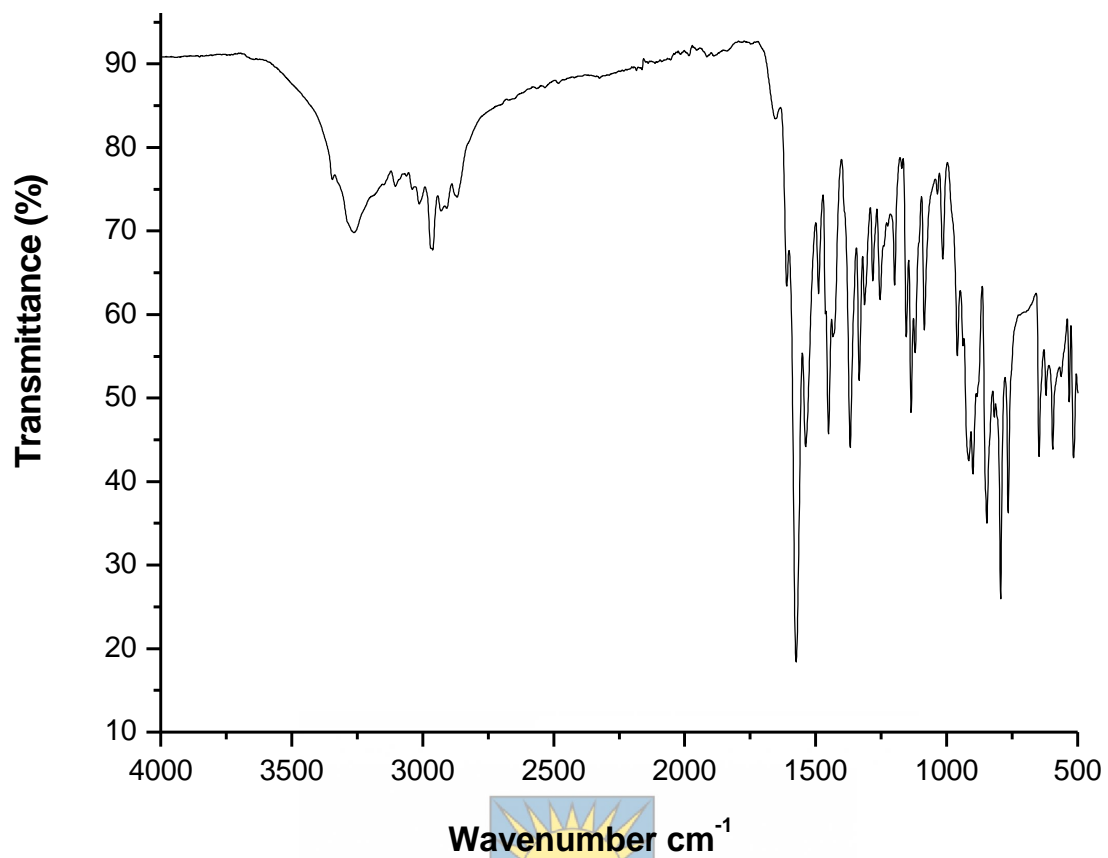
Figure 8: FTIR results of N-(3-aminopropyl)-7-chloroquinolin-4-amine

5.2.2. FTIR spectra's for hybrid compounds
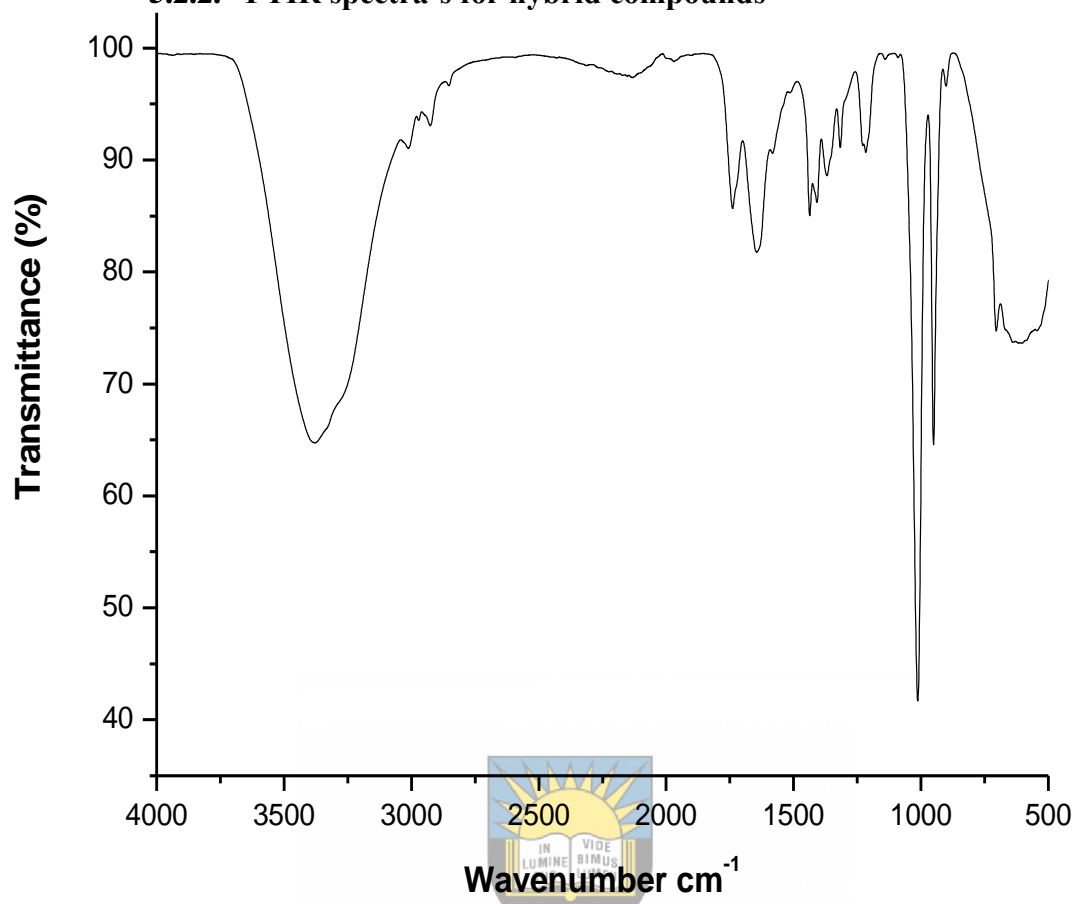
Figure 9: FTIR results of hybrid compound 9
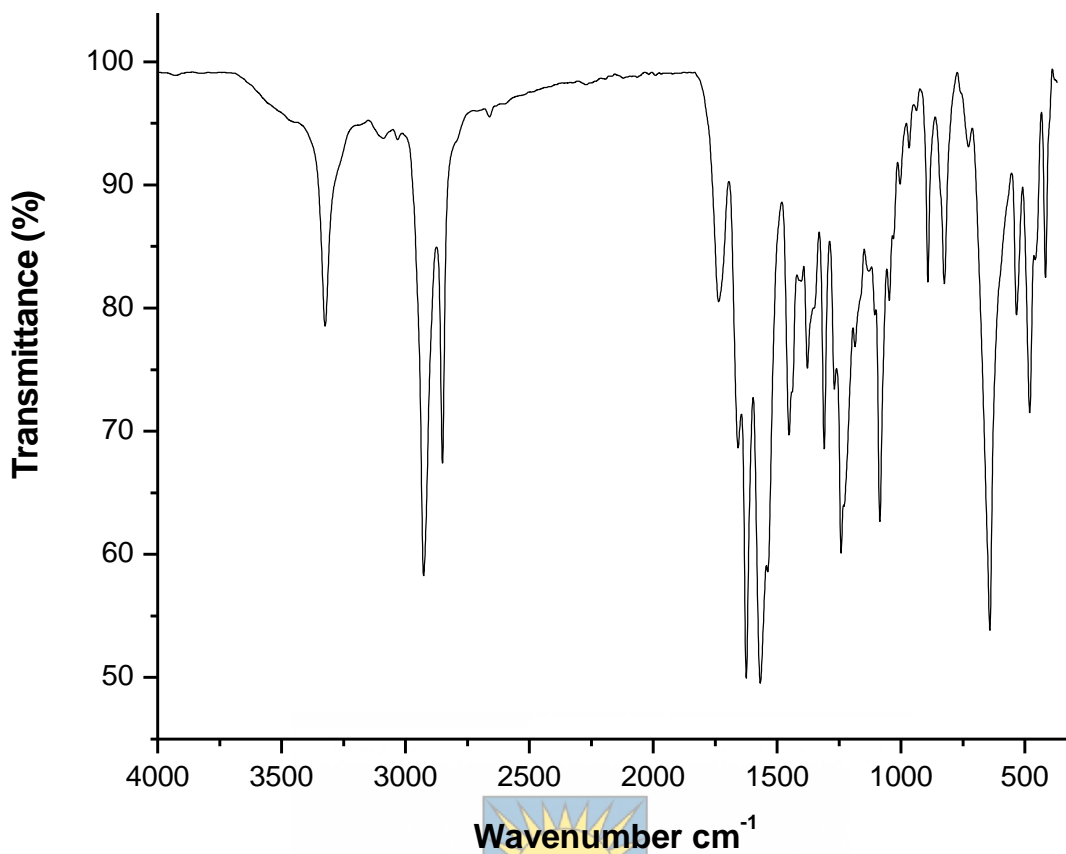
*Figure 10: FTIR results for hybrid compound **10a***
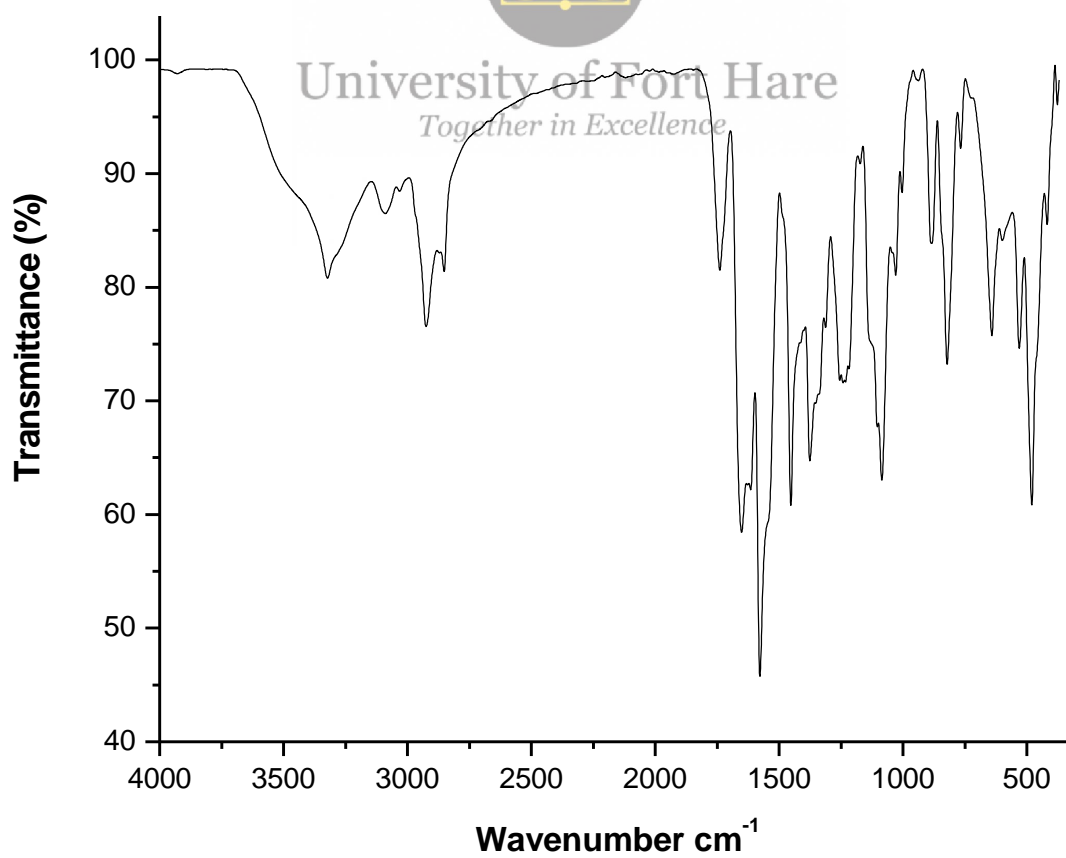
*Figure 11: FTIR results for hybrid compound **10b***
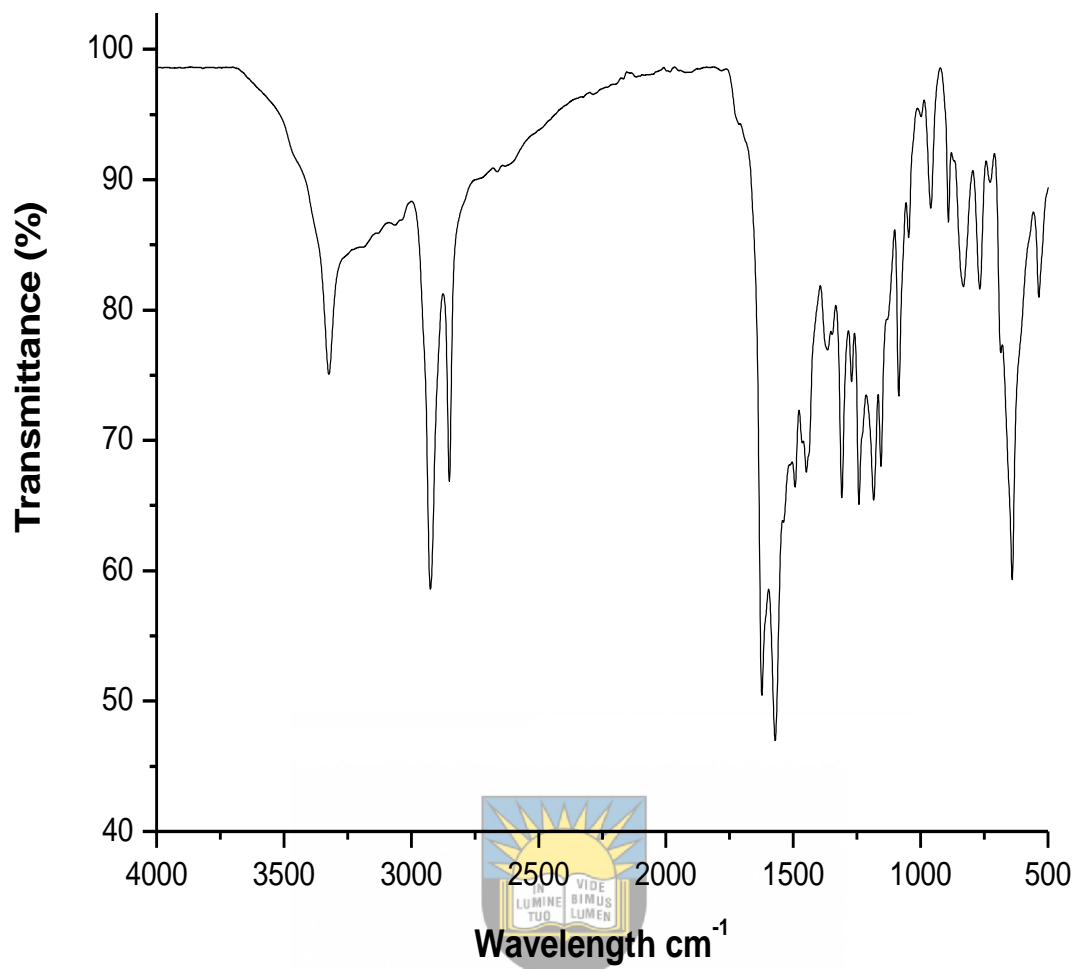
Figure 12: FTIR results for hybrid compound 11
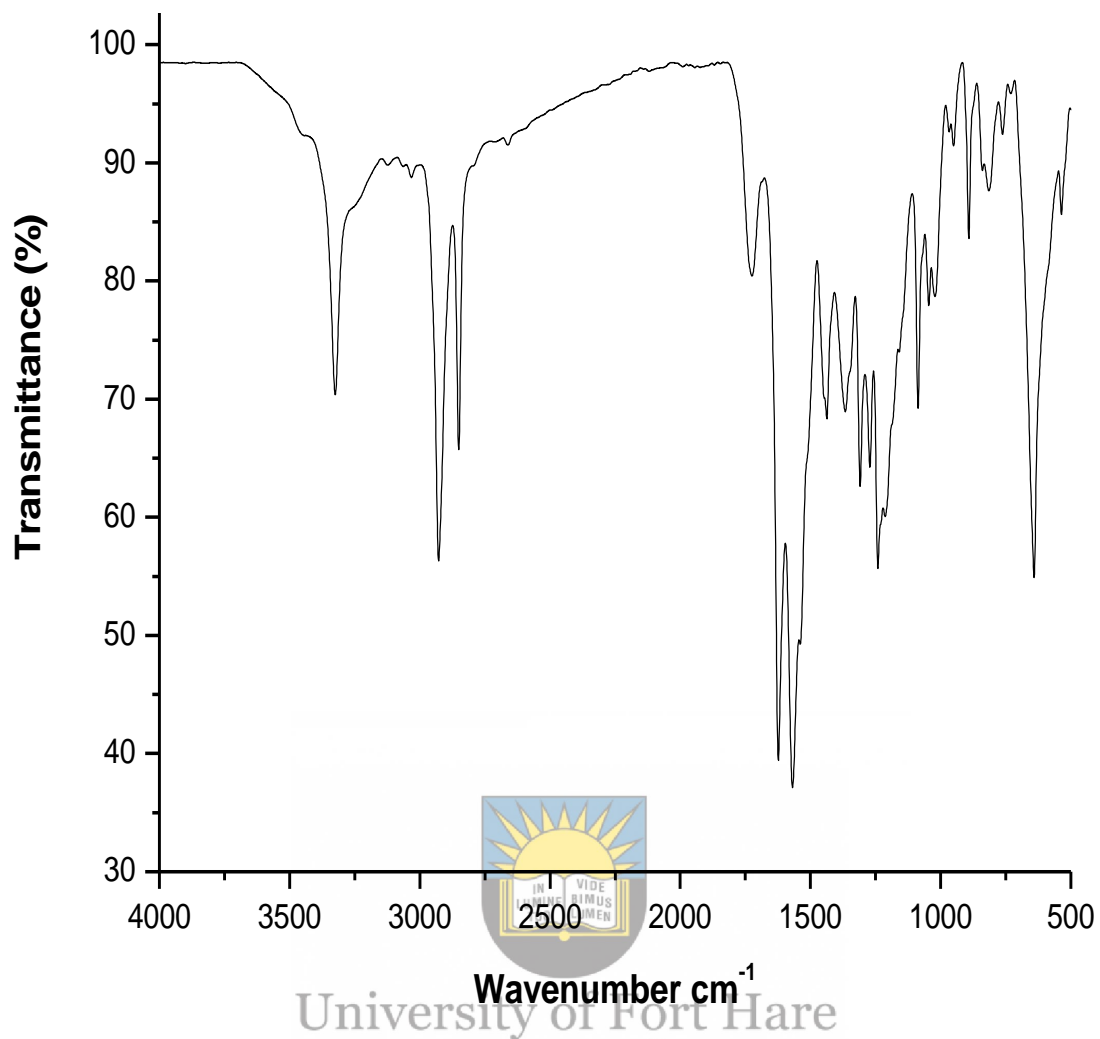
Figure 13: FTIR results for hybrid compound 3
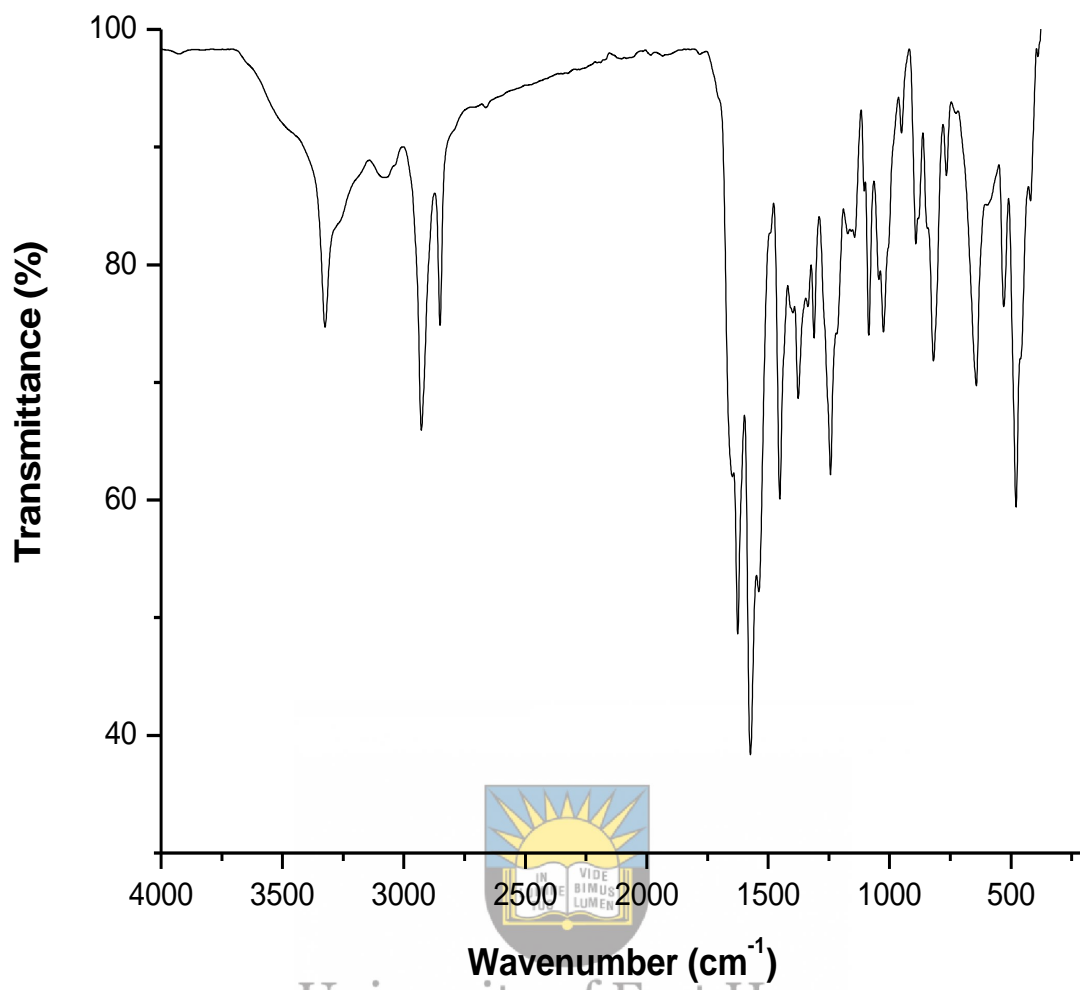
Figure 14: FTIR results for hybrid compound 4
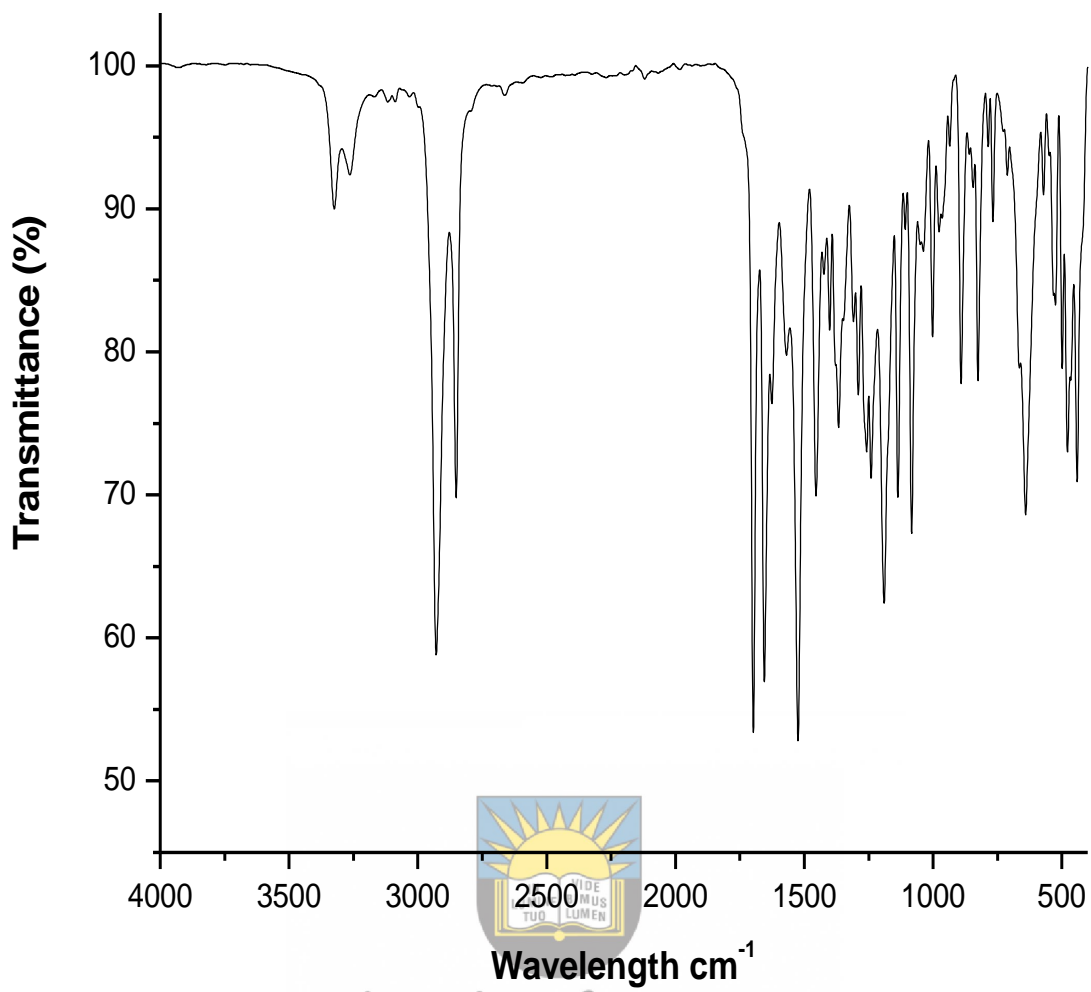
Figure 15: FTIR results for hybrid compound 6
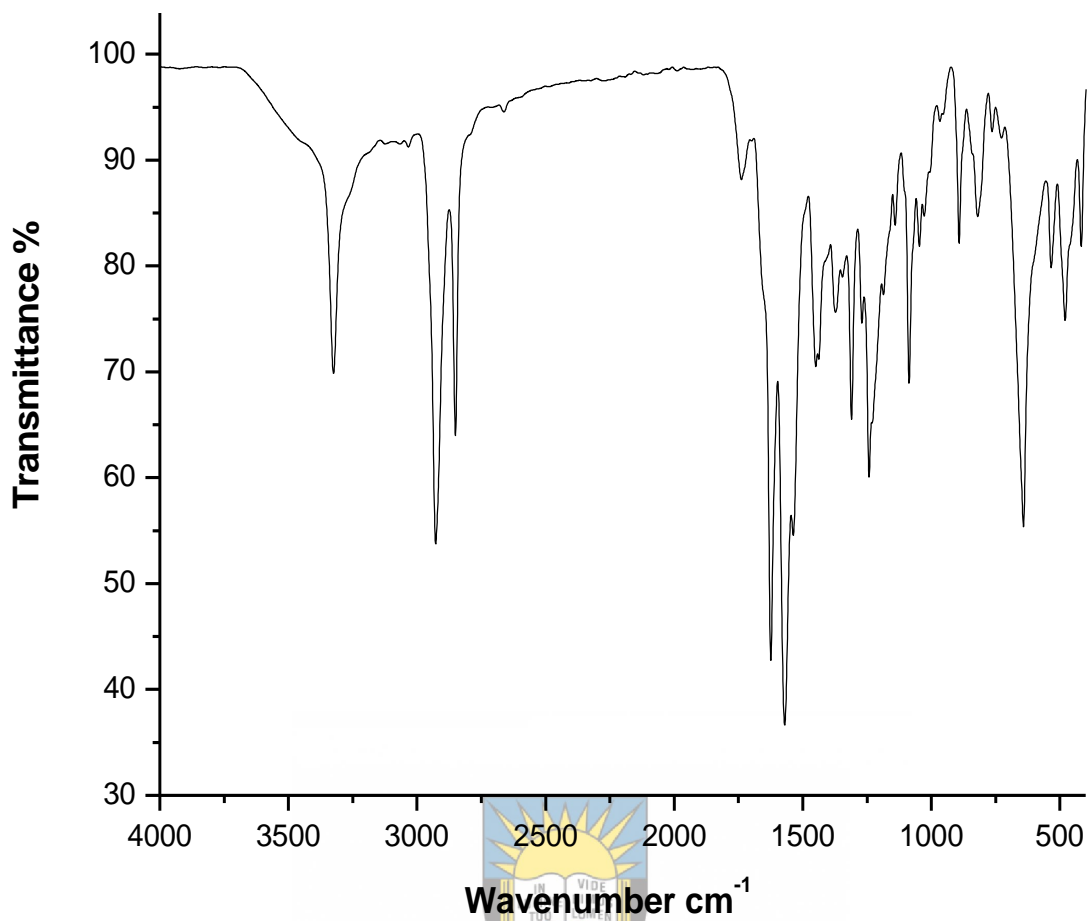
Figure 16: FTIR results for hybrid compound 8
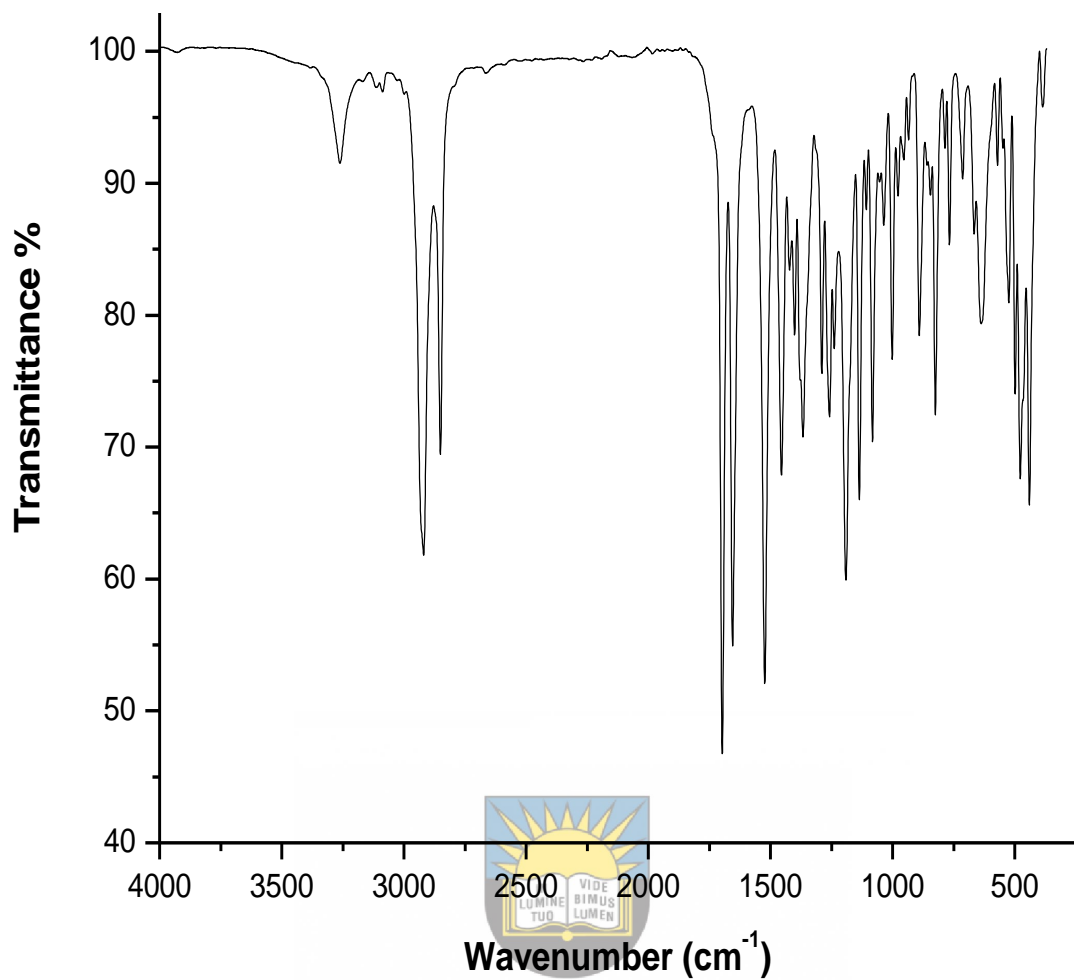
*Figure 17: FTIR results for hybrid compound **2a***

5.2.3. ^{13}CNMR spectra's
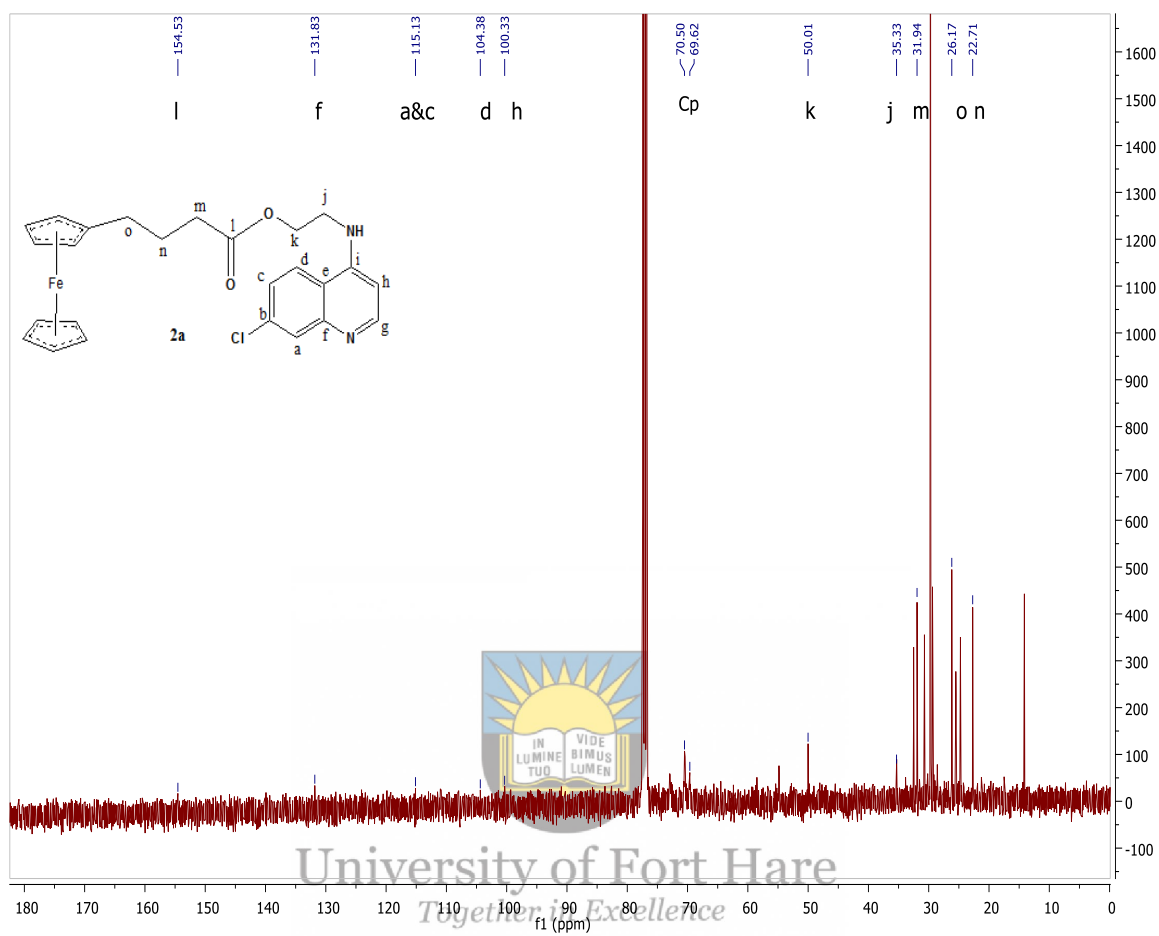
*Figure 18: ^{13}C NMR spectra (600 Hz, DMSO) for compound **2a***
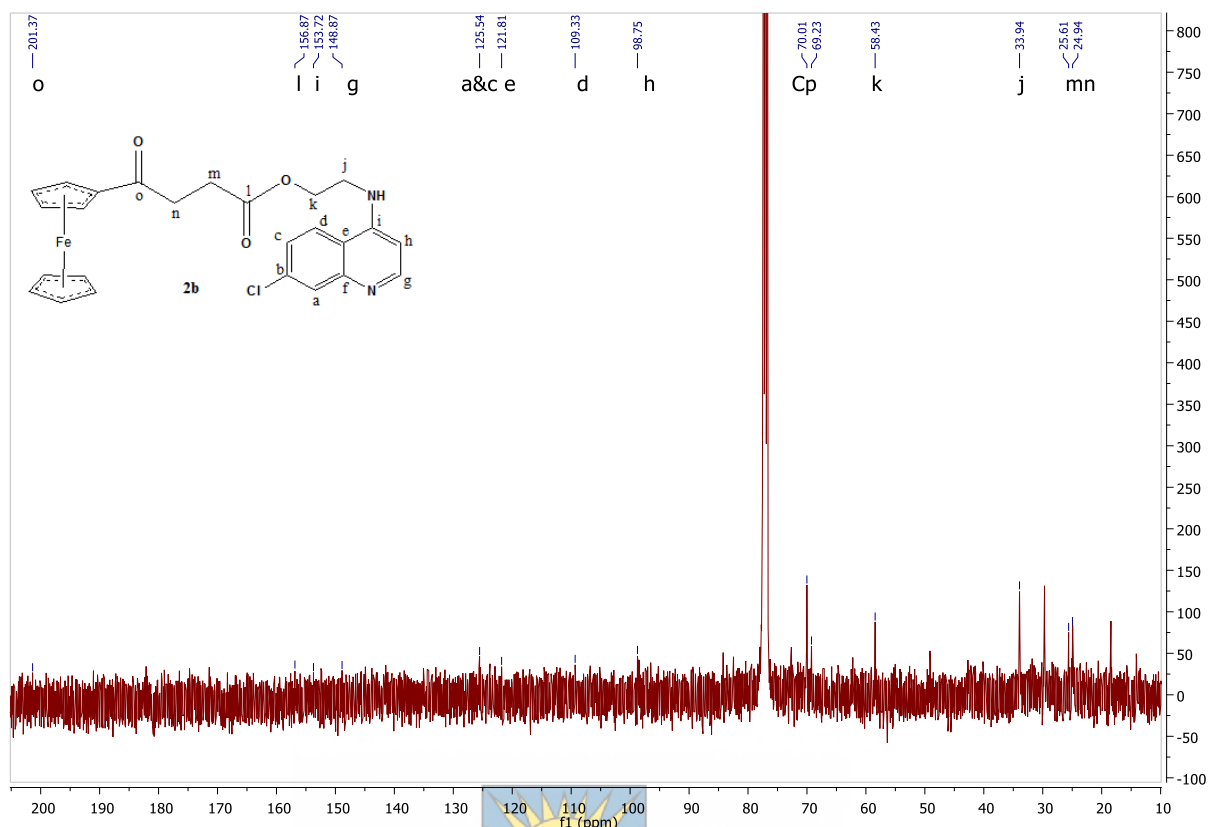
*Figure 19: ^{13}C NMR spectra (600 Hz, DMSO) for compound **2b***
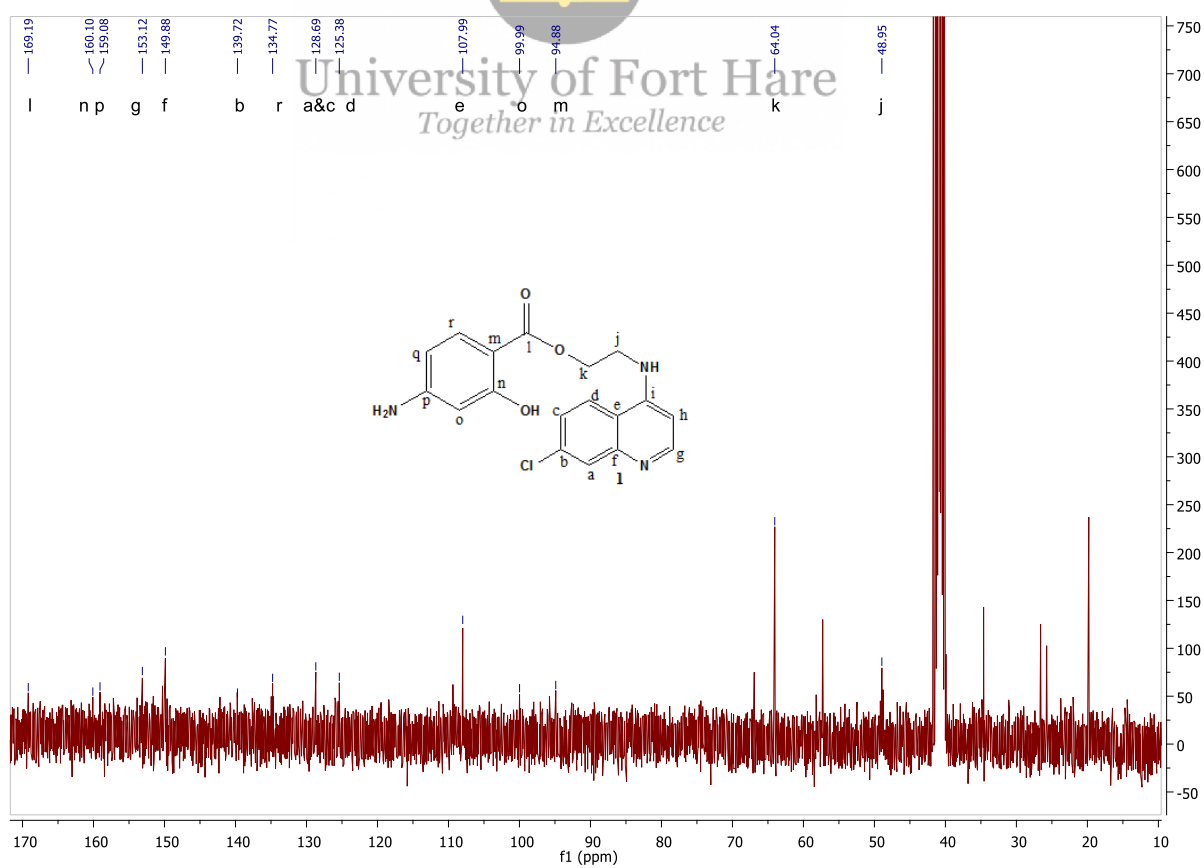
*Figure 20: ^{13}C NMR spectra (600 Hz, DMSO) for hybrid compound **1***
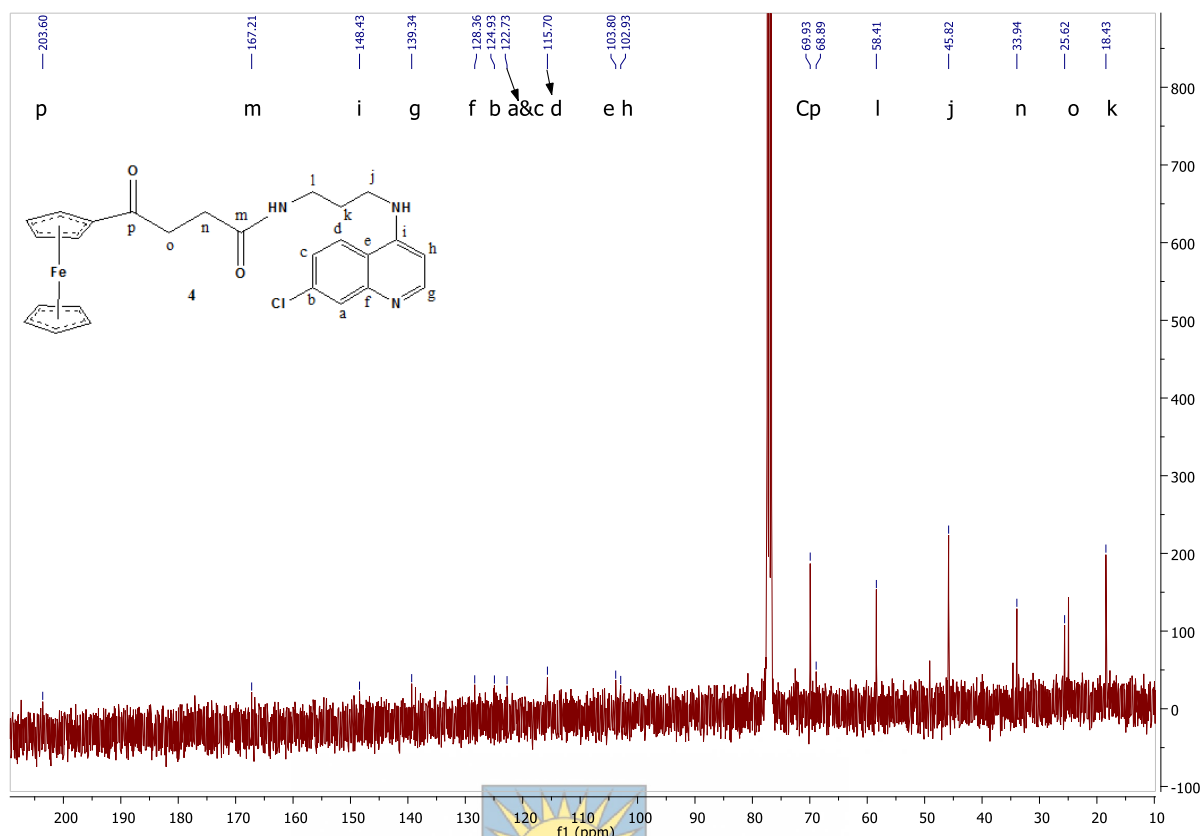
*Figure 21: ^{13}C NMR spectra (600 Hz, DMSO) for hybrid compound **4***
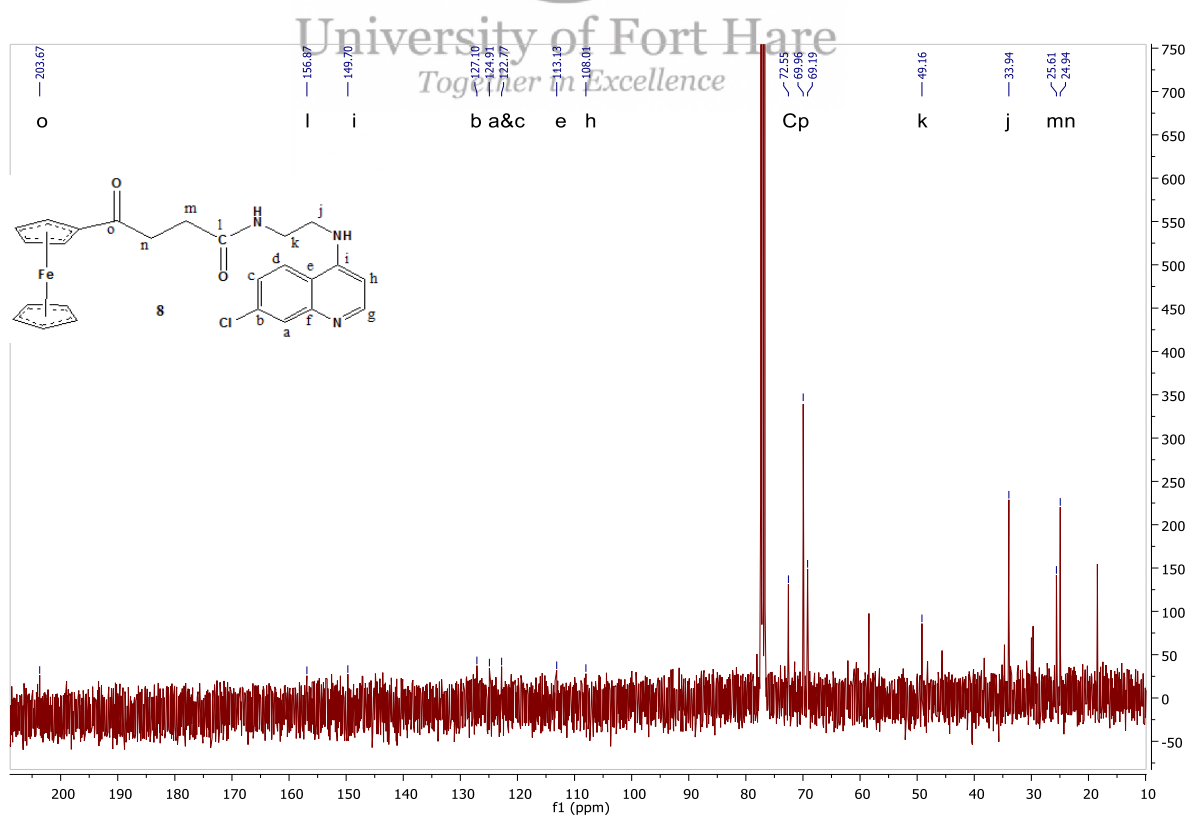
*Figure 22: ^{13}C NMR spectra (600 Hz, DMSO) for hybrid compound **8***
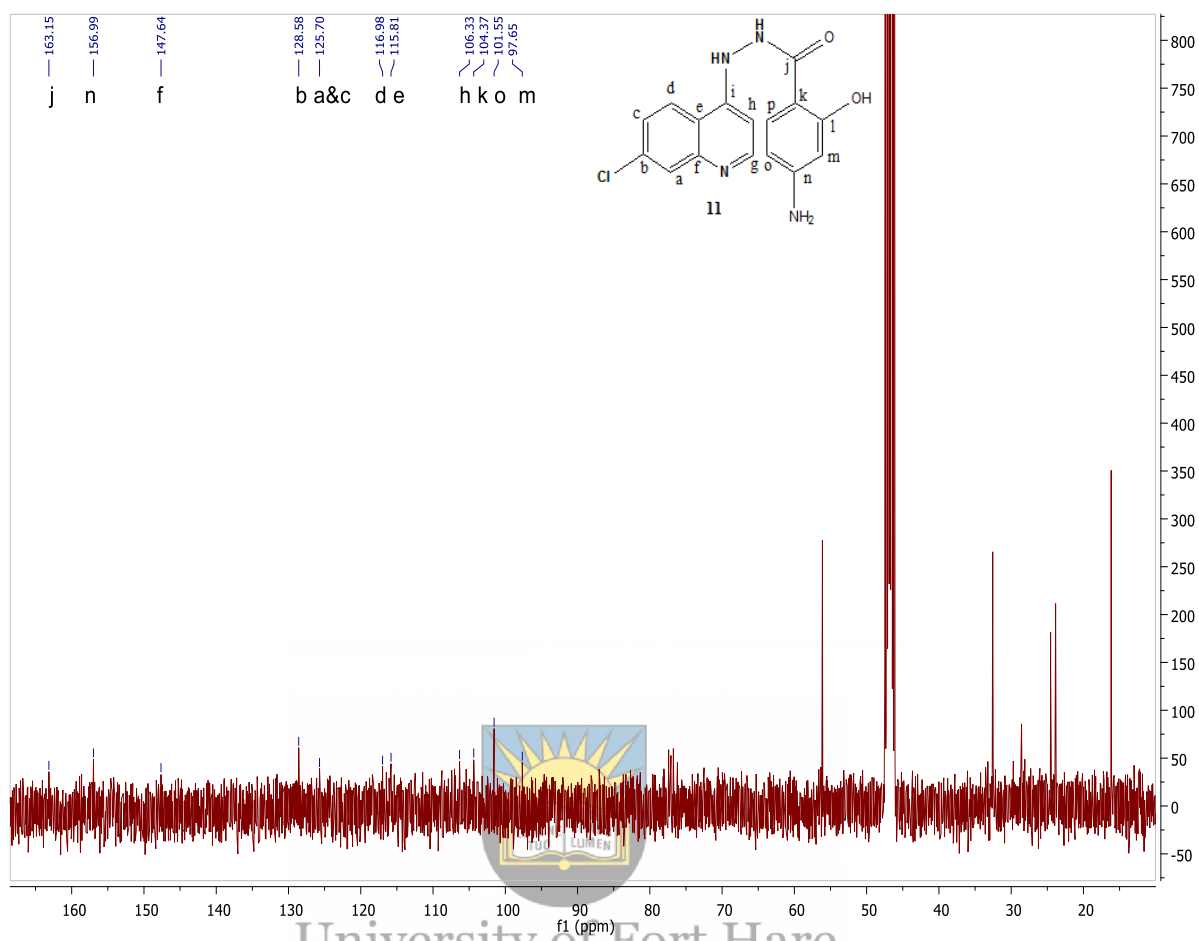
Figure 23: ¹³*C NMR spectra (600 Hz, DMSO) for hybrid compound* **11**
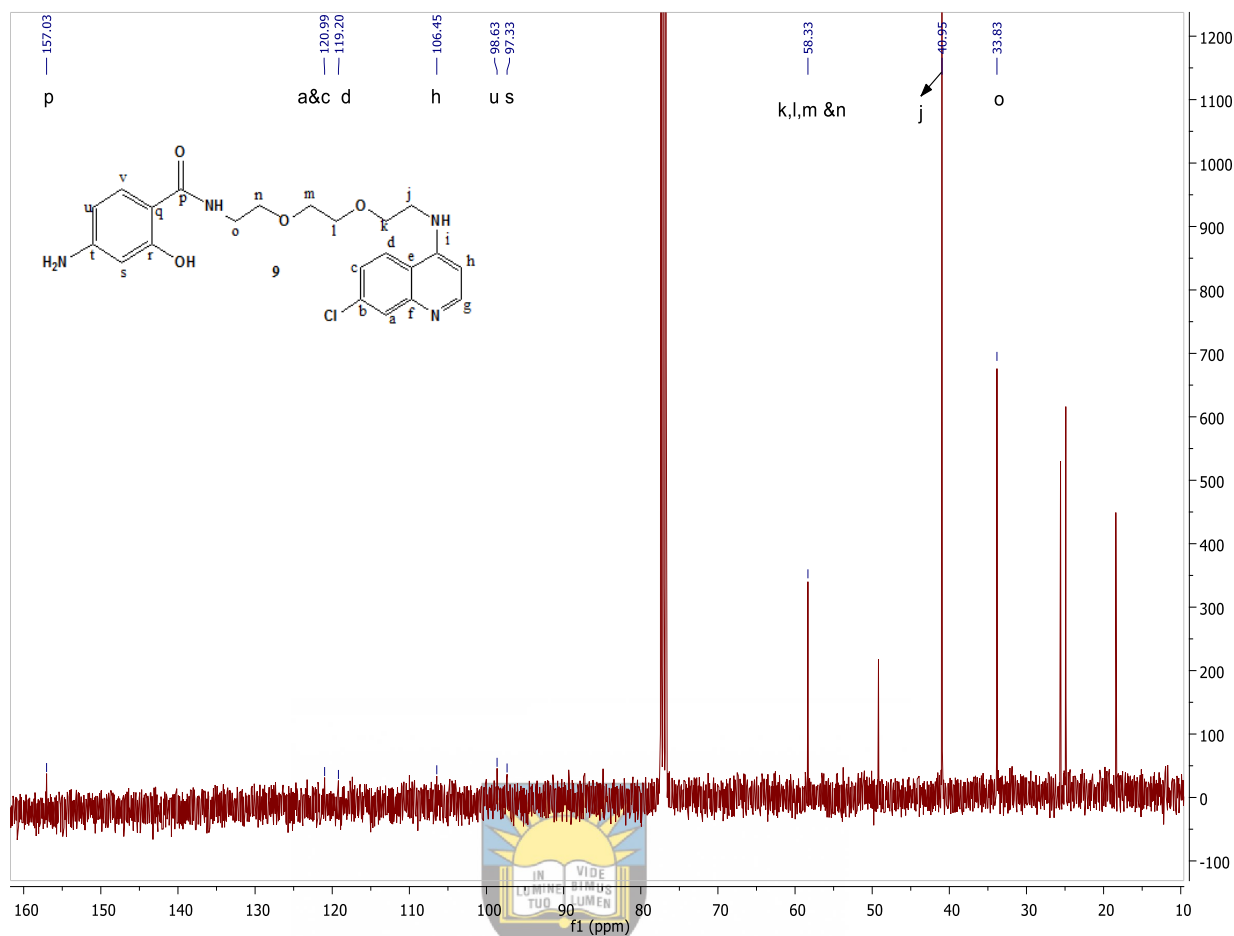
*Figure 24: ^{13}C NMR spectra (600 Hz, CDCl3) for hybrid compound **9***
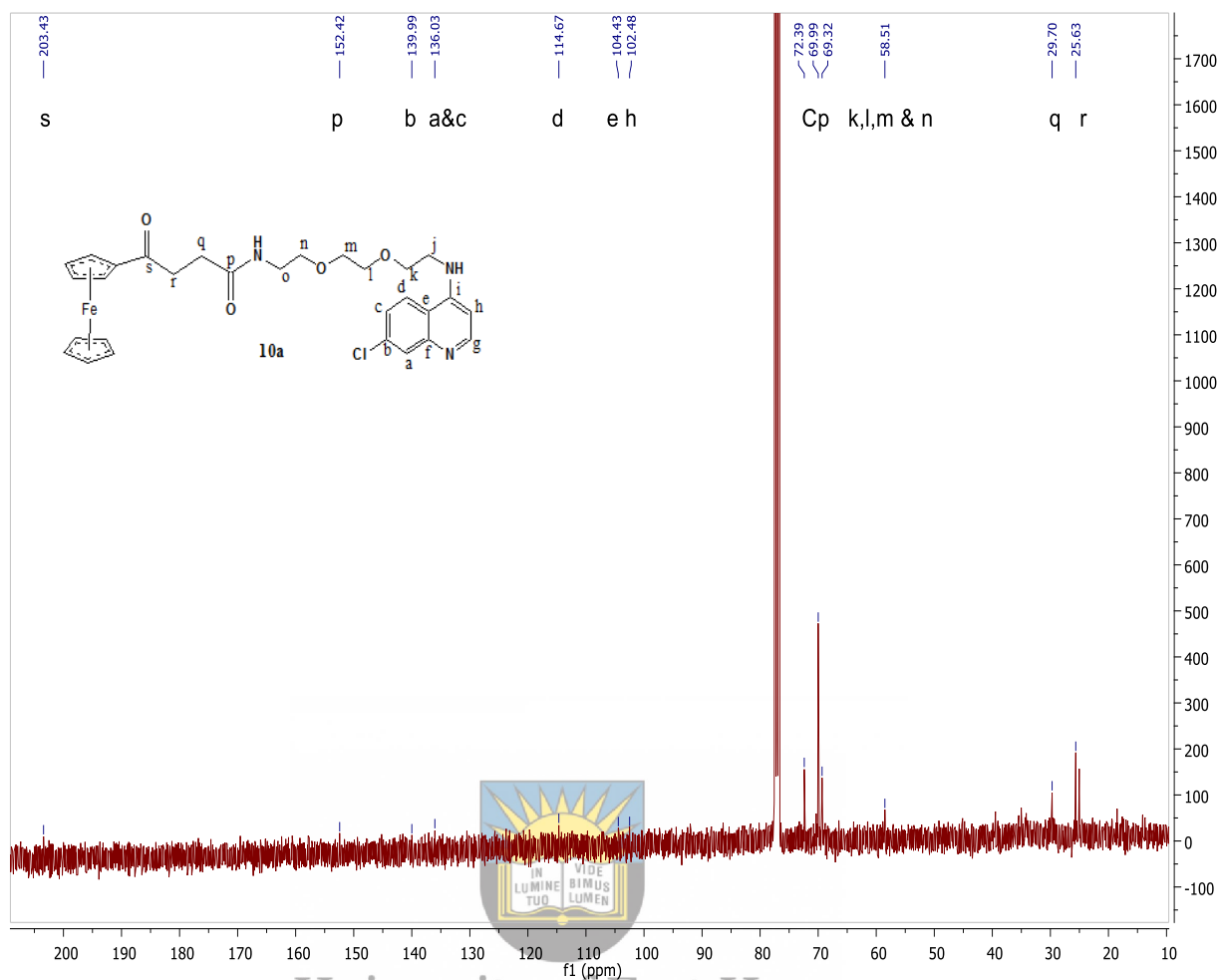
*Figure 25: ^{13}C NMR spectra (600 Hz, CDCl3) for hybrid compound **10a***
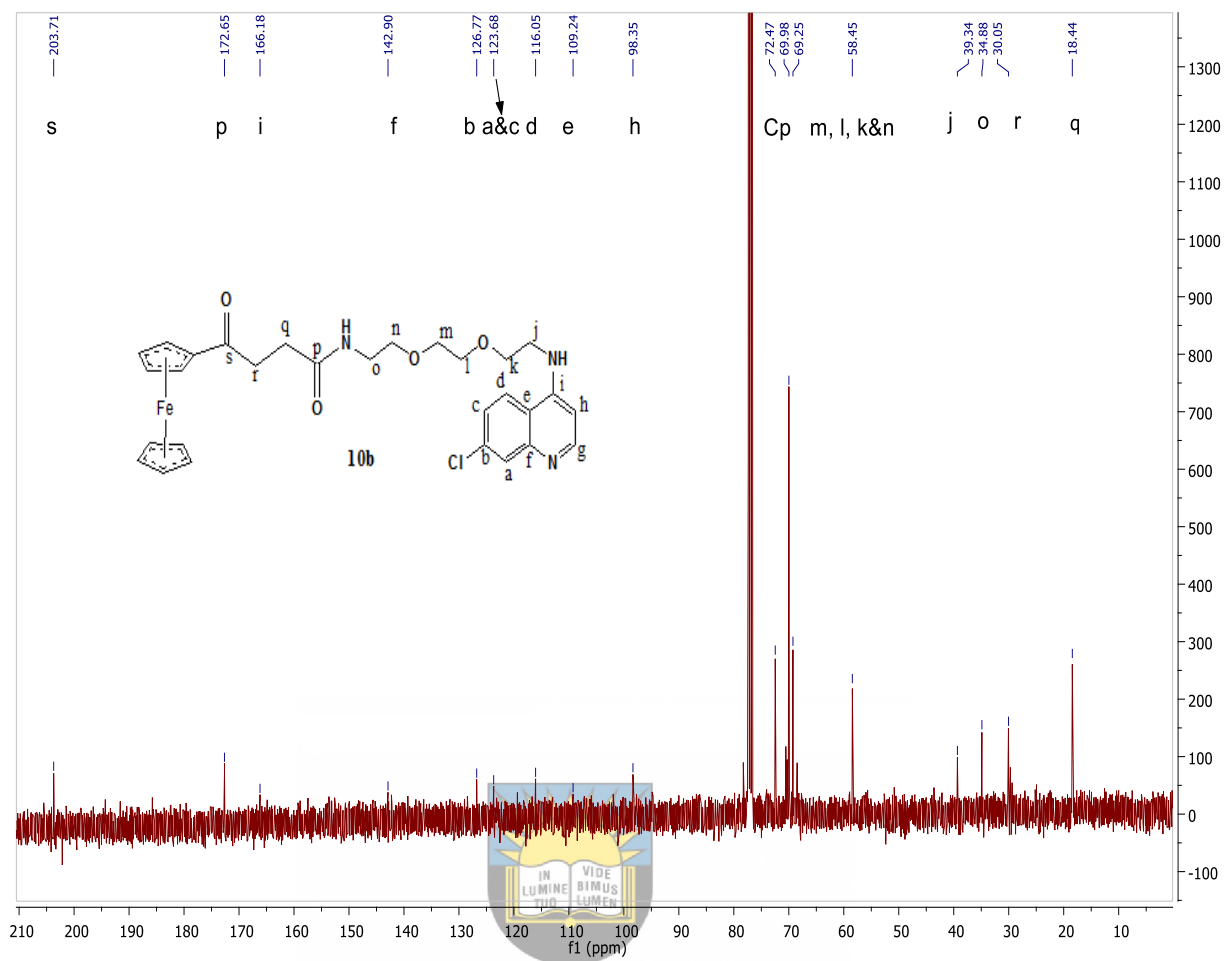
*Figure 26: ^{13}C NMR spectra (600 Hz, CDCl3) for hybrid compound **10b***
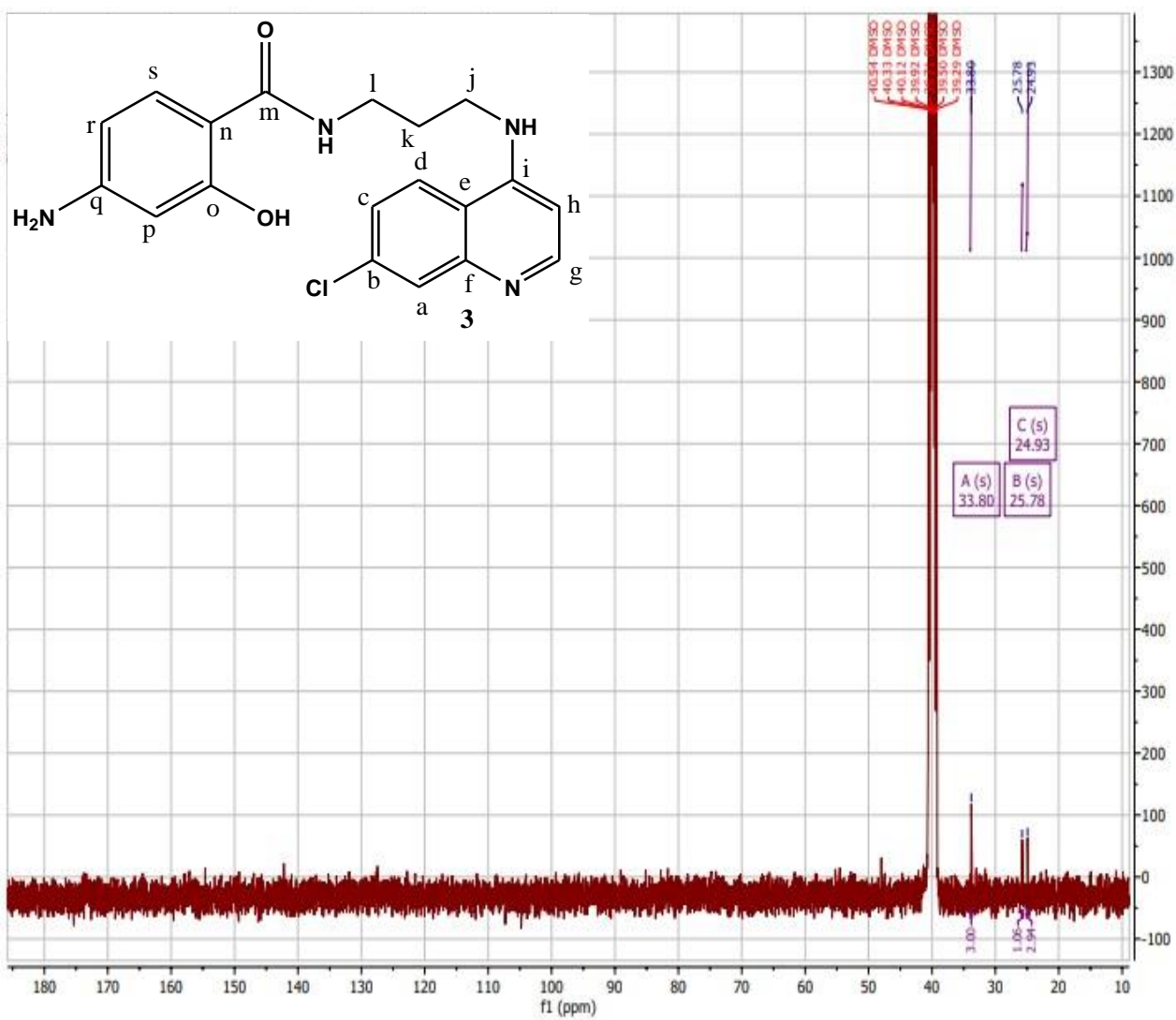
*Figure 27: ^{13}C NMR spectra (600 Hz, DMSO) for hybrid compound **3***
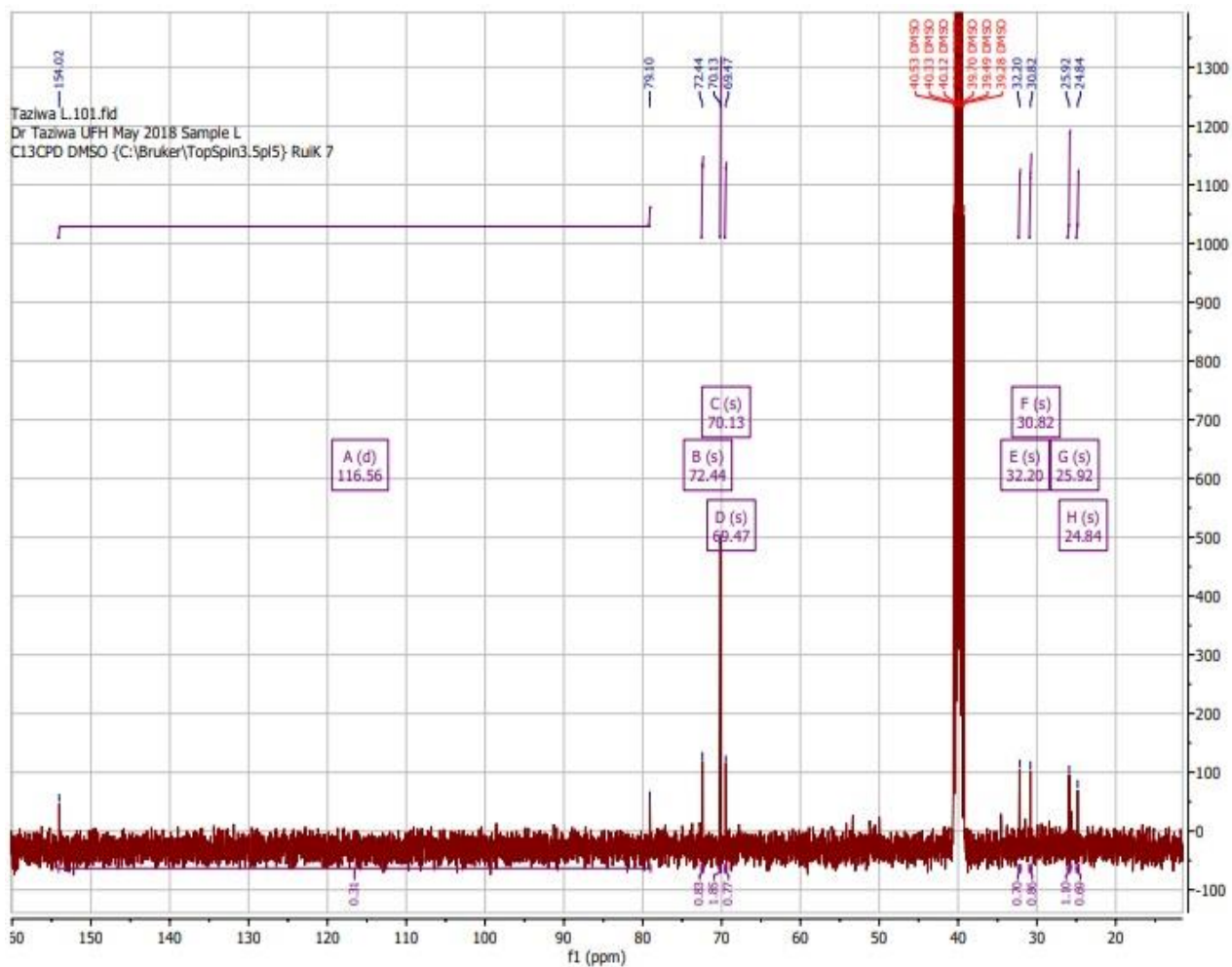
Figure 28: ^{13}C *NMR spectra (600 Hz, DMSO) for hybrid compound* **6a**
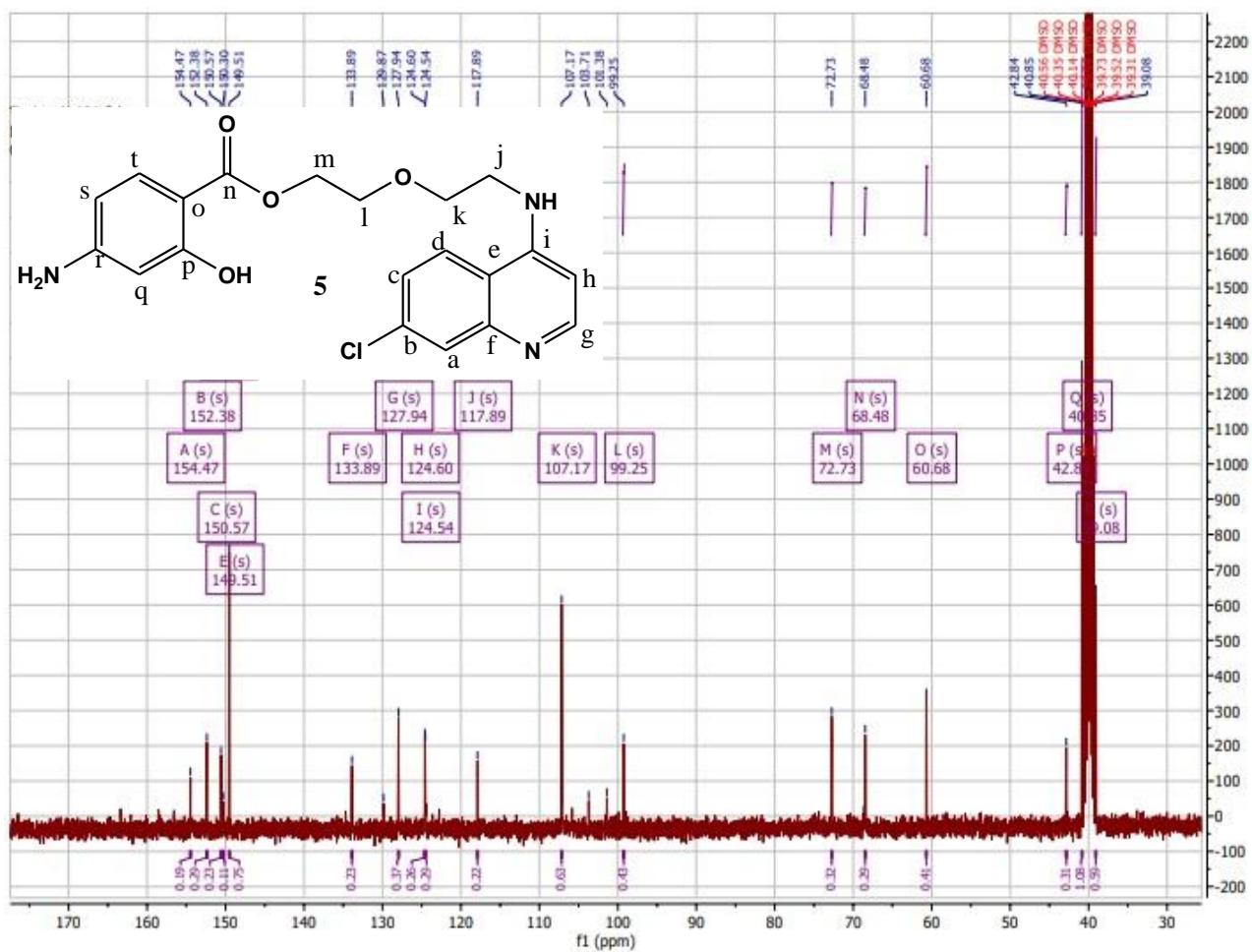
*Figure 29: ¹³C NMR spectra (600 MHz, DMSO) for hybrid compound **5***

5.2.4. ¹HNMR Spectra's
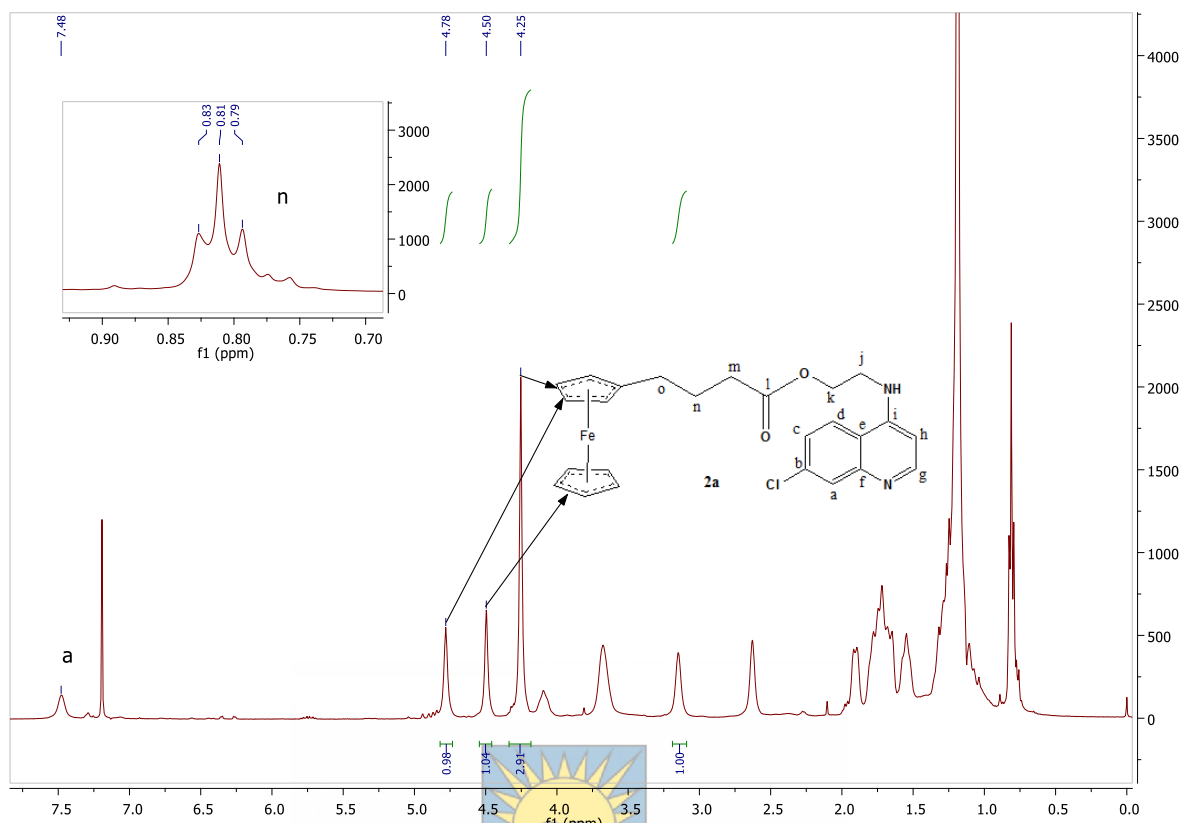
Figure 30: ¹H NMR spectra for compound 2a
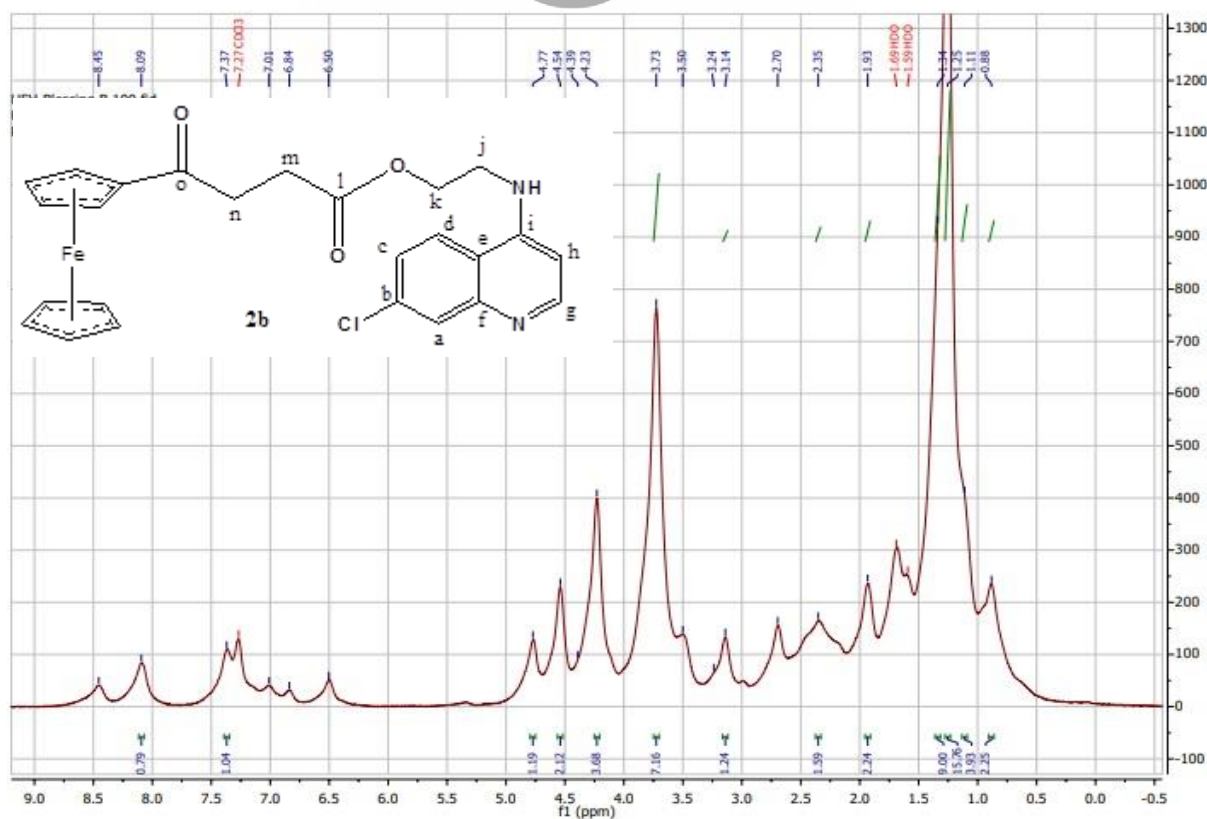
Figure 31: ¹H NMR spectra for compound 2b
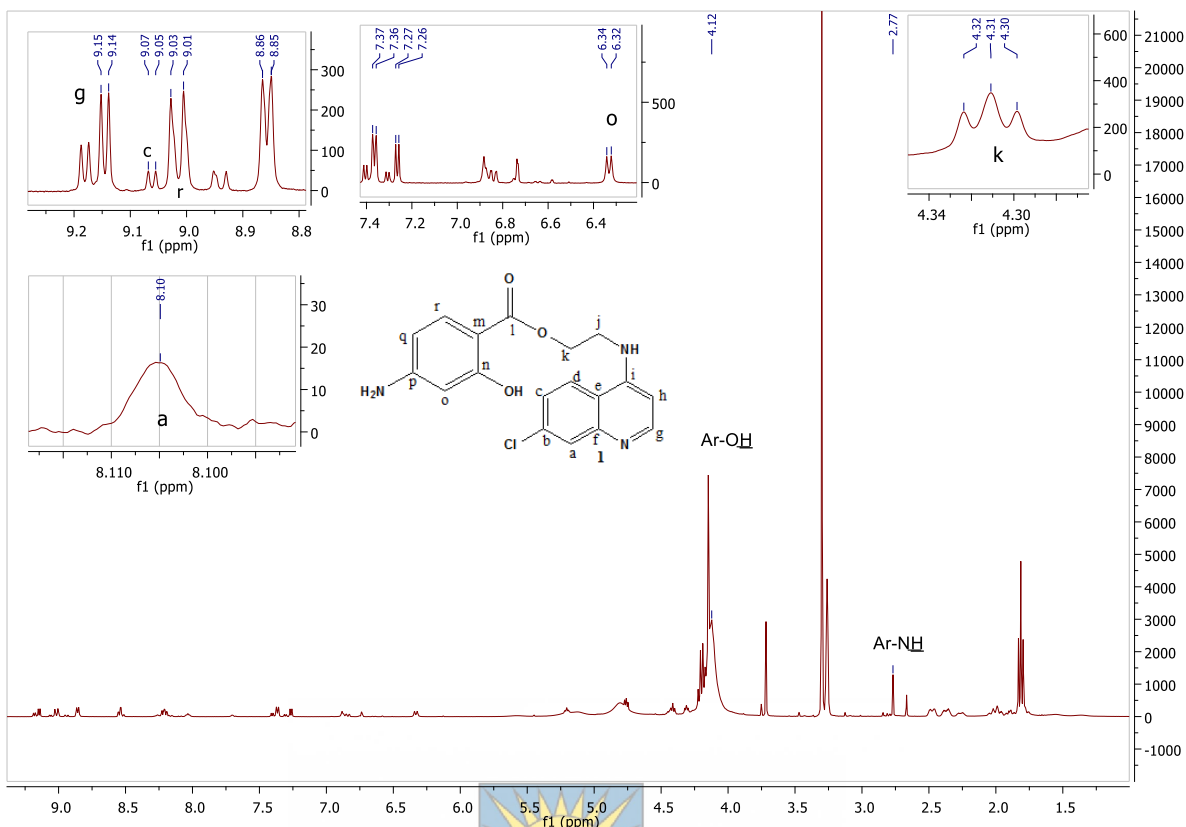
Figure 32: ^{1}H NMR spectra for hybrid compound 1
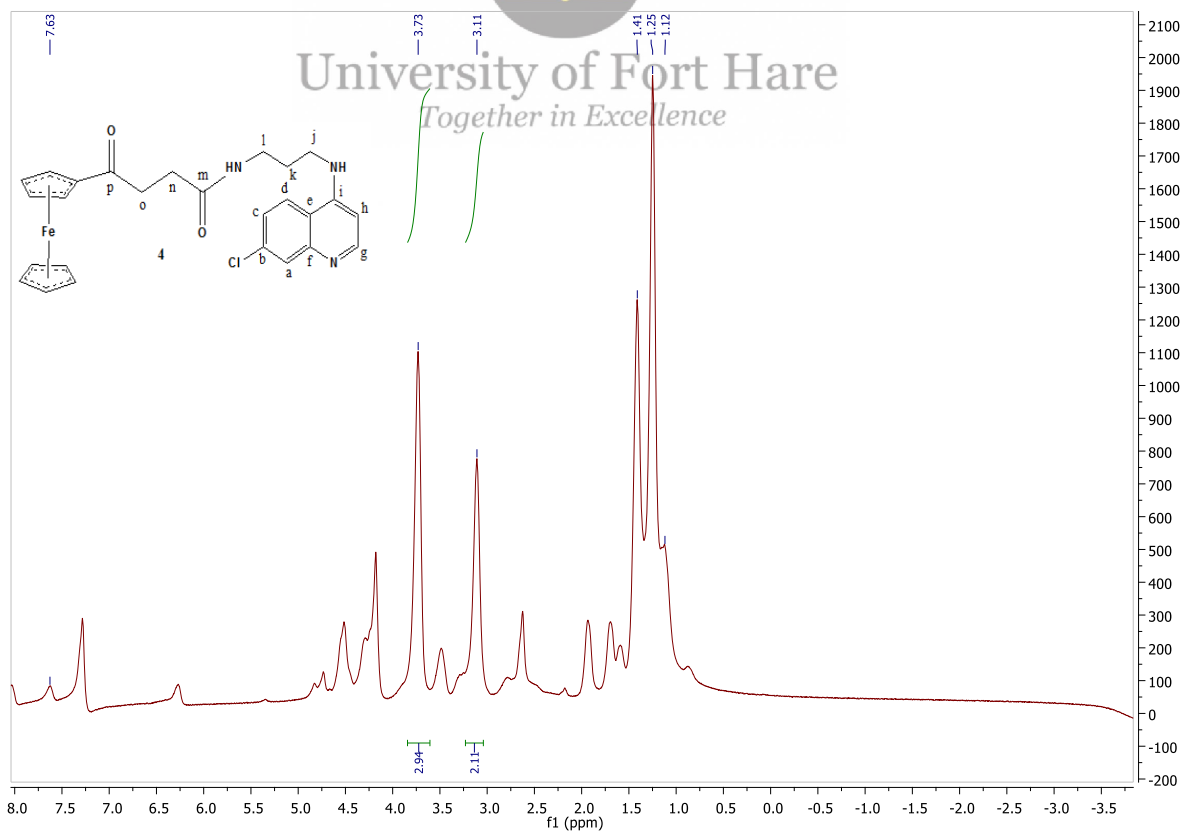
Figure 33: ^{1}H NMR spectra for hybrid compound 4
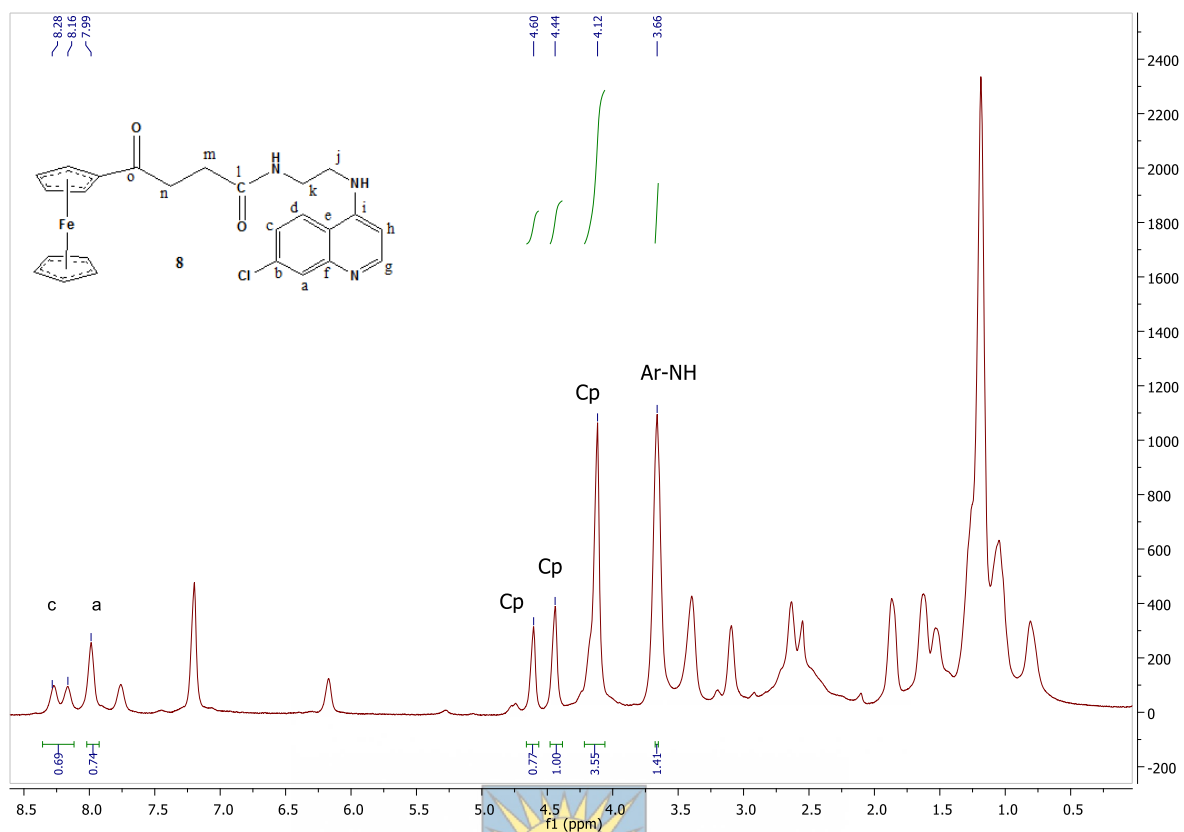
Figure 34: ¹H NMR spectra (400 Hz, CDCl3) for hybrid compound 8
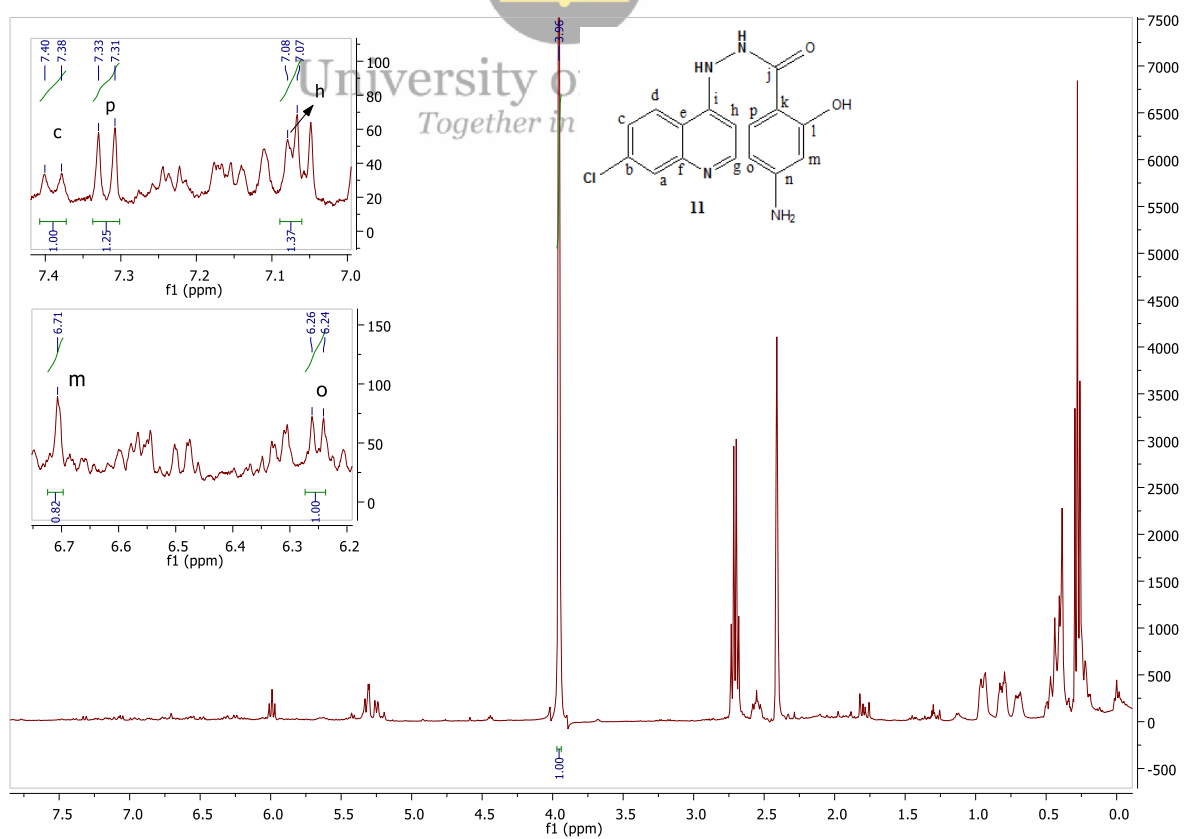
Figure 35: ¹H NMR spectra (400 Hz, DMSO) for hybrid compound 11
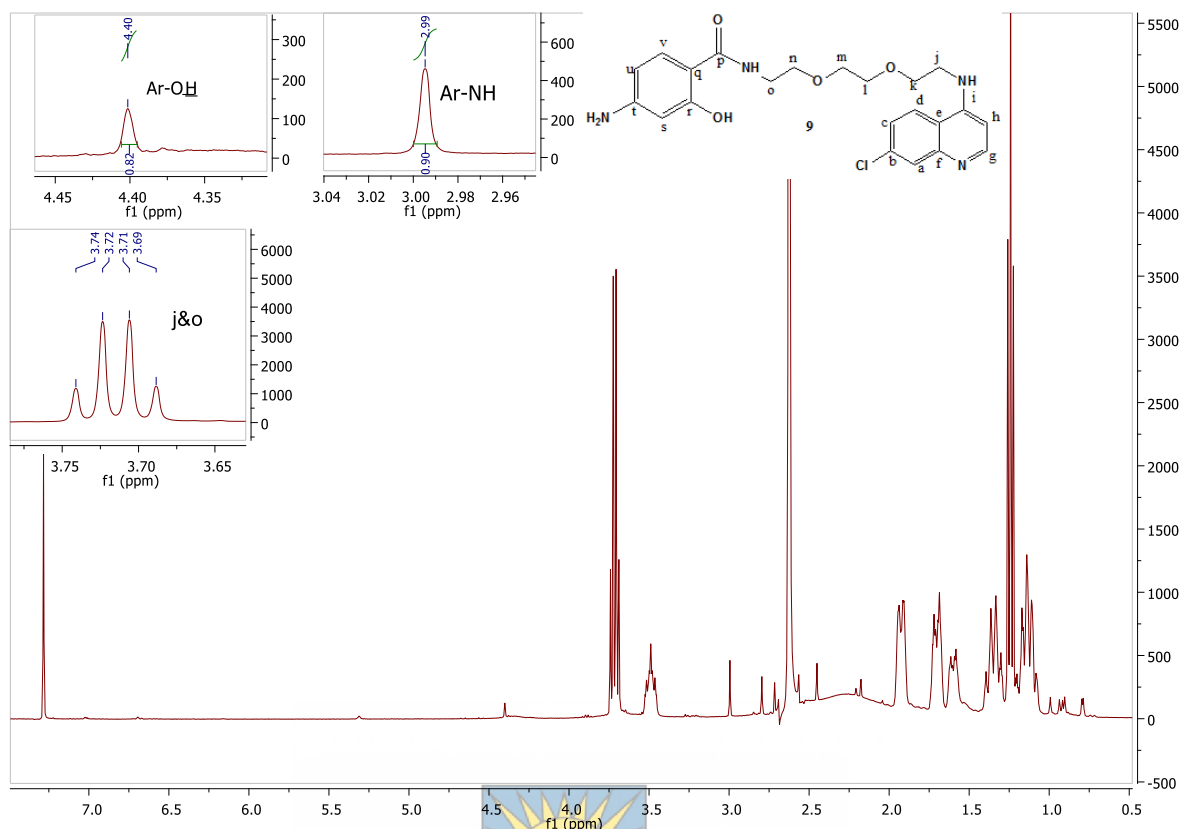
Figure 36: ^1H NMR spectra (400 Hz, CDCl3) for hybrid compound 9
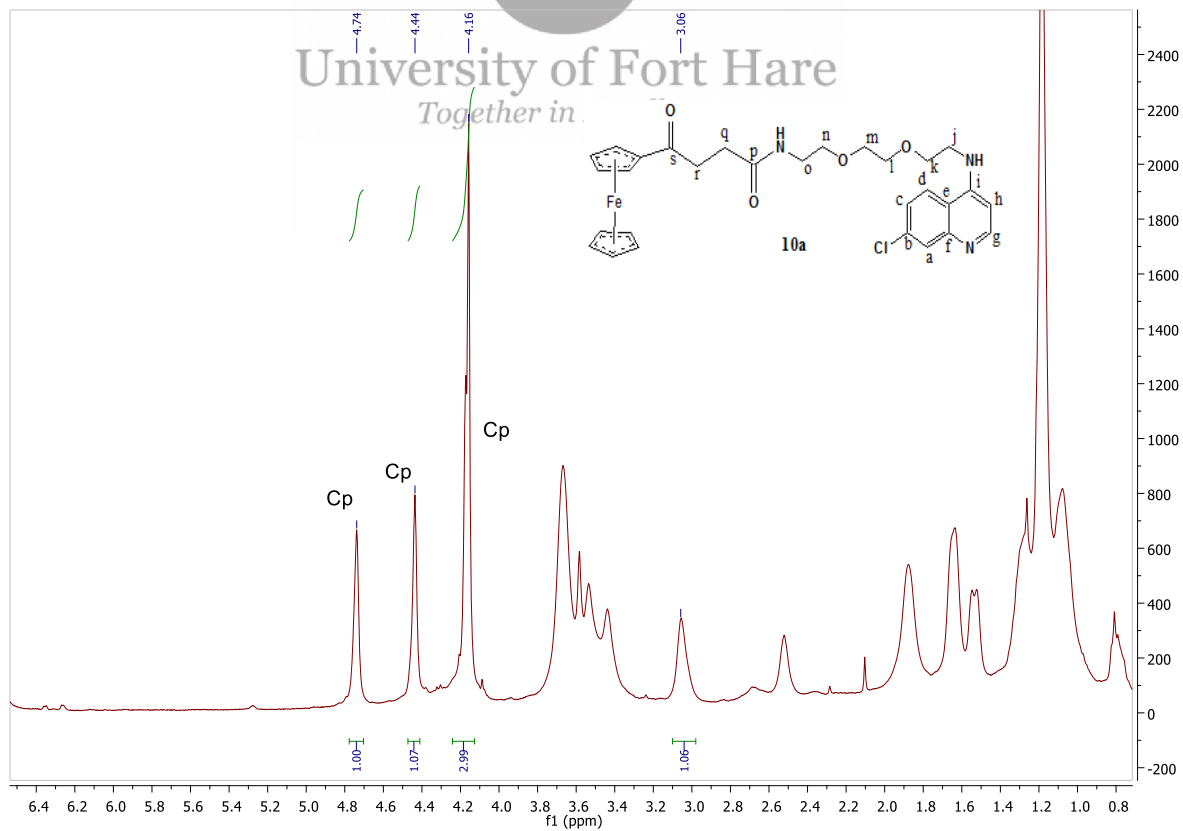
Figure 37: ^1H NMR spectra (400 Hz, CDCl3) for hybrid compound 10a
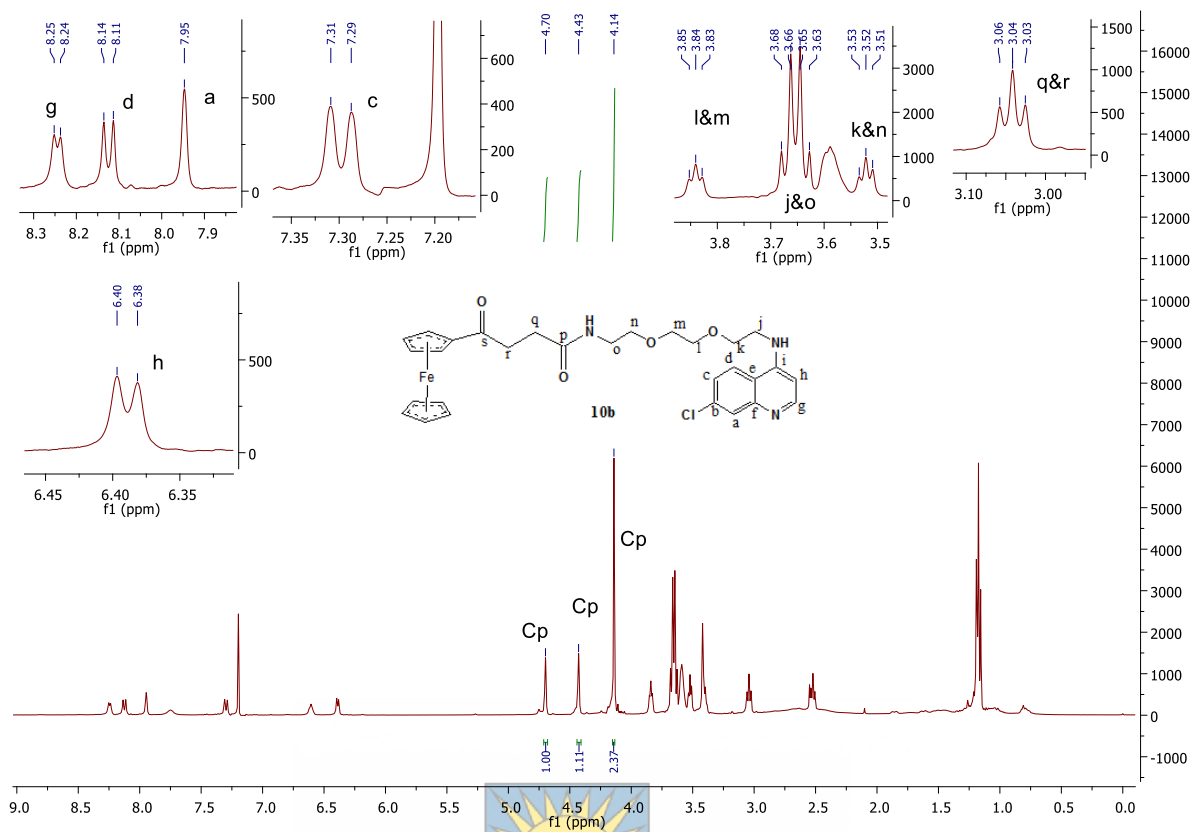
Figure 38: ¹H NMR spectra (400 Hz, CDCl3) for hybrid compound 10b
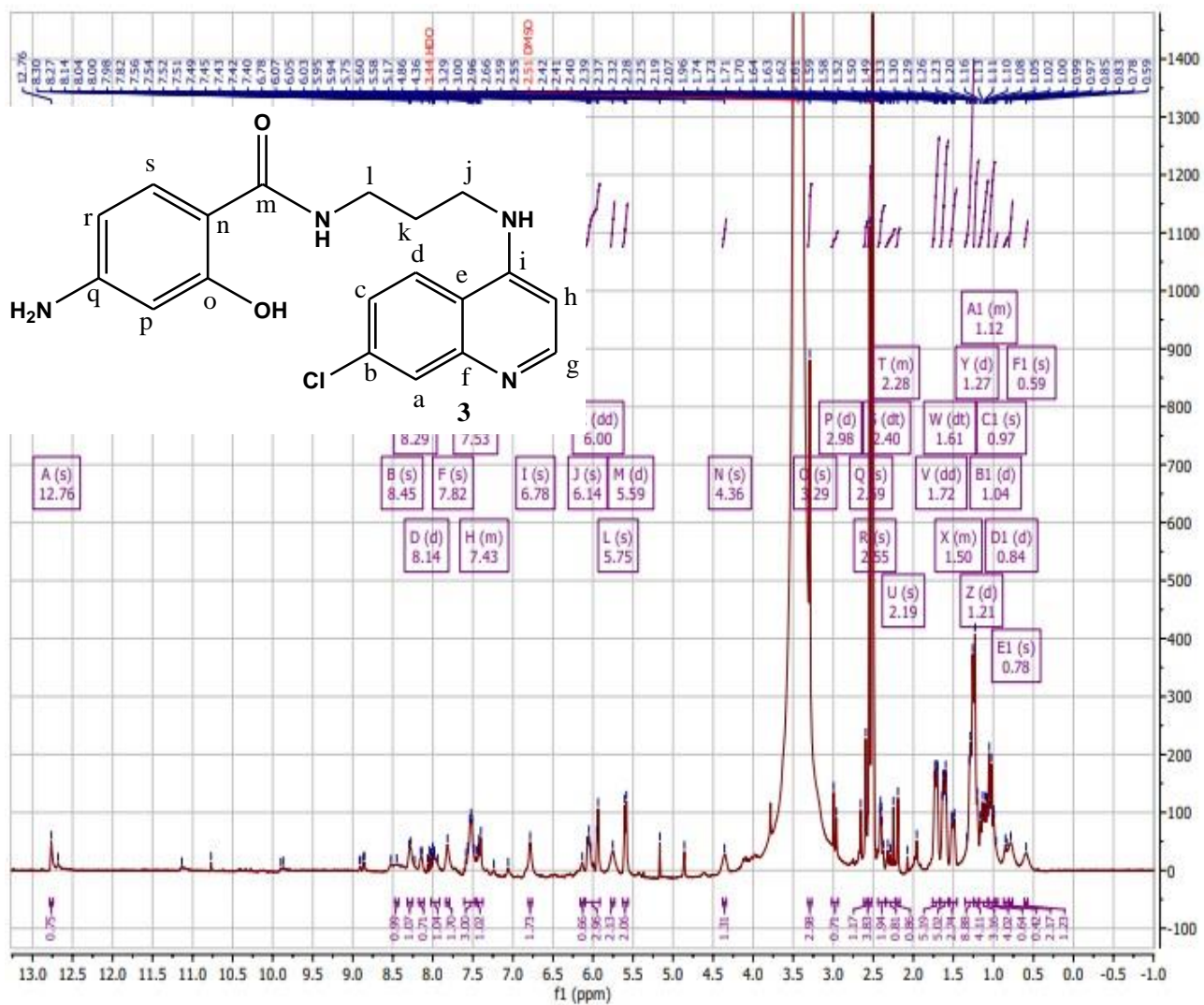
Figure 39: ^{1}H NMR spectra (400 Hz, DMSO) for hybrid compound 3
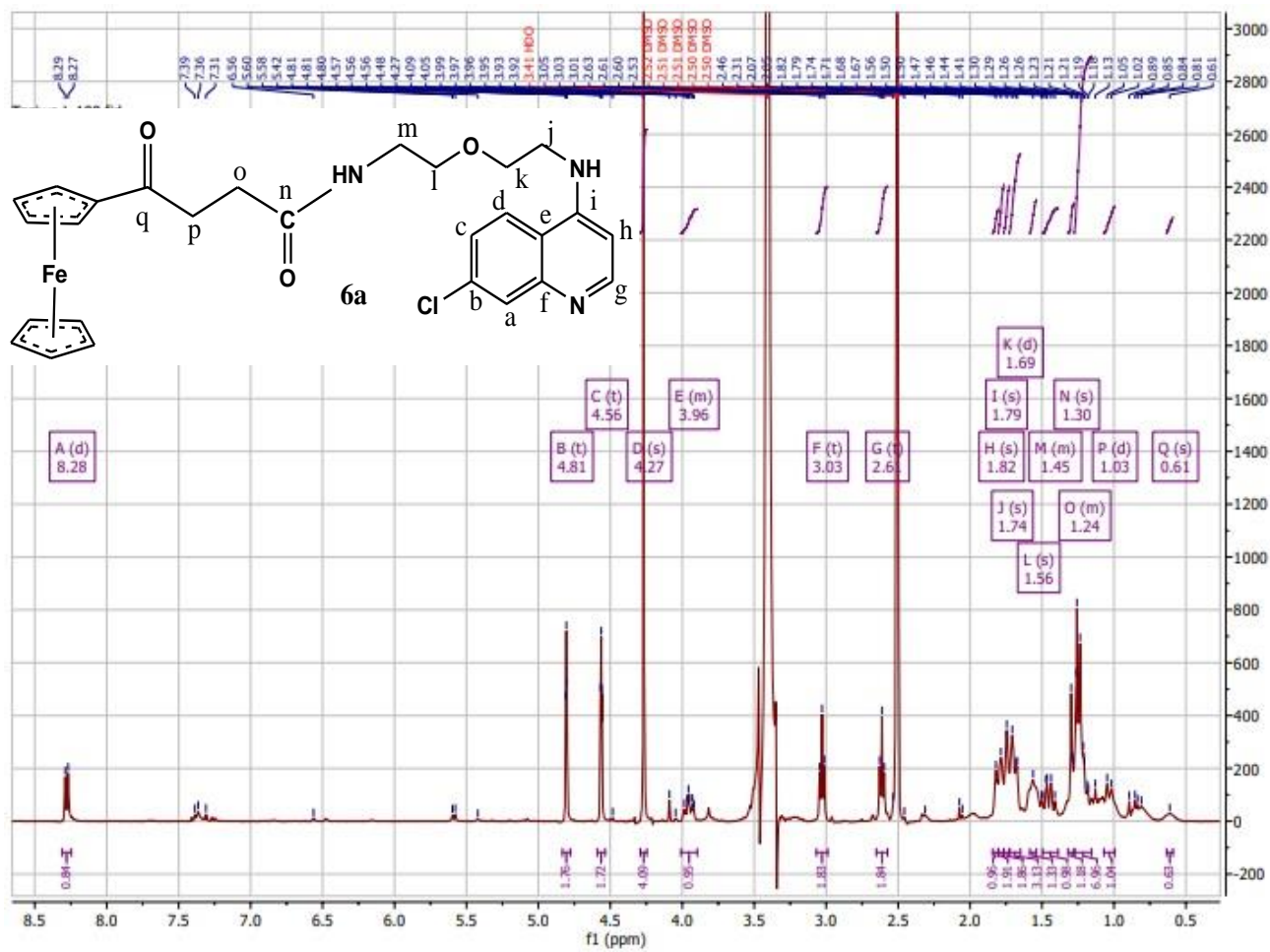
Figure 40: ^1H NMR spectra (400 Hz, DMSO) for hybrid compound 6a
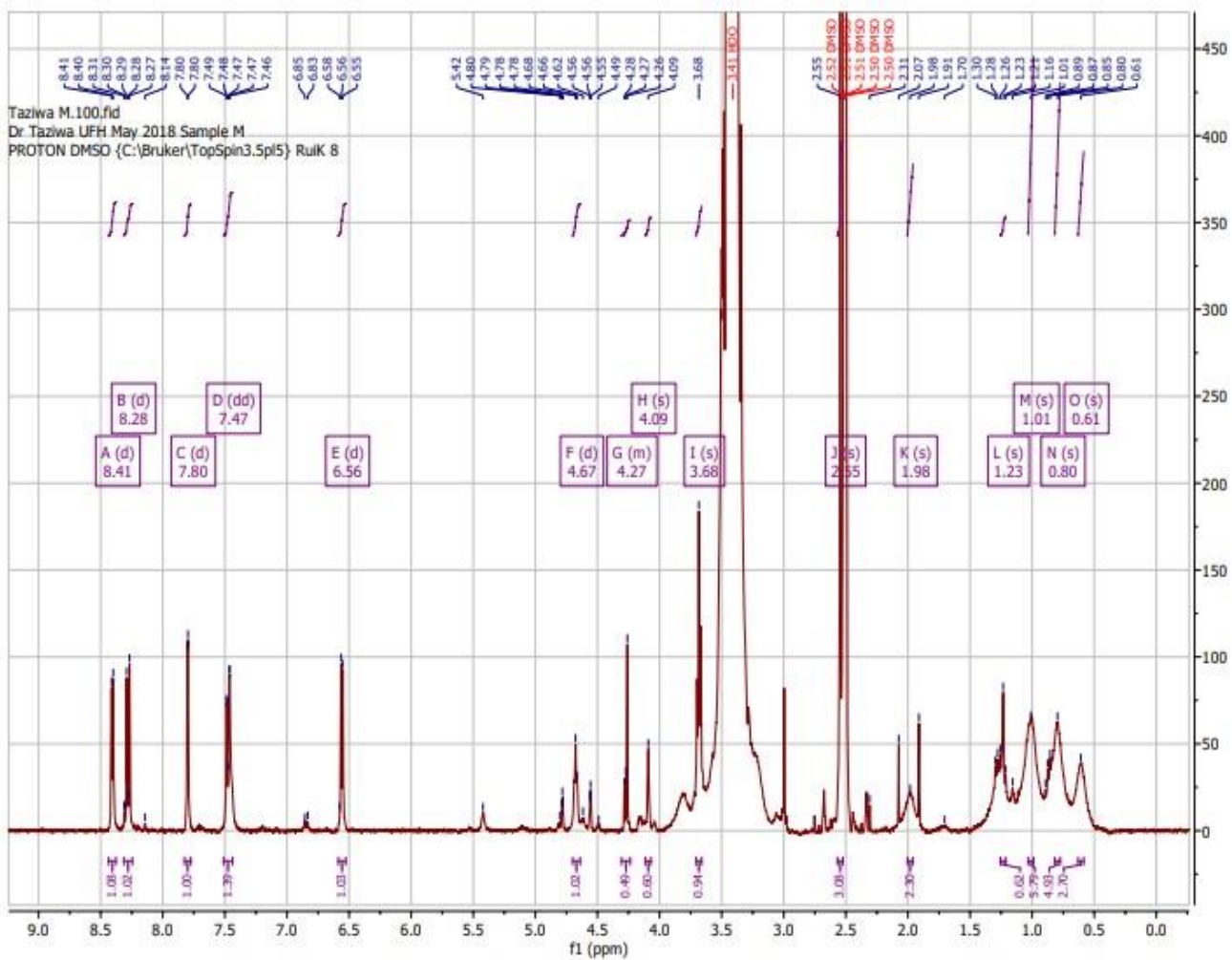
Figure 41: ^1H NMR spectra (400 Hz, DMSO) for hybrid compound 6b
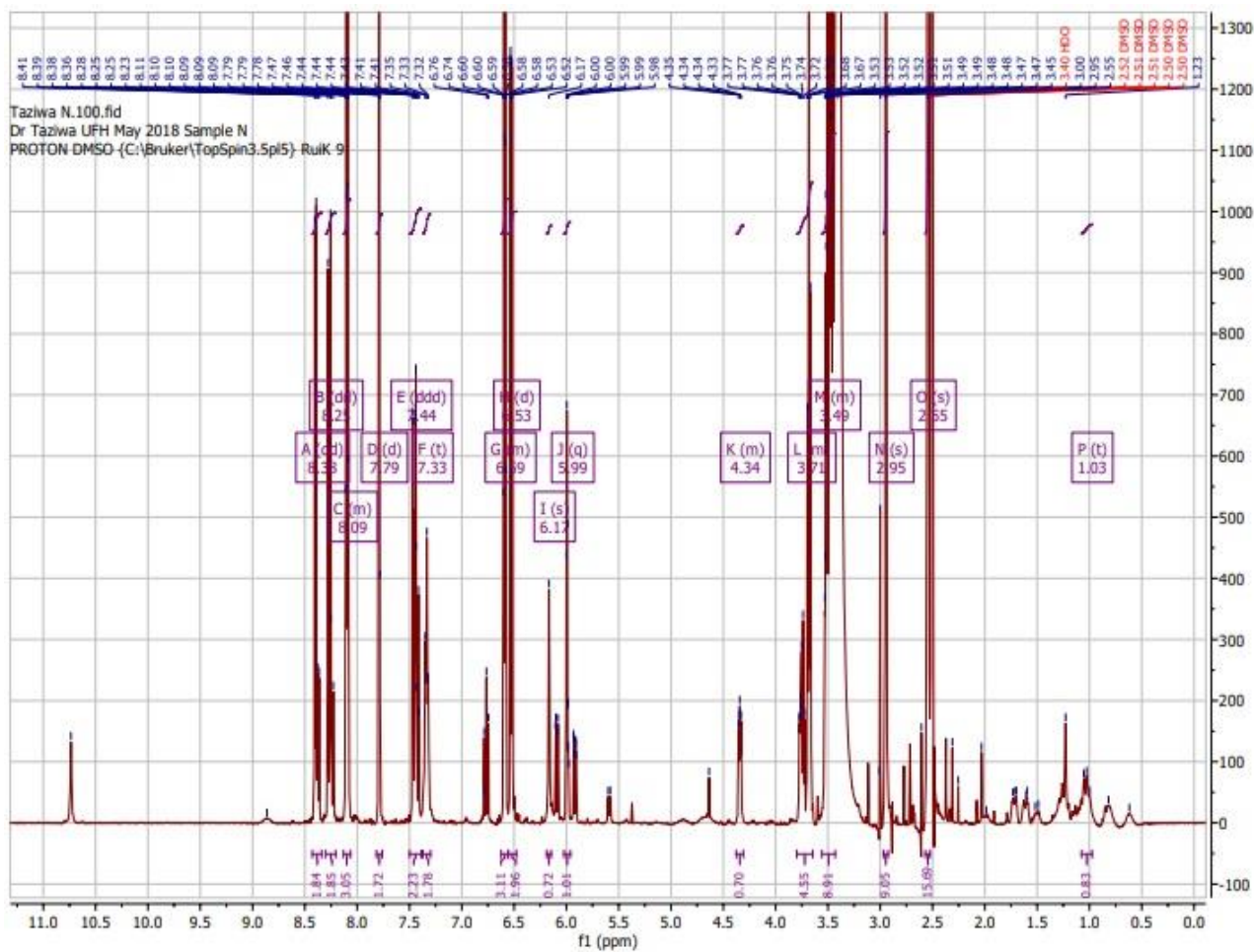
Figure 42:^{1}H NMR spectra (400 Hz, DMSO) for hybrid compound 5

5.2.5. LC-MS spectra's
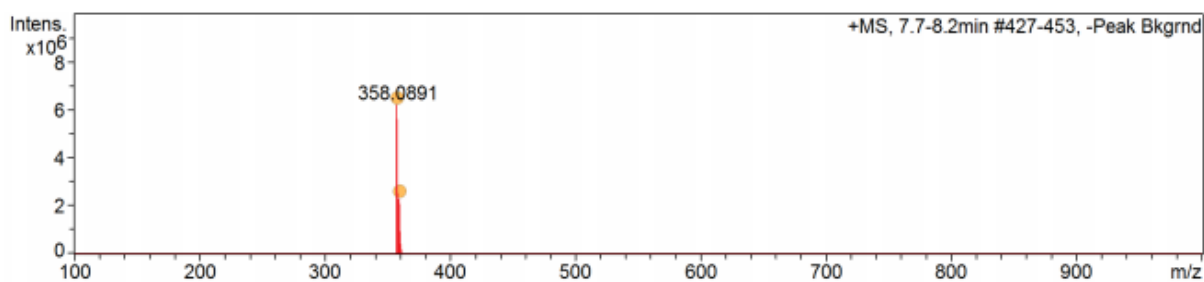
Figure 43: LC-MS results for Hybrid compound 1
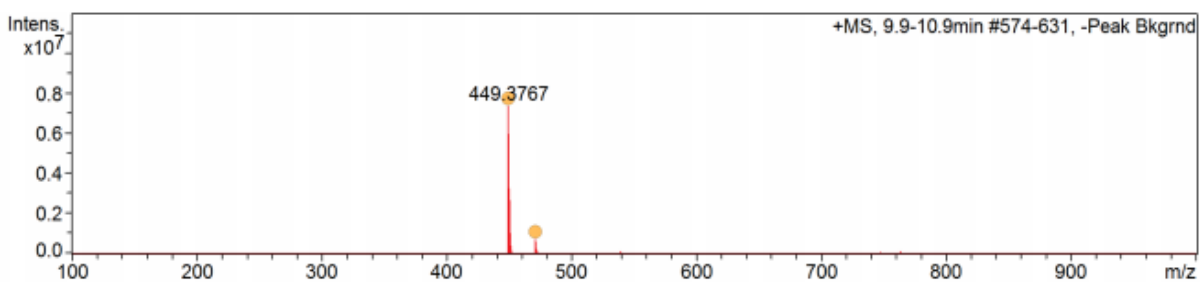
*Figure 44: LC-MS results for hybrid compound **2a***
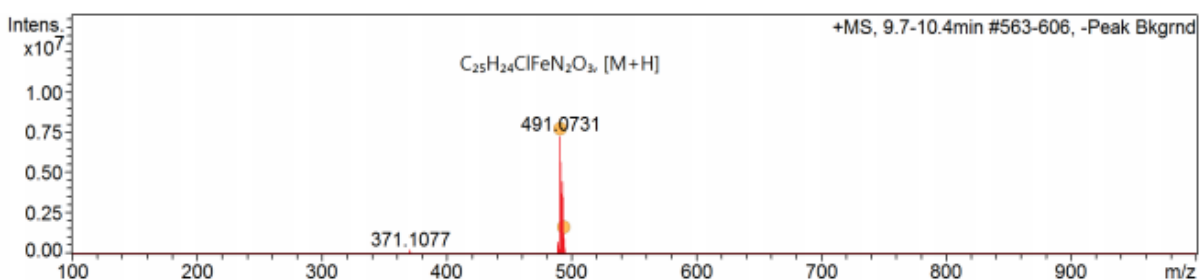
*Figure 45: LC-MS results for hybrid compound **2b***
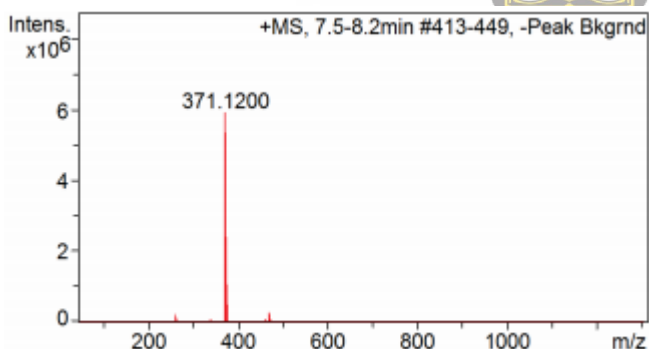
*Figure 46: LC-MS results for hybrid compound **3***
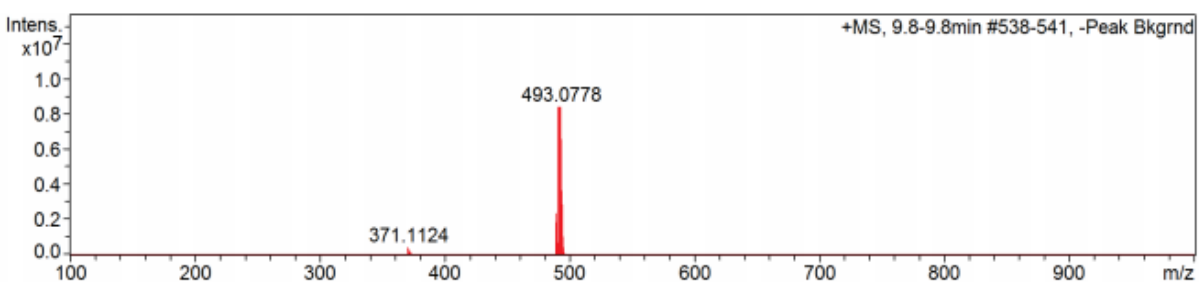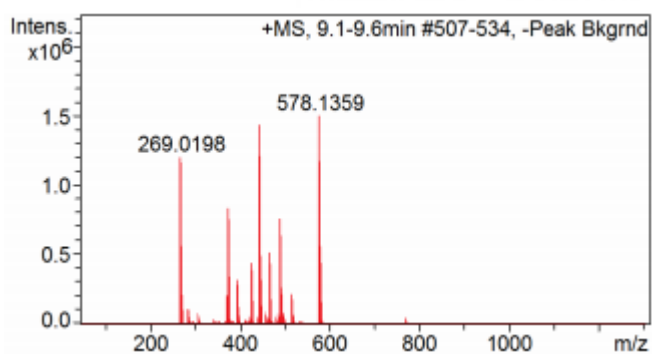

*Figure 47: LC-MS results for hybrid compound **4***

108
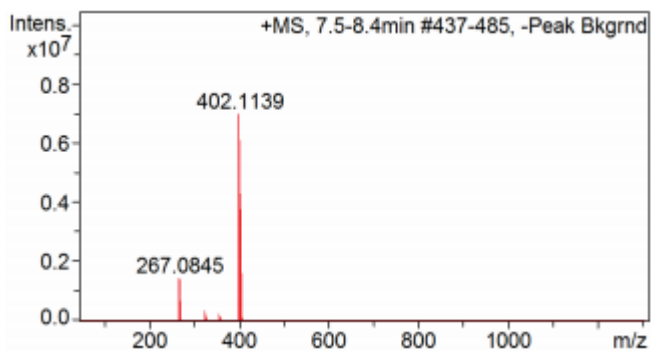
*Figure 48: LC-MS results for hybrid compound **5***
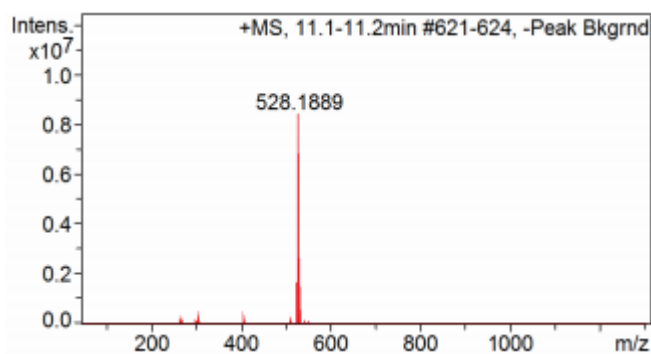
*Figure 49: LC-MS results for hybrid compound **6a***
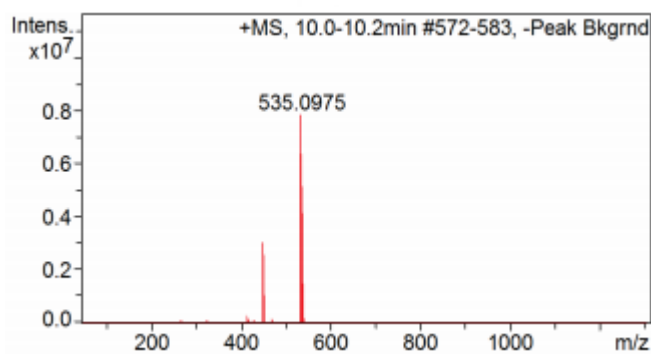
*Figure 50: LC-MS results for hybrid compound **6b***
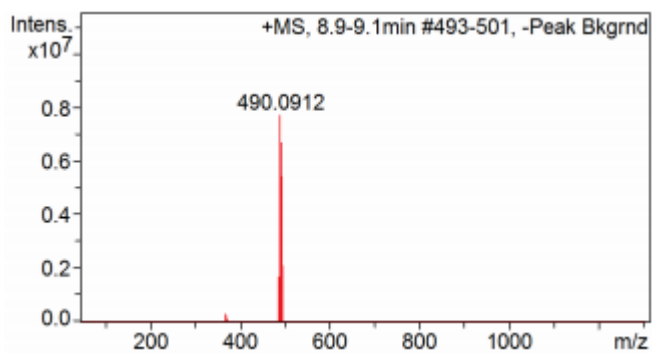
*Figure 51: LC-MS results for hybrid compound **8***
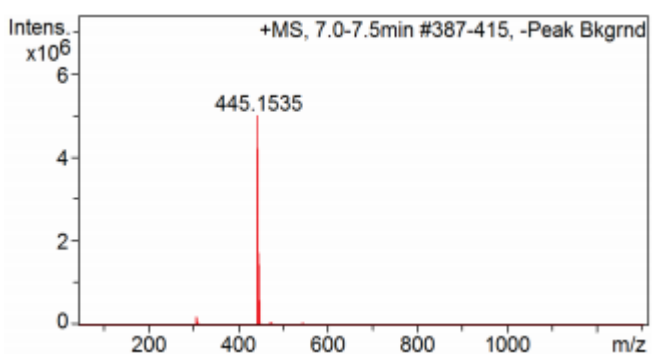
*Figure 52: LC-MS results for hybrid compound **9***

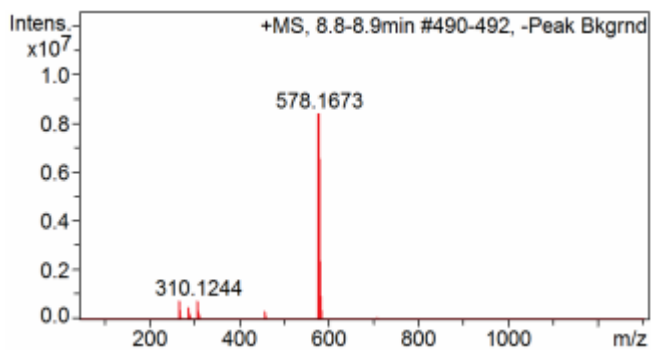*Figure 53: LC-MS results for hybrid compound **10a***

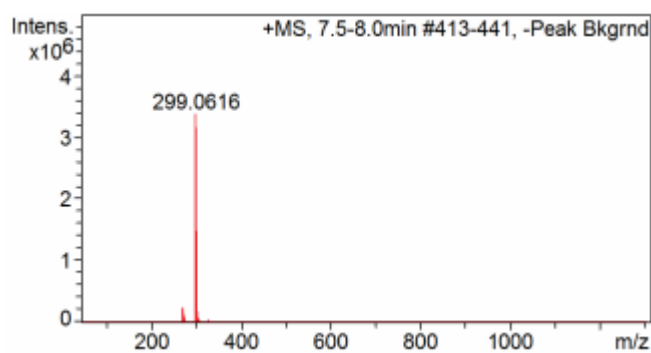*Figure 54: LC-MS results for hybrid compound **10b***

*Figure 55: LC-MS results for hybrid compound **11***

University of Fort Hare
Together in Excellence